

# **DEVELOPMENT OF NEWER CEMENTITIOUS BINDER FROM LIME SLUDGE AND ITS USE IN MORTAR**

Thesis submitted to AcSIR for the Award of the Degree of

**MASTER OF TECHNOLOGY**

in

**BUILDING ENGINEERING AND DISASTER MITIGATION**



by

**AASTHA SINGH**

**30EE15A01004**

Under the Supervision of

**Prof. S. K. SINGH**

**Prof. B. SINGH**



**CSIR – Central Building Research Institute**

Roorkee-247667, Uttarakhand, India

**May, 2017**

## CERTIFICATE

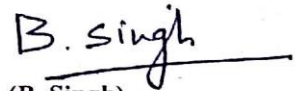
This is to certify that the work incorporated in this M. Tech. thesis entitled "*Development of Newer Cementitious Binder from Lime Sludge and its Use in Mortar*" submitted by *Ms. Aastha Singh* to Academy of Scientific and Innovative Research (AcSIR) in fulfilment of the requirements for the award of the Degree of Building Engineering and Disaster Mitigation, embodies original research work under our supervision. We further certify that this work has not been submitted to any other University or Institution in part or full for the award of any degree or diploma. Research material obtained from other sources has been duly acknowledged in the thesis. Any text, illustration, table etc. used in the thesis from other sources, have been duly cited and acknowledged.



**Aastha Singh**



**(S. K. Singh)**  
Professor,  
Structural Engineering Group  
CSIR-CBRI  
Roorkee



**(B. Singh)**  
Professor,  
Polymers, Plastics  
and Composites Group  
CSIR-CBRI  
Roorkee

## ACKNOWLEDGEMENT

First of all, I would like to thank God, the Almighty, for giving me everything to accomplish this thesis: Patience, health, wisdom, and blessing; and granting me the capability to proceed successfully.

I would like to express my deep and sincere gratitude to my supervisors, Dr. B. Singh, Professor, AcSIR, CSIR-Central Building Research Institute and Prof. S. K. Singh, Professor, AcSIR, CSIR-Central Building Research Institute for guiding me and giving their precious time, and also great ideas that enable me to complete this thesis. Their dynamism, vision, sincerity and motivation have deeply inspired me.

It is my great pleasure to acknowledge Dr. N. Gopalakrishnan, Director, CSIR-Central Building Research Institute, Roorkee for his generous support and useful advice to accomplish my project work.

I am also grateful to my seniors Humaira Athar and Kirthika and my lab mates Sandhya, Sameer, Hari Om, Nirmala, Naveen, Lalit and Joseph for their helping hand, moral support and encouragement whenever I needed.

I am also indebted to acknowledge, Mr. Rakesh Paswan, Scientist, Ms. Ishwarya G., Scientist, Mr. M. Reyazur Rahman M. Scientist, Ms. Surya Maruthupandian, Scientist, Dr. Jeeshan Khan, Scientist, Dr. Hemalata, Scientist, Mr. Rajesh Kumar, Scientist, Ms. Priyanka, Women Scientist, Mr. Srinivasan, Scientist, Dr. Rajni Lakhani, Senior Principal Scientist for their generous support and motivation to accomplish laboratory tests successfully.

My deepest gratitude to all who are closest to me, for their endless love, prayers and encouragement; my parents. Your support has helped me a lot to accomplish this project successfully.

(AASTHA SINGH)

## ABSTRACT

The objective of the present work is to develop low Portland clinker cement using high proportion of aluminosilicate pozzolana aiming at to reduce global warming (CO<sub>2</sub> emission). Various pozzolana such as fly ash, calcined clay and ground granulated blast furnace slag were selected for producing binder recipe. Alkaline lime sludge obtained from the paper industry was used as an alternative to limestone powder conventionally used for this purpose. The main approach is to dilute Portland cement with high volume of supplementary cementitious material in the presence of alkaline activator. Dilution of Portland cement content reduces the effectiveness of SCM activation unless an alkaline activator can be added. Consequently, the compatibility of the two cementitious gels, C-S-H (the main reaction product of the ordinary Portland cement) and N-A-S-H (the main product of the alkaline activation of aluminosilicate materials), may have important technological implications for future cementitious systems in which both products might be expected to precipitate.

The lime sludge was thermo-chemically activated at 850°C in presence of sodium hydroxide to convert its crystalline state to non-crystalline state. The hydraulic properties of resulting sludge were evaluated as per IS: 1727-99 for use in Portland cement and its value obtained was ~4.2 MPa. Various recipes comprised of cement clinker, pozzolana (fly ash, calcined clay and ground granulated blast furnace slag) and thermo-chemically activated lime sludge were formulated by varying pozzolana as well as lime sludge proportions. The Blaine's surface area and particle size distribution of the resulting mixes was found in the range of 500-626 m<sup>2</sup>/kg and 16.78 to 41.77 μm. It was concluded that, lime sludge based binder had more fineness than the Portland cement (285 m<sup>2</sup>/kg Blaine's surface area). The lime absorption characteristic of these mixes was determined according to BS EN 196 (Part 5). All the mixes exhibited lime absorption value below the saturation line in lime solubility curve plotted between calcium oxide concentration and hydroxyl ion concentration showing their adequate pozzolanicity. The strength forming phases in the mixes were analyzed with the help of XRF, XRD, FTIR, SEM-EDAX and TGA. The oxide composition indicated that CaO, SiO<sub>2</sub> and Al<sub>2</sub>O<sub>3</sub> content in the mix were in the range of 38-48 %, 26-32 % and 17-25 % respectively. The higher intensity of absorption bands in region 990 - 1120 cm<sup>-1</sup> for lime sludge based binder over Portland cement indicated more reaction product formation which are related to strength development. The

existence of alite/ belite phase in the region 30-32° 2 $\theta$  of XRD supported strength development in hardened pastes. Needle and Prismatic type crystals as observed in FE-SEM were adequately viewed in the mix. Based on these results, it is concluded that cementitious binder containing GGBS/calclined clay and thermo-chemically activated lime sludge gives optimum results.

Rheological studies of lime sludge based cementitious binders were carried out as a function of water-cement ratio, superplasticizer doses and lime sludge content. The mix followed Bingham fluid rule. Hysteresis loop between shear stress and shear rate of mix indicated its shear thickening behaviour. The workable mix (zero yield stress) was obtained at 0.2 % superplasticizer content. Hydration behaviour of various binders was studied with the help of isothermal conduction calorimetry by varying pozzolana and lime sludge proportion. It was observed that reduced induction period and increased height of acceleration peak indicated fast setting and more strength of lime sludge based binder compared to Portland cement. This is mainly attributed to formation of calcium carboaluminate hydrate, C<sub>3</sub>AH<sub>6</sub> (the reaction between calcium aluminate hydrate and thermo-chemically activated lime sludge), C-A-S-H and other phases. The total heat (proportional to reaction products) of lime sludge binder was higher than the Portland cement. Adding activated lime sludge into mix resulted intense acceleration peak indicating the possibility of higher strength development than the Portland cement in the hardened pastes. Based on the results, it was found that lime sludge binder containing GGBS/calclined clay exhibited superior performance than those of Portland cement.

The physical properties of developed thermo-chemically activated lime sludge binder (25%) were evaluated according to IS: 4031. The results were compared with the requirements of IS: 269. It was found that the developed binder satisfied the criteria laid down in the Standard. Life cycle analysis of lime sludge based binder was carried out using SIMA PRO software. It was observed that global warming in terms of CO<sub>2</sub> emission was reduced by 51% when compared with the Portland cement. Abiotic depletion potential in terms of depletion of resources was reduced by 50% showing its sustainability over the Portland cement.

It is concluded that thermo-chemically activated lime sludge based binder can be used as an alternative to Portland cement in many applications. The development of these kinds of hybrid cements based on low energy clinker and low lime mixes may encourage the utilization of unused lime sludge produced from various industries.

# CONTENTS

Certificate	i
Acknowledgement	ii
Abstract	iii
<b>CHAPTER 1: INTRODUCTION</b>	<b>1</b>
1.1 General	1
1.2 Objectives	3
1.3 Scope of the study	3
1.4 Methodology	3
1.5 Structure of thesis	4
<b>CHAPTER 2: LITERATURE REVIEW</b>	<b>5</b>
2.1 General	5
2.2 Building Lime	6
2.2.1 Classification and Application of Building Lime	6
2.2.2 Lime Production Technology	6
2.2.3 Hydraulic Lime	9
2.3 Lime Sludge	10
2.3.1 Types of Lime Sludge.	11
2.3.1.1 Paper Sludge	13

2.3.1.2	Sugar Sludge	14
2.3.1.3	Carbide Sludge	14
2.3.1.4	Chromium Sludge	15
2.3.1.5	Phospho-Chalk	15
2.3.1.6	Soda Ash Sludge	15
2.3.2	Applications of lime sludge	15
2.3.3	Theory of calcination	15
2.4	Calcined Clay	16
2.4.1	Chemical composition of calcined clay	17
2.5	Ground granulated blast furnace slag	18
2.6	Fly ash	19
2.7	Limestone	20
2.8	Gypsum	22
2.9	Blended cement	22
2.9.1	Advantages of blended cement	22
2.10	Global research and development trends	23
2.11	Research trends in India	23
2.12	Research significance	24
2.13	National need	25
2.14	Identified research gaps	26
<b>CHAPTER 3:</b>	<b>EXPERIMENTAL INVESTIGATIONS</b>	<b>27</b>
<b>3.1</b>	<b>Introduction</b>	<b>27</b>

<b>3.2 Materials</b>	27
3.2.1 OPC 43 grade cement clinker	27
3.2.2 Lime sludge	27
3.2.3 Calcined clay	32
3.2.4 Ground granulated blast furnace slag	33
3.2.5 Fly ash	34
3.2.6 Limestone	34
3.2.7 Gypsum	35
<b>3.3 Preparation of materials</b>	35
3.3.1 Activation of lime sludge	35
3.3.2 Grinding	35
3.3.3 Inter-grinding of mixes	36
<b>3.4 Optimization of mixes</b>	37
<b>3.5 Testing methods</b>	37
3.5.1 Specific surface area	37
3.5.2 Particle size distribution	39
3.5.3 X-ray diffractometer	40
3.5.4 FE-SEM and EDAX	41
3.5.5 Thermogravimetric analysis and differential thermal gravimetric	42
3.5.6 Fourier transform infrared spectroscopy	43
3.5.7 Consistency	44
3.5.8 Setting time	44



3.5.9	Flow table	45
3.5.10	Lime reactivity	45
3.5.11	Fratini test	47
3.5.12	Isothermal calorimeter	47
3.5.13	Specific gravity	48
3.5.14	Soundness	48
3.5.15	pH	50
3.5.16	Rheology	50
3.5.17	Compressive strength	51
<b>CHAPTER 4:</b>	<b>RESULTS AND DISCUSSION</b>	<b>53</b>
<b>4.1</b>	<b>Characterisation of cementitious binders</b>	<b>53</b>
4.1.1	Lime reactivity and pozzolanicity	53
4.1.2	Blaine specific surface area	55
4.1.3	Particle Size Distribution	55
4.1.4	X-ray Fluorescence spectroscopy (XRF)	58
4.1.5	X-ray Diffraction (XRD)	59
4.1.6	Fourier Transform of Infrared spectroscopy	60
4.1.7	FE-SEM - EDAX	61
4.1.8	Thermal gravimetric analysis (TGA/DTG)	66
<b>4.2</b>	<b>Rheological Studies of binders</b>	<b>69</b>
<b>4.3</b>	<b>Hydration Studies of binders</b>	<b>73</b>
<b>4.4</b>	<b>Properties of lime sludge based cementitious binders</b>	<b>78</b>

	4.4.1 Specific gravity	78
	4.4.2 Soundness	78
	4.4.3 pH	79
	4.4.4 Consistency and setting time	81
	4.4.5 Compressive Strength	82
	<b>4.5 Life cycle assessment</b>	<b>88</b>
<b>Chapter 5:</b>	<b>Conclusion</b>	<b>93</b>
	<b>References</b>	<b>95</b>
	List of figures	x
	List of tables	xv

## LIST OF FIGURES

Fig. 1.1	Cement production and growth in cement demand with respect to years	1
Fig. 1.2	Methodology for development of new lime sludge based cementitious binder	4
Fig. 2.1	Pantheon Temple, Rome	5
Fig. 2.2	Charminar, Hyderabad	5
Fig. 2.3	A partially mechanized vertical shaft lime kiln	8
Fig. 2.4	An innovative single-tier lime hydrator	8
Fig. 2.5	The production process of lime sludge	14
Fig. 2.6	The chemical composition of calcined clay	17
Fig. 2.7	The chemical composition of GGBFS	18
Fig. 2.8	The chemical composition of fly ash	19
Fig. 3.1	Photographic view of clinker	27
Fig. 3.2	Raw lime sludge from paper industry	28
Fig. 3.3	Characterization of raw lime sludge	29
Fig. 3.3 (a)	SEM image of raw lime sludge	29
Fig. 3.3 (b)	EDAX analysis of raw lime sludge showing elements present	29
Fig. 3.4	XRD analysis of raw lime sludge	29
Fig. 3.5	TGA/DTG curve of raw lime sludge	30
Fig. 3.6	FTIR spectrum of raw lime sludge	30
Fig. 3.7	TGA/DTG curve of calcined clay	32

Fig. 3.8	TGA/DTG curve of GGBFS	33
Fig. 3.9	TGA/DTG curve of limestone	34
Fig. 3.10	FTIR spectrum of limestone	35
Fig. 3.11	Grinding procedure of blended cement	36
Fig. 3.11 (a)	Planetary ball mill for grinding	36
Fig. 3.11 (b)	Inter-grinding mix	36
Fig. 3.11 (c)&(d)	Planetary ball mill jars for grinding	36
Fig. 3.12	The experimental setup of the automatic Blaine's apparatus	39
Fig. 3.13	The photographic view of X-ray Diffractometer	40
Fig. 3.14	Field emission scanning electron microscope for fractographic examination	41
Fig. 3.15	TGA/DTA instrument for determining weight loss of a material	42
Fig. 3.16	FTIR instrument for obtaining infrared spectrum of a material	43
Fig. 3.17	The Vicat's apparatus for measuring consistency of cement	44
Fig. 3.18	The Vicat's apparatus showing setting time of a blended cement	45
Fig. 3.19	Flow table for determining mortar flow	46
Fig. 3.20	Mortar cubes for lime reactivity	46
Fig. 3.21	Experimental setup of Fratini test	47
Fig. 3.22	TAM air isothermal calorimeter for hydration kinetics	48
Fig. 3.23	Le Chatelier's flask of determining specific gravity of blended cement mixes	49
Fig. 3.24	Le Chatelier's apparatus for soundness of blended cement mixes	49

Fig. 3.25	The experimental setup for determining pH of blended mixes from pH meter	50
Fig. 3.26	M3500 viscometer for determining rheology of a blended cement paste	51
Fig. 3.27	Universal testing machine for compressive strength of paste	51
Fig. 3.28	Compressive strength of specimens	52
Fig. 3.28 (a)&(b)	Casting of mortar cubes for different blended cements	52
Fig. 3.28 (c)&(d)	Mortar testing on compressive testing machine	52
Fig. 4.1	Fratini curve showing pozzolanic reactivity of pozzolana	54
Fig. 4.2	Particle size distribution curve of Portland cement and various cementitious binders	57
Fig. 4.3	Particle size distribution curve of cementitious binder (calcined clay and GGBFS) containing different percentage of thermo-chemically activated lime sludge	57
Fig. 4.4	XRD of lime sludge based cementitious binders	60
Fig. 4.5	FTIR of unhydrated cementitious binder with varying GGBFS, calcined clay and lime sludge	61
Fig. 4.6	SEM images of lime sludge based cementitious binder	62
Fig. 4.6 (a)	Portland cement	62
Fig. 4.6 (b)	Sample 1	62
Fig. 4.6 (c)	Sample 2	62
Fig. 4.6 (d)	Sample 3	62
Fig. 4.6 (e)	Sample 4	63
Fig. 4.7	EDAX analysis of Portland cement and thermo-chemically activated lime sludge based cementitious binders	63

Fig. 4.7 (a)	Portland cement	63
Fig. 4.7 (b)	Sample 1	63
Fig. 4.7 (c)	Sample 2	64
Fig. 4.7 (d)	Sample 3	64
Fig. 4.7 (e)	Sample 4	64
Fig. 4.8	TGA/DTG curve of sample 1	67
Fig. 4.9	TGA/DTG curve of sample 2	67
Fig. 4.10	TGA/DTG curve of sample 3	68
Fig. 4.11	TGA/DTG curve of sample 4	68
Fig. 4.12	TGA/DTG curve of OPC 43 cement	69
Fig. 4.13	A general flow behaviour of cement paste	69
Fig. 4.14	Shear stress versus shear rate graph of blended cement pastes and OPC 43 cement paste	70
Fig. 4.15	Viscosity versus shear rate of blended cement pastes and OPC 43 cement paste	71
Fig. 4.16	Hysteresis loop of shear stress versus shear rate	72
Fig. 4.16 (a)	OPC 43 cement paste	72
Fig. 4.16 (b)	Blended cement with 15% LS	72
Fig. 4.16 (c)	Blended cement with 30% LS	72
Fig. 4.17	Yield stress versus lime sludge content	73
Fig. 4.18	Shear stress versus shear rate of lime sludge based binder for different superplasticizer doses	73
Fig. 4.19	General representation of hydration of cement paste	74

Fig. 4.20	Normalised heat flow versus time curve of lime sludge based binder with different pozzolana	76
Fig. 4.21	Normalised heat versus time curve of lime sludge based binder with different	76
Fig. 4.22	Normalised heat flow versus time curve of lime sludge based binder with varying lime sludge and pozzolana content	77
Fig. 4.23	Normalised heat flow versus time for optimised mix with varying lime sludge content	77
Fig. 4.24	Normalised heat versus time for optimised mix with varying lime sludge content	78
Fig. 4.25	Compressive strength versus time graph for lime sludge based binder with different pozzolana	83
Fig. 4.26	Compressive strength versus time graph for lime sludge based binder with varying lime sludge and pozzolana content.	83
Fig. 4.27	Compressive strength versus time graph for lime sludge based binder with varying lime sludge content	84
Fig. 4.28	FTIR spectra of hydrated cementitious binders	85
Fig. 4.29	TGA curve of hydrated cement paste	85
Fig. 4.30	TGA curve of hydrated lime sludge based binder	86
Fig. 4.31	FE-SEM images of hydrated cementitious binder	86
Fig. 4.31 (a)	Portland cement	86
Fig. 4.31 (b)	lime sludge based binder	86
Fig. 4.32	Product Life Cycle	88
Fig. 4.33	Lime sludge based binder production in SimaPro 7.0	90
Fig. 4.34	OPC 43 cement paste production in SimaPro 7.0	91
Fig. 4.35	LCA of blended cement and OPC 43 cement	92

## LIST OF TABLES

Table 2.1	Chemical composition of Indian lime sludge	12
Table 2.2	Particle size distribution of Indian lime sludge	12
Table 2.3	Mineralogical composition of Indian lime sludge	13
Table 3.1	Physical characteristics of raw lime sludge	28
Table 3.2	The chemical composition of raw lime sludge, calcined clay, GGBFS and fly ash	31
Table 3.3	The particle size distribution of raw lime sludge, calcined clay and limestone	32
Table 3.4	Physical characteristics of calcined clay	33
Table 3.5	Blended cement mixes for optimisation	37
Table 3.6	Blended cement mixes for final investigations	38
Table 3.7	Blended cement mixes with variation of lime sludge and pozzolana	38
Table 4.1	Lime reactivity of pozzolana with lime sludge	53
Table 4.2	Fratini test results for pozzolanic materials	55
Table 4.3	Blaine surface area of lime sludge based cementitious binders	56
Table 4.4	Particle size distribution of lime sludge based cementitious binders	58
Table 4.5	Chemical composition of lime sludge based cementitious binders with different pozzolana	59
Table 4.6	EDAX analysis of lime sludge based cementitious binder and Portland cement	65



Table 4.7	Elemental composition of thermo-chemically activated lime sludge based cementitious binders and Portland cement	65
Table 4.8	Specific gravity of lime sludge based cementitious binders.	79
Table 4.9	Soundness of lime sludge based binder	80
Table 4.10	The pH of lime sludge based cementitious binders	80
Table 4.11	The initial and final setting time of lime sludge based blended cements	81
Table 4.12	Comparative properties of lime sludge based binder and ordinary Portland cement	87
Table 4.13	Composition of lime sludge based cementitious binder in LCA	89
Table 4.14	Composition of OPC 43 cement paste	90
Table 4.15	Utilised inventories with data source in SimaPro 7.0	91



# CHAPTER 1

## INTRODUCTION

### 1.1 General

Cement is one of the main ingredient of concrete construction and second largest used material after water. Due to exponential growth of population in recent years, demand for construction increased and thus increase in cement demand, as shown in Fig. 1.1 (Department of industrial policy and promotion, 2016). However, production of cement is one of the most significant sources of greenhouse gases. About 8% of the total anthropogenic CO<sub>2</sub> emission is generated by cement industry, worldwide (Trends in global CO<sub>2</sub> emission, 2015). Production of one ton of cement emits approximately one ton of carbon-dioxide. The researchers are working to develop newer sustainable cementitious materials by replacing cement clinker with other industrial by-products having pozzolanic properties and hydraulic activity as supplementary cementitious materials/ newer binder (Khatri *et al.*, 1995, Toutanji *et al.*, 2004, Segui *et al.*, 2012). Some of the successfully used industrial wastes as supplementary cementitious materials are fly ash, ground

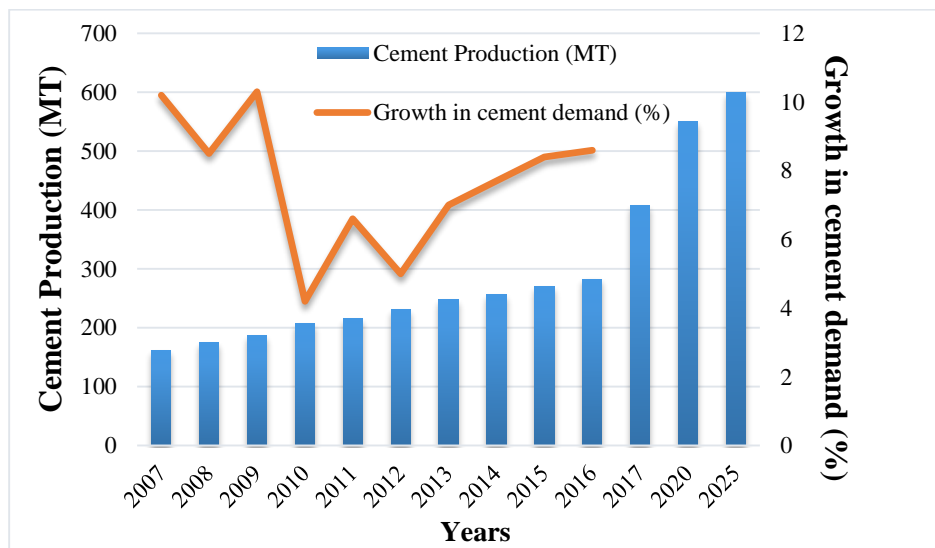


**Fig. 1.1: Cement production and growth in cement demand with respect to years (Department of Industrial Policy & Promotion, 2016)**

granulated blast furnace slag, silica fume, etc. which offers benefits like potential savings in natural resources and energy, reduction in CO<sub>2</sub> emission including reduction in landfill hazard. One such industrial by-product is lime sludge.

In India, every year about 300 million tons of industrial waste is generated from the agro-industrial processes out of which about 4.5 million tons of lime sludge is generated (Garg and Singh, 2005 and CPCB, 2006). Lime sludge is generally obtained from paper, acetylene, sugar, fertilizer, soda ash and sodium chromate industries.

India produces about 2.6% of the world's paper and out of that 45% is the sludge produced. Raw materials that are used for production are wood, bamboo, straw and agricultural waste (CRI-ENG-SP 965, 2000). Paper sludge generally consists of organic cellulose fiber material and inorganic clay material. This is disposed of either directly to landfill or after incineration reducing the amount of sludge but still a considerable sludge is available for disposal. Paper sludge consists of lime in the form of calcium carbonate which after processing can be used in construction industry by partial replacement of cement (CRI-ENG-SP 965, March 2000, National Council for Cement and Building Materials)

After incinerating lime sludge in the range of 650 °C – 900 °C, the resultant calcined material may contain reactive lime (CaO) which contributes chemically to the Portland cement ingredient (CPCB, 2006). Lime sludge is therefore potentially suitable as an ingredient in the cement kiln feed, contributing calcium and silica for the manufacture of blended cements.

Potential uses of lime sludge in construction products include use in board products such as plasterboard, alternative fuels for cement manufacture and brick manufacture. The main limiting factor is the difficult nature of the material's physical properties and its high moisture content. Improper disposal of these wastes on land lead to unproductive land for vegetation also possible degree of contamination of ground and surface water.

Owing to such a high volume of waste and its potential for re-use, the construction industry presents a large forefront in recycling and reusing of lime sludge which shall not only solve the waste management problem, but may also serve as new resource for construction industry.

## **1.2 Objectives**

After extensive literature review it can be concluded that lime sludge can be used to develop a new binder and can be utilized for making a mortar and concrete, which will utilize waste product and reduce CO<sub>2</sub> emission and hence is a sustainable technology.

The objectives of the present study is to develop newer cementitious binder by partial replacement of ordinary Portland cement clinker with lime sludge (paper industry waste), calcined clay (metakaolin) and ground granulated blast furnace slag (GGBFS).

## **1.3 Scope of the study**

The study involves experimental investigations on development of newer cementitious binder from lime sludge and its use in cement-sand mortar. The scope of the study envisages are as under:

1. Characterization and processing of lime sludge:  
pH, moisture content, chemical composition, and hydraulic reactivity.
2. Lime sludge based cementitious binder and its hydration studies
3. Formulation of binders with other pozzolanic materials along with its hydration kinetics, phase analysis and microstructure of hydrated paste (XRF, XRD, SEM, TGA/DTA), setting time, soundness, fineness, pH, rheology, water absorption, and strength development.
4. Mortar based on developed lime sludge based binder:  
Mortar flow, compressive strength.
5. Life cycle assessment of developed cementitious binder.

## **1.4 Methodology**

The methodology adopted in present investigations to develop a blended cement having cement clinker with lime sludge, calcined clay and GGBFS to reduce clinker factor and utilise waste from industry. The methodology is illustrated as below:

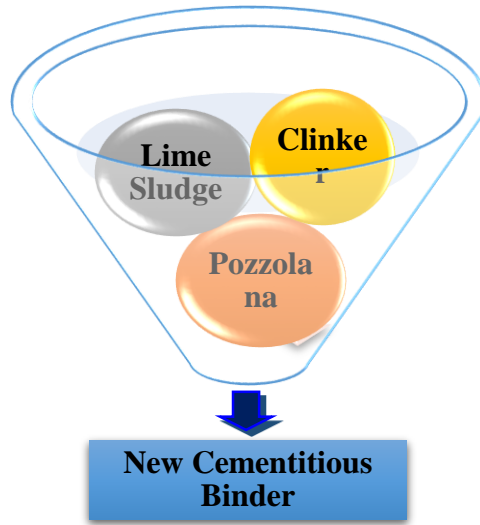


**Fig. 1.2: Methodology for development of new lime sludge based cementitious binder**

## 1.5 Organisation of thesis

A thesis is structured into 5 chapters. A brief description of each chapter is given below:

**Chapter 1:** This chapter deals with the introduction of the subject.

**Chapter 2:** This chapter describes a detailed literature survey on cementitious binders with reference to the application in mortars and concrete. The chapter throws light on general background of building lime and lime sludge, cementitious binders and research and development trends. Based on this, identification of research gaps and statement of problem is discussed.

**Chapter 3:** This chapter deals with the experimental details of the project. This includes characterisation of raw materials, optimization of proportioning, preparation of pastes and mortars and their physio-mechanical and microstructural characterization methods.

**Chapter 4:** This chapter deals with characterisation, initial flow, compressive strength and microstructural details of new cementitious binder.

**Chapter 5:** This chapter describes the conclusion drawn from the study along with future scope of work.

The references are presented at the end of the thesis.

# CHAPTER 2

## LITERATURE REVIEW

### 2.1 General

Lime is a material which is extensively used as a building material for over thousand years. It is often used in the form of lime wash, lime mortars, renders, plaster etc. Lime is generally used for the repair of heritage buildings, it is preferred because it is vapour permeable and reduces the risk of trapped moisture. Free lime absorbs carbon dioxide in its setting process. Lime binders are durable and have stood the test of time, certain examples are Pantheon Temple in Rome for 2000 years (Fig. 2.1) and Caesar's Tower at Warwick Castle for 600 years (Holmes, 2002) Charminar in Hyderabad for 426 years (Fig. 2.2) was made by using lime mortar and many such ancient buildings are there that are made using lime. Lime is obtained from a natural resource called limestone, it is necessary to find an alternative to preserve natural resources for sustainable development. Lime sludge is a waste product that is obtained from many industries such as paper, sugar etc. It can be used as an alternative to limestone in building raw materials.

CO<sub>2</sub> pressures facing the construction industry and increasing demand of ordinary Portland cement are providing increasing emphasis to reduce the use of OPC as the primary binder

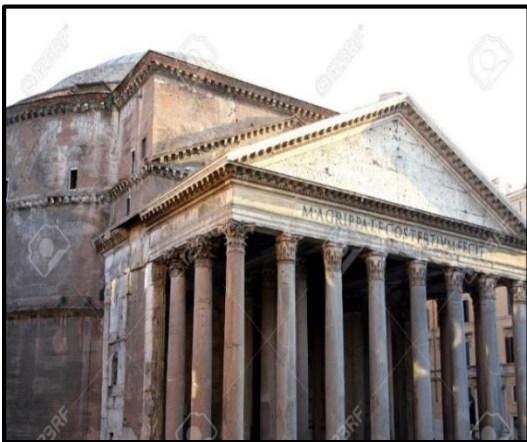


**Fig. 2.1: Pantheon Temple, Rome**



**Fig. 2.2: Charminar, Hyderabad**

phase in concrete. Reduction in OPC use can be obtained by replacing OPC with supplementary cementitious materials such as metakaolin, fly ash, slag (Falla *et al.*, 2015) also

waste products from other industries such as lime sludge, rice husk ash, paper sludge etc. Many researchers have worked on using supplementary cementitious materials for making blended cements. Extensive work has been done on limestone calcined clay cement. This cement allows to reduce the clinker factor up to 50% (Emmanuel, 2015).

## **2.2 Building Lime**

The term "lime" comes from the word limestone. Limestone rocks were converted to lime powder by burning (calcination). Lime is extensively used in building and roads, lime concrete, mortar and plaster, stabilised bricks, autoclaved calcium silicate bricks (sand-lime bricks), flyash-sand lime bricks, and cellular concrete. The BIS has formulated a comprehensive IS specification on building lime in 1973 as per IS: 712 and then later 3<sup>rd</sup> revision was done in 1984. Lime is a versatile chemical used in the paper industry for re-causticisation and as precipitated calcium carbonate for producing alkaline paper, for distemper and white washing, for water and effluent treatment and possess many other uses.

### ***2.2.1 Classification and Application of Building Limes***

The classification of lime sludge as per IS: 712-1984 is as under:

Class A - Eminently hydraulic lime used for structural purposes.

Class B - Semi-hydraulic lime used for masonry mortars, lime concrete and plaster undercoat.

Class C - Fat lime used for finishing coat in plastering, whitewashing, composite mortars, etc. and with addition of pozzolanic materials for masonry mortar.

Class D - Magnesium/dolomitic lime used for finishing coat in plastering, white washing, etc.

Class E - *Kankar lime* used for masonry mortars.

Class F - Siliceous dolomitic lime used for undercoat and finishing coat of plaster.

### ***2.2.2 Lime Production Technology***

The calcination of lime takes place through the chemical reaction:



The reaction takes place at around 900 °C, at which uncontrollable reactions may take place. Optimum heat and temperature at the proper place and time is very important to render the



process energy efficient. It is also necessary to avoid the retention time of lime at the highest temperature in order to avoid the ill-effects of excessive heat which produces dead burnt lime.

Building lime specifications also stipulate the low limits of sulphate, phosphate, chloride and magnesium oxide, but permit quite high percentages of silica (SiO<sub>2</sub>), alumina (Al<sub>2</sub>O<sub>3</sub>), and iron oxide (Fe<sub>2</sub>O<sub>3</sub>). The lime made of kankar, an earthen limestone, contains 25 to 30% of SiO<sub>2</sub>+ Al<sub>2</sub>O<sub>3</sub>+ Fe<sub>2</sub>O<sub>3</sub> and still considered as a good building lime.

The quality of lime produced depends on the rate of calcination, the nature of the limestone and the fuel, the suction created by the natural draught of the kiln and the maximum temperature achieved in the kiln. In 1970s, CSIR-Central Building Research Institute (CBRI), Roorkee introduced an improved design – a partially mechanised vertical shaft kiln lined with the refractory bricks, together with the check on the size of limestone and coal for 10 to 15 tons of lime production per day (Fig. 2.1). The kiln is provided with masonry shaft with RCC columns and rings. Expansion joints in the masonry have been provided to avoid cracking tendency in such type of structures as thermal expansion is bound to occur during calcinations operations.

The Bureau of Indian Standards brought out codes of practice for production of limes (IS: 1849 and IS: 1861). The lime produced in kilns is quicklime which is an unstable product and has a very limited shelf life. This depends on the packaging, weather and storage conditions. It gets air slaked and carbonated with atmospheric moisture and carbon dioxide and renders it unsuitable for use. For most of the applications the quick lime is first converted into a more stable hydrated lime.



A lime hydrator of a capacity of 10 tons per 8 hour shift, capable of continuously hydrating quicklime at atmospheric temperature, was designed and developed at CSIR-CBRI in 1975-76. An innovative single-tier lime hydrator was developed as shown in Fig. 2.2. Hydrated lime for building requires controlled chemical reactivity and plasticity.

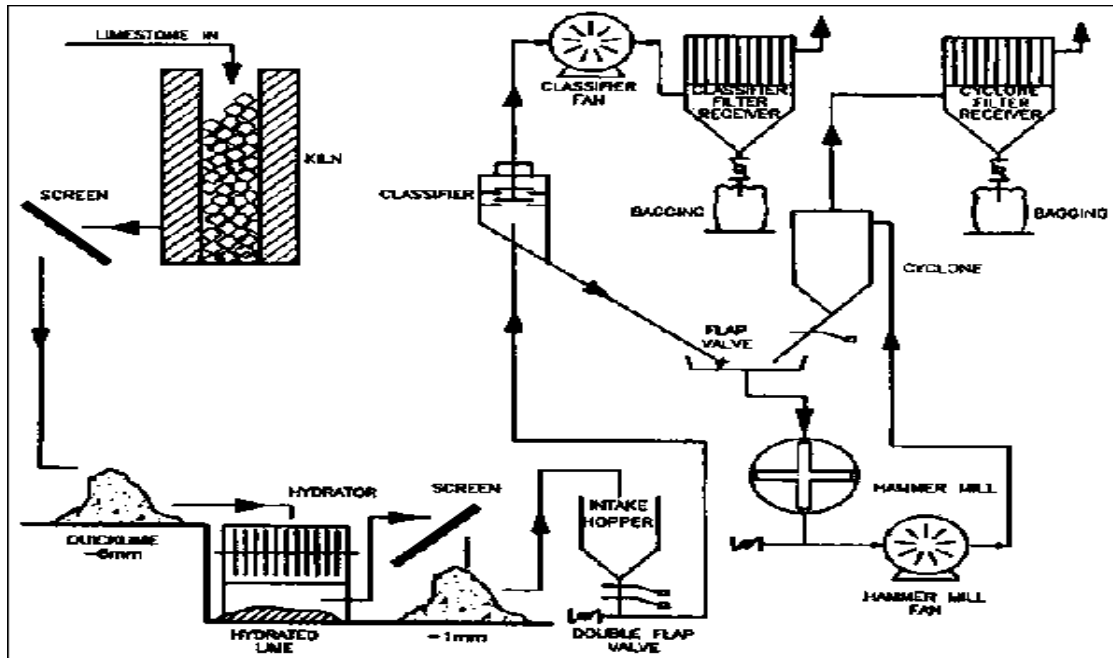


Fig. 2.3: A Partially Mechanized Vertical Shaft Lime Kiln (Energy Efficiency in Construction, 1995)

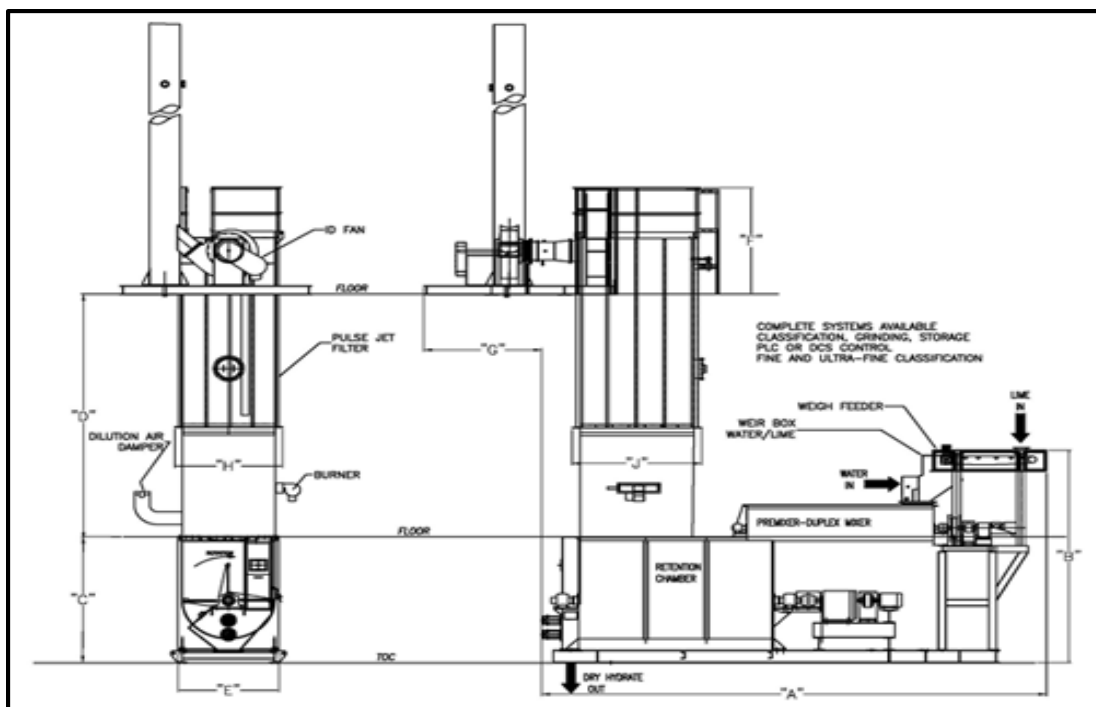


Fig. 2.4: An Innovative Single-Tier Lime Hydrator (Jain *et al.*, 1993)

### ***2.2.3 Hydraulic Lime***

Hydraulic Lime is a term generally used for lime (CaO) or slaked lime (Ca(OH)<sub>2</sub>) that are used for making lime mortar, which sets through hydration. The term hydraulic lime covers materials that vary in properties such as setting times and strength development. Hydraulic lime is characterised by good workability, low shrinkage, and salt and frost resistance, adequate compressive and good flexural strength. The properties of hydraulic lime are influenced by the existence of certain impurities and by the methods of burning and slaking. Based on clay content hydraulic lime is categorised in three categories, these are: feebly, moderately and eminently hydraulic lime (Vicat, 1837).

***Feebly hydraulic lime:*** Normally contains 12% reactive clay. The putty will set like soft soap between 1 and 6 months, and the material can be knocked up for reuse.

***Moderately hydraulic lime:*** Normally contains 12% to 18% reactive clay. The putty will set like hard soap within 1 month, but can still be knocked up for reuse.

***Eminently hydraulic lime:*** Normally contains 18% to 25% reactive clay. The putty will set hard in less than a week.

The more hydraulic the limes the harder and more impervious will be the resulting mortar. While using lime for the conservation of historic buildings care should be taken to match the properties of the mortar to the characteristics of the stone as well as to the degree of exposure on site. Lime has been known to mankind since the time of ancient civilization. It finds extensive application in building and in numerous chemical and other industries.

Most of the uses to which lime is put are such which require that quicklime should first be converted into the form of hydrated lime. Hydrated lime can be produced as dry hydrate, putty, slurry or lime water. The main distinguishing characteristic of which is the amount of excess water they contain.

According to hydraulic properties (setting under water and by reaction with CO<sub>2</sub> in the air) lime can be categorized as:

- Natural Hydraulic Lime (NHL): The hydraulic properties exclusively result from the chemical composition of the raw material. No additions are allowed (EN-459).

- Hydrated Hydraulic Lime (HHL): It is the US equivalent of the European NHL (ASTM C-141).
- Hydraulic Lime (HL): Consists of lime and other materials such as cement, blast furnace slag, fly ash, limestone filler and other suitable materials (EN-459).
- Formulated Lime (FL): Consists mainly of hydrated lime and or NHL with added hydraulic and/or pozzolanic material (EN-459).
- Pozzolanic Hydraulic Lime (PHL): Consists mainly of hydrated lime with one or more pozzolana with possible inclusion of inert filler. When cement is present even in traces (can be up to 20% of binder weight), it is labelled as PHL (ASTM C-1707).

Benefits of using lime as building material are:

- Walls breathe better and moisture can evaporate easier.
- Expansion joints can be avoided.
- Insulation is improved and cold bridging reduced.
- No risk of salt staining.
- Alterations can be carried out easily and masonry units can recovered later.
- Masonry life was increased.
- CO<sub>2</sub> emissions in the manufacture of lime less than cement and during carbonation the mortars and renders reabsorb considerable quantities of CO<sub>2</sub> from the atmosphere.

### **2.3 Lime Sludge**

Limestone is the most widely used mineral in the chemical industry and generally one of the by-products/wastes from these chemical industries is a lime bearing sludge. Lime sludge is generated from paper, acetylene, sugar, fertilizer, sodium chromate and soda ash industries. All the lime sludge other than carbide sludge contains lime as calcium carbonate. The carbide sludge from acetylene industry mainly contains lime as calcium hydroxide. This sludge essentially contains lime as major constituent. However, their chemical compositions vary considerably depending upon the composition of limestone used in the parent process as shown in Table 2.1. The particle size distribution and mineralogical composition of India lime sludge are shown in Table 2.2 and Table 2.3 respectively (CPCB, 2006).

All sludge contain some deleterious constituents/ contaminants, which come from the process through which they are generated, e.g. the phospho-chalk from fertilizer industry contains 5-9%  $\text{SO}_3$ , 1.5%  $\text{P}_2\text{O}_5$  and 2% fluoride as major contaminants. Similarly, paper, sugar and chromium sludge contain free alkalies up to 2%. The chromium sludge and carbide sludge in addition also contain chromium up to 10% and chloride up to 2% respectively. The presence of these deleterious constituents/ contaminants restricts their bulk utilization in making cement and related building materials (CPCB, 2006). Detailed investigations were carried out on the utilization of lime sludge from various industries. The study has revealed that sludge from paper industry can be utilized up to 74% (dry basis) as a component of raw mix for the manufacture of cement clinker. In addition to it around 30% (dry basis) lime sludge can also be utilized for the manufacture of masonry cement. Due to the presence of deleterious constituents in higher quantities carbide sludge can be used only up to 30% whereas level of utilization for other sludge could reach to only 10% in the manufacture of cement clinker. The sludges are disposed of wet in the form of slurry/filter cake into lagoons/settling tanks and is considered potential health and environmental hazards.

### ***2.3.1 Types of Lime Sludge***

Based on the process of generation, lime sludge can be categorised as:

- a) Paper Sludge
- b) Sugar Sludge
- c) Carbide Sludge
- d) Chromium Sludge
- e) Phospho-chalk
- f) Soda Ash Sludge

Table 2.1 shows the chemical composition of Indian lime sludge and Table 2.3 shows the mineralogical composition of Indian lime sludge. Fineness and particle size distribution of slurries varies dewatering and sedimentation characteristics. Also, these characteristics vary with their chemical contaminants. Particles size distribution of Indian lime sludge is shown in Table 2.2.

**Table 2.1: Chemical Composition of Indian Lime Sludge (CPCB, 2006)**

Constituents	Paper %	Phospho-chalk %	Carbide %	Sugar %	Chromium %	Soda Ash %
<b>LOI</b>	35-40	34-38	25-30	40-50	20-35	34-38
<b>CaO</b>	45-50	45-50	60-70	42-50	35-40	44-48
<b>Al<sub>2</sub>O<sub>3</sub></b>	2-5	0.3-0.5	1-3	2-2.5	3-5	1.5-3.0
<b>Fe<sub>2</sub>O<sub>3</sub></b>	1-1.5	0.3-0.5	0.1-0.25	2-2.5	-	1-2
<b>SiO<sub>2</sub></b>	4-6	3-5	4-6	1.5-4.5	4-6	4-7
<b>SO<sub>3</sub></b>	-	5-9	0.2-0.3	1-2	-	-
<b>P<sub>2</sub>O<sub>5</sub></b>	-	1-1.05	Trace	-	-	-
<b>F<sup>-</sup></b>	-	1-2	-	-	-	-
<b>Cl<sup>-</sup></b>	-	-	0.2	-	-	6-10
<b>MgO</b>	1.5-2.0	-	0.2-0.5	4-10	3-6	1-2
<b>Na<sub>2</sub>O/K<sub>2</sub>O</b>	0.5-1.5	-	0.02-0.2	1-2	1-1.8	-
<b>Cr<sub>2</sub>O<sub>3</sub></b>	-	-	-	-	8-10	-

**Table 2.2: Particle Size Distribution of Indian Lime Sludge (CPCB, 2006)**

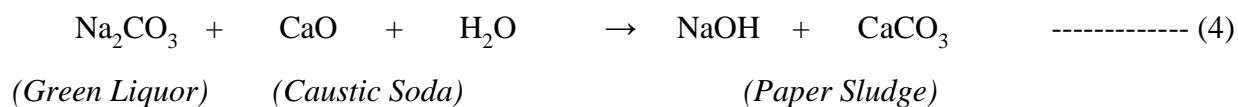
Particle Size (microns)	Paper Sludge %	Fertiliser Sludge %	Carbide Sludge %	Sugar Sludge %	Chromium Sludge %	Soda Ash Sludge %
+90	2	2	-	6	4	6
-90 + 45	8	60	8	8	12	16
-45 + 30	10	20	62	40	12	42
-30 + 10	72	12	20	24	60	26
-10 + 5	8	4	6	16	8	6
-5	-	2	4	6	4	4

**Table 2.3: Mineralogical Composition of Indian Lime Sludge (CPCB, 2006)**

S. No.	Sludge	Mineralogical Composition		Deleterious Constituents Present
		Minor Phase	Major Phase	
1.	Paper Sludge	Calcite	$\alpha$ -quartz, silicate	Phosphates, Fluorides, Ammonia
2.	Phospho-chalk	Calcite	$\alpha$ -quartz, silicate	Alkalies, Chloride
3.	Carbide Sludge	Calcium hydroxide	$\alpha$ -quartz, silicate	Alkalies, Chloride
4.	Sugar Sludge	Calcite	$\alpha$ -quartz, silicate	Sulphite, Organic Matter
5.	Chromium Sludge	Calcite	Chromium, Ferrite	Chromium, Alkalies
6.	Soda Ash Sludge	Calcite	$\alpha$ -quartz, silicate	Chloride

### 2.3.1.1 Paper Sludge

The principal process for producing chemical pulps in paper industries is the Kraft process; where the mixtures of sodium sulphide and sodium hydroxide are used as pulping chemicals. The production process of paper sludge is shown in Fig.2.5 (NPTEL, Lecture 26, and Chemical Technology II). In the process, calcined lime is used for regeneration of caustic soda by conversion of soda ash (green liquor) leaving behind calcium carbonate sludge as a waste.



Calcium carbonate thus produced is washed with water and filtered to recover alkalies. Various properties of paper sludge is identified by many researchers such as Thomsaet *al.*, (1987), Liawet *al.*, (1998), Boniet *al.*, (2004), Fava *et al.*, (2011), Maheswaran (2011), Lisbonaet *al.*, (2012) Xu *et al.*, (2014) and Abdullah *et al.*, (2015).

### 2.3.1.2 Sugar Sludge

Sugar sludge commonly known as press mud, a by-product from the sugar industries is obtained during the carbonation process as calcium carbonate. In the sulphate process, the sludge mainly

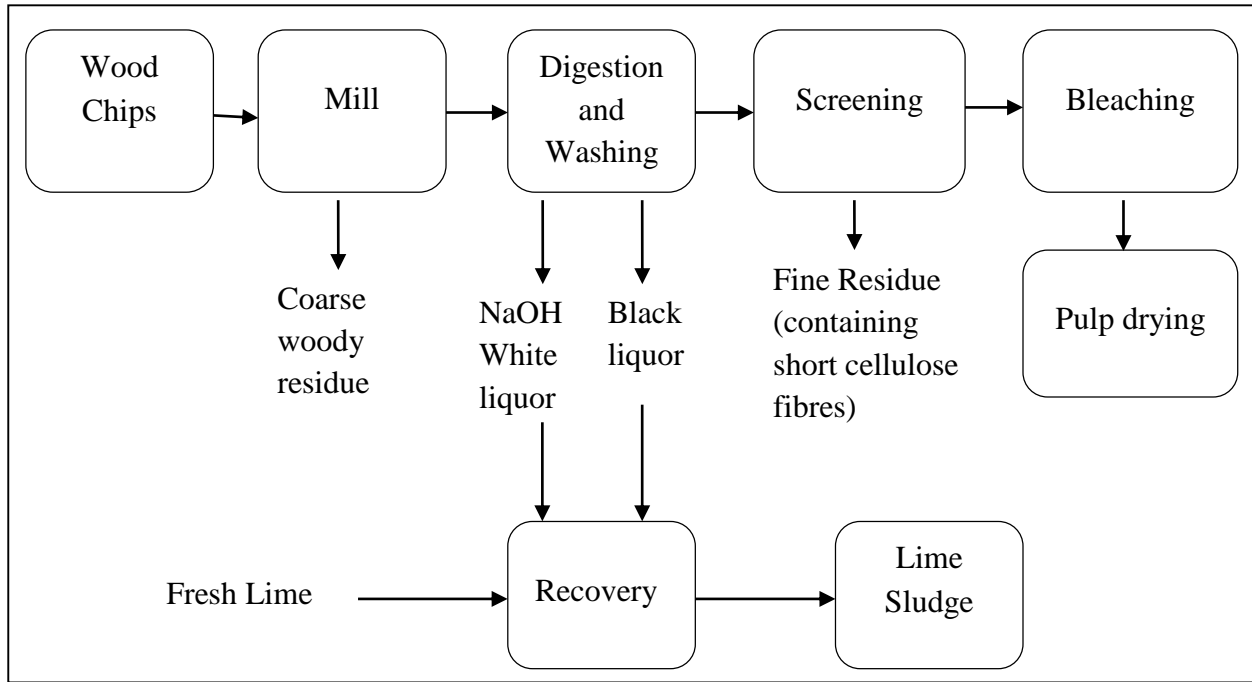
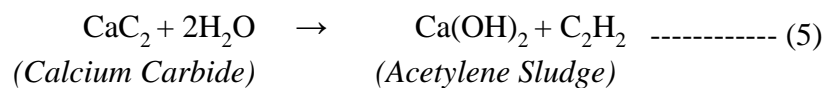


**Fig. 2.5: Production Process of Lime Sludge**

contains calcium sulphate and is generally used as a fertilizer. The carbonate sludge is disposed of wet with solid content ~10%.

### 2.3.1.3 Carbide Sludge

Calcium carbide is manufactured by the interaction of limestone and carbon as a starting material for the manufacture of acetylene gas in acetylene industries. Most carbide acetylene processes are wet processes from which hydrated lime,  $\text{Ca(OH)}_2$ , commonly known as a sludge is obtained as a by-product.



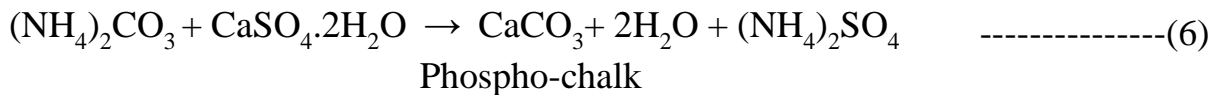


### **2.3.1.4 Chromium Sludge**

Chrome ore (chromite  $\text{FeO}\cdot\text{Cr}_2\text{O}_3$  i.e. 68%  $\text{Cr}_2\text{O}_3$ , 32%  $\text{FeO}$ ) is calcined with limestone and soda ash and digested with water to extract soluble chromium salts and the resultant residue is rejected as the carbonated sludge. The sludge generally contains soluble chromium salts and is considered deleterious for the environment and therefore it is generally converted to insoluble salts before disposal.

### **2.3.1.5 Phospho-Chalk**

Calcium carbonate sludge, generally known as phospho-chalk is a by-product waste obtained in the process of manufacture of ammonium sulphate, through the reaction of carb liquor and phospho-gypsum (a by-product from the phosphoric acid manufacture) in the fertilizer industries.



### **2.3.1.6 Soda Ash Sludge**

Lime bearing sludge is also generated from soda ash manufacturing industry. The soda ash sludge essentially contains calcium carbonate with associated impurities of sulphide and chloride depending upon the process of manufacture.

### **2.3.2 Applications of Lime Sludge**

1. As a raw material for the manufacture of cement
2. Manufacture of lime pozzolana bricks/ binders
3. For recycling in parent industry
4. Manufacture of building lime

### **2.3.3 Theory of calcination**

Manufacture of lime involves thermal decomposition of calcium carbonate under certain conditions of temperature and pressure. The dissociation of  $\text{CaCO}_3$ , the main chemical compound in lime sludge takes places as per reaction:



The reaction indicates that for one gram molecule of  $\text{CaCO}_3$ , it is necessary to spend 42.53 kcal heat. Accordingly for obtaining one kg of lime ( $\text{CaO}$ ) from  $\text{CaCO}_3$ , the heat energy required will be about 750 Kcal which includes energy for dissociation as well as that needed to bring to the threshold state of dissociation. The mechanism of calcium carbonate decomposition is as follows:

- a) When heating a cube of calcium carbonate from room temperature to calcining temperature, it first expands prior to dissociation.
- b) Surface calcination, starts, the pore volume increase, and the sample volume remain constant.
- c) When calcination is complete, the sample has the maximum pore volume and simple volume is still largely unchanged.
- d) With further temperature increase and longer calcination limes, crystals grow and sintering begins, both pore volume and sample volume decrease. The dissociation temperature of  $\text{CaCO}_3$  can vary from 800-1000°C.

*Parameters affecting Calcination:*

- a) When heating a cube of calcium carbonate from room temperature to calcining temperature, it first expands prior to dissociation.
- b) Surface calcination, starts, the pore volume increase, and the sample volume remain constant.
- c) When calcination is complete, the sample has the maximum pore volume and simple volume is still largely unchanged.
- d) With further temperature increase and longer calcination limes, crystals grow and sintering begins, both pore volume and sample volume decrease. The dissociation temperature of  $\text{CaCO}_3$  can vary from 800-1000°C.

## **2.4 Calcined Clay**

Calcined clay consists of various clay minerals which is suitable for substitution of cement as a pozzolanic material which will reduce  $\text{CO}_2$  emissions. It is easily available and has low carbon content which will lead for production of sustainable concrete. Calcined clay is

anhydrous aluminium silicate. The pozzolanic reactivity of calcined clay is in the increasing order of illite, montmorillonite, and kaolinite. Calcined clay leads to depletion of portlandite and promote the formation of additional CSH phases in the hydrated cement which will lead to pore refinement and denser microstructure (Trumer, 2015).

#### 2.4.1 Chemical Composition of calcined clay

The chemical composition of calcined clay is shown in Fig. 2.6. Calcined clay is mainly composed of  $\text{SiO}_2$  and  $\text{Al}_2\text{O}_3$  which will react with  $\text{CaO}$  from cement clinker.

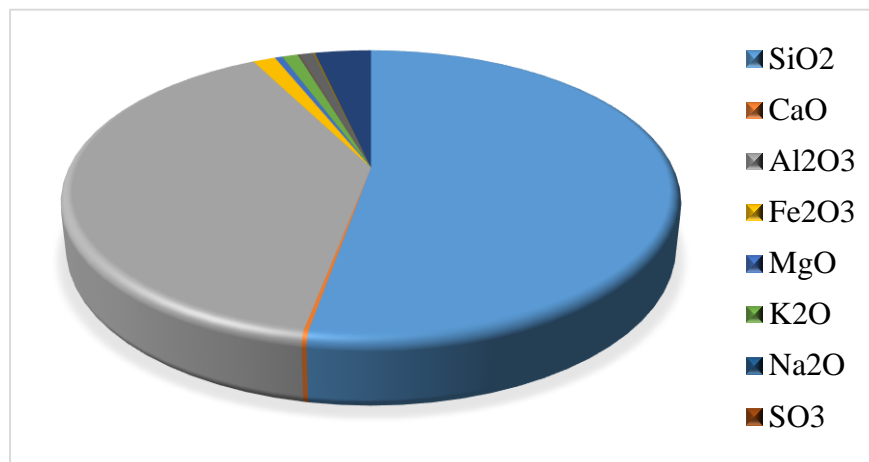


**Fig. 2.6: The chemical composition of calcined clay (Beuntner *et al.*, Danner *et al.*, Chatterjee A. K., Bao *et al.*)**

Calcined clay is produced by heating natural kaolin to high temperature in a kiln. At about  $700^\circ\text{C}$ , dihydroxylation of kaolin is completed and a poorly crystalline meta-kaolin (calcined clay) is formed which will act as a pozzolanic concrete additive. Due to reasonable aluminium content in calcined clay it will enhance the limestone reactivity in blended cement resulting in formation of  $\text{CO}_3\text{-AFm}$  (hemi- and/or mono-carboaluminate) (Falla, 2015). Ternary mixture of clinker, metakaolin and limestone seems to be beneficial in the reduction of carbonation.

In a chloride attacked concrete, when cement is replaced by 4% metakaolin in repair concrete it will lead to longer service life and will also reduce the  $\text{CO}_2$  emission by 50%. (Petcherdchoo, 2015). Calcined clay with lowest density are most de-hydroxylated which will result in highest

reaction potential. Thermal activation of any clay with 25% kaolin content is possible (Thienel, 2015).

## 2.5 Ground granulated blast furnace slag (GGBFS)

Ground granulated blast-furnace slag (GGBFS) is used with portland cement in concrete for many applications. Concrete made with GGBFS has many advantages such as workability, improved durability and economic benefits (ACI 233R-03). The drawback in the use of GGBFS in concrete is that the rate of hydration is slow and hence strength development is considerably slower than the Portland cement concrete under standard 20°C curing conditions, although for same water/binder ratio the ultimate strength is higher (Garcia *et al.*, 2001 and Roy *et al.*, 1982). Therefore, ground granulated blast-furnace slag is not used where high early age strength is required. Fig. 2.6 gives the chemical composition of GGBFS.

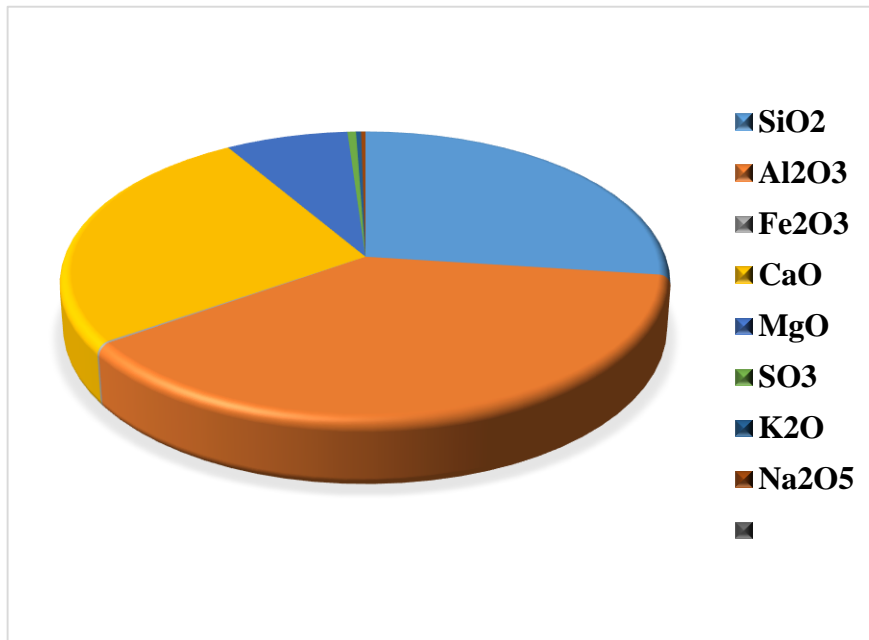


**Fig. 2.7: Chemical composition of GGBFS (Garcia *et al.*, Roy *et al.*, and Escalante *et al.*)**

The early strength development of GGBFS concrete can be achieved by curing at high temperature. As GGBFS content in cement increases, the w/c ratio for same workability increases. Therefore, GGBFS enhances the workability. The GGBFS content is optimised to 50-59% of total binder content till which compressive strength increases and more addition

will lead to decrease in compressive strength (Oner *et al.*, 2007). GGBFS improves the pore structure of concrete which reduces the chloride diffusion coefficient (Luo *et al.*, 2003). GGBFS in concrete are more durable than Portland cement concrete in aggressive environments under the action of salts and acids and the durability of concrete increases with increasing amounts of GGBFS. A more durable concrete mix for agricultural use in silos can be specified by incorporating GGBFS as a partial substitute for OPC (Pavia *et al.*, 2008)

## 2.6 Fly ash

Fly ash is a by-product of coal combustion. It is inexpensive and is widely available product. For the sustainable development it is necessary to reduce the use of natural resources such as limestone and clay. Fly ash is a waste product whose disposal is an issue, therefore it is a suitable for use as construction material. Fly ash is used as a partial replacement of cement to improve the workability of fresh concrete. When it replaces about 20-30% of cement, it will be effective in thermal cracking, sulphate attack or alkali silica expansion. (Mehta, 2004). Fly ash reduces the water cement ratio and also enhances the compressive strength of concrete. Fig. 2.7 shows the chemical composition of fly ash.

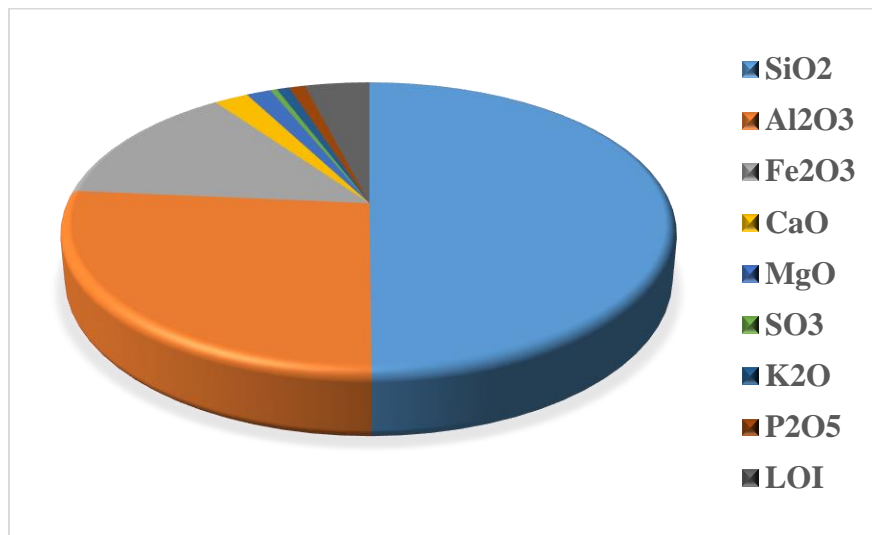


**Fig. 2.8: Chemical composition of fly ash (Mehta K., Hossain)**

Abrasion resistance of concrete mixtures with up to 35% cement replacement by fly ash had similar results of concrete without fly ash. Abrasion resistance of concrete beyond 35% cement

replacement, decreased slightly up to 55% cement replacement (Hossain, 1999). Chloride ion permeability at 91 days is highest with 35% replacement and it lowers with 45% replacement (ASTM C 1202). The paste with 30% replacement of cement with ultra-fine fly ash (Class C) has more refined structure than paste with 30% fly ash replacement of cement which will lead to high capillary pore pressure in ultra-fine fly ash cement paste, leading to more cracks and large crack area than paste with 30% fly ash replacement of cement.

## **2.7 Limestone**

Limestone is a sedimentary rock whose main constituent minerals are calcite and aragonite, which are different crystal forms of calcium carbonate. Limestone is used for making cement clinker along with clay. Limestone is extensively used in cement production for decades. It is also used as a filler in concrete.

Thongsanitgarn *et al.* (2011), studied that the compressive strength of Portland-limestone cement pastes decreased in all ages with an increasing amount of limestone due to the dilution effect. The limestone particle size has influence on the observed compressive strength values. It was confirmed that compressive strength increased with the fineness of limestone. From the standard consistency results, it seems that limestone has no effect on water requirement compared to Portland cement. Moreover, the increase in level of fine particles caused requires much water. Both initial and final setting time of Portland limestone cement pastes were decreased with an increasing of limestone content at the same fineness. At the same level replacement, the cement pastes using small-sized limestone show lower setting time than those using large-sized limestone.

Barrett *et al.* (2014), observed that ordinary Portland cement (OPC), Portland limestone cement (PLC) and PLC-slag systems had similar early age shrinkage, stress development, and cracking behaviour. While the PLCs have higher Blaine fineness values than OPC, they also have fewer very large cement particles and more very finely ground limestone particles. The PLCs therefore exhibit self-desiccation and a pore size distribution that does not increase shrinkage stresses at service level relative humidity.

Falchi *et al.* (2015), prepared water repellent mortars by using different hydrophobic compounds as admixtures. Calcium and zinc stearates, silane/siloxane products (as liquid

solution and powder) were mixed into limestone cement mortars for obtaining in-bulk water-repellent mortars suitable for building protection and resistant to the degrading action of water. Siloxane products conveyed good water repellent effectiveness, without strongly influencing the setting and hydration of the binder, while the zinc stearates slowed down the hydration reactions.

Diab *et al.* (2016), studied for short and long term, the use of limestone up to 10% had not a significant reduction in concrete properties. It is not recommended to use blended limestone cement in case of sulphate attack. The use of limestone cement containing up to 25% limestone has insignificant effect on corrosion resistance before cracking. The use of 10% limestone powder as cement replacement decreases SO<sub>2</sub>, NO<sub>x</sub>, CO, CO<sub>2</sub> and THC emissions by 10.2%. Also, the reductions of raw materials were 2.3% and 10.5% for limestone and clay, respectively. Additionally, the reductions of fuel and electricity were 10.5% and 4.8%, respectively.

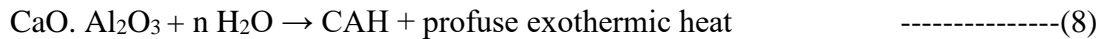
Tsivilis *et al.* (2000), studied the properties and the behaviour of limestone cement concrete and mortar. Portland limestone cements of different fineness and limestone content have been produced by inter-grinding clinker, gypsum and limestone. In order to have compatible results, the produced cements were selected to have the same level of strength. Portland limestone cement, containing up to 20% limestone, presents satisfactory concrete strength and workability, while the sorptivity and the chloride permeability seems to be similar to the pure cement concrete. Limestone cement concretes indicate lower resistance to freezing and thawing compared with the pure cement concrete. Portland limestone cement, containing 20% limestone, shows the optimum protection against rebar corrosion. Furthermore, the limestone additions decrease the carbonation depth and the total porosity of the mortar.

Torres *et al.* (2003), studied that mortar prisms made with Portland-limestone cement were stored in air and in 1.8% magnesium sulphate solution at 5°C and have been examined over a period of 5 years. The limestone content in the samples varied from 0% to 35%, but the water to cement plus limestone powder ratio was kept constant. The prisms stored in magnesium sulphate solution were all showing clear signs of deterioration, increasing in intensity with limestone content. The mortar prism with 5% limestone replacement was, however, degraded

in comparison with the ordinary Portland cement control prism; it was found that formation of thaumasite due to sulphate attack caused the degradation.

## 2.8 Gypsum

Gypsum is a soft sulfate mineral which is composed of calcium sulfate di-hydrate i.e.  $\text{CaSO}_4 \cdot 2\text{H}_2\text{O}$ . Gypsum is used in cement industry for controlling the rate of hardening of the cement. During the manufacturing of cement, after clinker is being cooled off, a small amount of gypsum is added during the final grinding process. Setting of cement is controlled by gypsum. If gypsum is not added to cement clinker it will lead to flash setting due to rapid hydration of calcium aluminate compound to form calcium aluminate hydrate (CAH). The heat released will make matrix stiff which will minimise the mixing process. Calcium aluminate hydrate will not contribute in strength development and will hamper the hydration of calcium silicate. Chemical reaction without adding gypsum is shown in equation (8).



Hence, it is important to change reaction course of  $\text{C}_3\text{A}$  which is achieved by adding sulphate salts. Aluminate tend to react with  $\text{SO}_3$  which will prevent its reaction with water (Bhanumathidas, 2004). Gypsum is also used for making boards and mortars in building construction.

## 2.9 Blended Cement

Blended cements are defined as hydraulic cements (ACI 116) which consists of intimate and uniform blending of number of different materials. Blended cements are made by inter-grinding and/or blending of Portland cement clinker with the other materials such as mineral admixtures/additives like GGBFS, silica fume and fly ash. Blended cements are widely used nowadays and their optimal and efficient use also offers economic benefits. They are being used for pavement and bridge deck constructions.

### 2.9.1 Advantages of Blended Cement

The advantages of blended cement can be classified into two categories:



- a) Technical advantages: Blended cements are finer than OPC which reduces the permeability of concrete and hence enhances durability. Also due to fineness, reactivity of cement also increases which leads to higher strength. The partial replacement of Portland cement clinker with other cementitious materials in different proportions can attain sulfate resistance and resistance to alkali silica reaction.
- b) Environmental advantages: Mineral admixtures that are waste products from steel and thermal plants are used in blended cement and hence conserve natural resources such as limestone etc. Blended cement reduces the clinker factor and hence CO<sub>2</sub> emission is reduced.

## 2.10 Global Research and Development Trends

Morsy S. M. (2005) studied the effect of temperature on hydration kinetics and stability of hydration phases of metakaolin-lime sludge-silica fume system, according to him the hardened pastes cured at 60°C possess higher values of compressive strength than that cured at 20°C. He used ratio of 1:1 for lime sludge and metakaolin. For both temperatures CSH was formed at an early stage but then C<sub>2</sub>ASH<sub>8</sub> (gelhenite) and C<sub>4</sub>AH<sub>13</sub> were formed, and then C<sub>3</sub>ASH<sub>6</sub> (hydrogarnet) was formed which is the predominant phase in the samples cured at 60°C which is responsible for strength gain at this temperature.

Xu W. *et al.* (2014) studied the utilization of lime-dried sludge (LDS) for producing cement. He utilized lime dried sludge <15% and observed that α-C<sub>2</sub>S phase formation increased with excessive LDS while the C<sub>3</sub>S structure decreased which results in a decreased compressive strength. Also, with the addition of trace elements from sludge, the clinker burn ability of cement clinker was lowered and with that the temperature required for liquid phase formation as well as for the acceleration of sintering process.

## 2.11 Research trends in India

Dave N. G. and Mehrotra S. P. (1992), suggested that due to shortage of cementitious materials and their increasing demand leads to increase in need of alternate cementitious materials such as carbide lime, GGBFS and fly ash for making high strength binders from waste. They checked properties of 3 binders and observed to have superior properties than ordinary Portland cement.

Pandey S. P., and Sharma R. L. (2000), studied the influence of mineral additives on the strength and porosity of OPC mortar, according to them addition of mineral additives in OPC increased porosity of mortar and decreased strength. When lime sludge was added with OPC and limestone it gave similar results of volume and overall histogram of pore range at 7 and 28 days as OPC due increase in rate of hydration.

According to Garg and Singh (2006), cementitious binder can be produced by blending industrial wastes such as fly ash, phosphogypsum plaster ( $\beta$ -hemihydrate), lime sludge with OPC in suitable proportions. For strength development of cementitious binders, Ettringite, CSH and Wollastontie were the major hydraulic products responsible. Also, with increase in curing period, water absorption and porosity of cementitious binders increased which indicated absence of leaching and increased level of stability towards water. Variation in strength development was observed at different temperatures i.e. 27 °C, 40 °C and 50 °C subjected to alternate wetting and drying cycles, it is due to variable hydration of binders. Also, when subjected to alternate heating and cooling cycles at 27 °C, 40 °C and 50 °C, strength decreases on increase in temperature and maximum fall of strength was observed at 50 °C.

Maheswaran S. *et al.* (2011), studied the partial replacement of cement with lime sludge. According to him, Sludge content of 10% or more cement replacement leads to decrease in concrete mechanical properties. Lime sludge was calcined at 750°C and properties for 10%, 20% and 30% replacement level was checked and it was observed that compressive strength and split tensile strength were decreasing with increasing replacement level.

Sahu V. and Gayathri V. (2014), studied the partial replacement of cement with lime sludge and fly ash in mortar. He observed that by increasing lime sludge and decreasing fly ash content in cement mortar, strength increased. It was observed that large amount of alumina and silica in fly ash and calcium oxide in lime sludge makes them compatible with each other and hence can replace cement to a large extent.

## **2.12 Research Significance**

The emission of carbon dioxide is a serious worldwide problem leading to greenhouse effects. One of the most important industries causing carbon dioxide emission is cement production. The utilisation of supplementary cementing materials (e.g. blast furnace slag, fly ash, silica

fume, natural pozzolana and limestone) is a well-known and advantageous strategy to reduce carbon dioxide emissions.

The lime sludge generated from the waste water treatment units of the paper mills is one of the major wastes in paper industry. Because of its large daily output and limited landfill space, although being classified as general commercial wastes, the waste has a tremendous adverse effect on the development of paper industry. Because the lime sludge consists of high calcium carbonate and moisture content, they can be recycled into constructional materials. Some domestic paper factories had developed the sludge incineration systems to reduce the amount of sludge and also to solve the problem of insufficient landfill sites. However, the sludge still contains 30% non-flammable materials which are collected in the form of ashes after incineration, and the amount is still considered sizeable.

### **2.13 National Need**

The increased tempo of constructional activities in the country and the short fall in cement production, have brought together the need of alternate cementing materials.

The concrete industry has been getting beat up for the past decade over the large carbon footprint of cement, and as cement manufacturing releases a significant amount of carbon dioxide into the environment. In India, there is enough limestone for the production of cement and lime but in various states such as J&K, Punjab, U.P, West Bengal, Bihar, Orissa, Kerala and large parts of Maharashtra do not possess enough limestone deposits and this restricts the growth of cement and lime industries. This calls for looking into use of various industrial wastes in making low cost cementitious binders and building blocks. One of the major possibilities is the use of mining and mineral wastes into making ready to use masonry mortars, bagged and supplied in the same manner as cement.

Also, with increase in the industrialization, waste generation is increasing. So, if this waste can be utilized in construction activities as building material so that CO<sub>2</sub> emission can be reduced with decrease in the problem of disposal of waste then a sustainable technology can be obtained that will decrease pollution by reducing amount of CO<sub>2</sub> and will be economic and will utilize a waste product.

## 2.14 Identified Research Gaps

Based on the literature review done in this chapter, following are the identified research gaps:

- a) Work has been reported to use lime sludge as filler to a level of 5-10% by weight in Portland cement.
- b) No work has been reported regarding the use of processed lime sludge (thermo-chemical activation) as an integral part of cement to make high strength cementitious binders. This may enhance the loading up to level of 30-40% by weight.
- c) Utilization of lime sludge in place of limestone in making Portland Limestone Cement is also the need of hour. Effort is needed in this direction.

## **CHAPTER 3**

### **EXPERIMENTAL INVESTIGATIONS**

#### **3.1 Introduction**

This chapter describes the material used for investigation, their processing and characterisation, fabrication of blended cements, casting and curing of cement paste and mortar, physical, calorimetric, microstructural studies and rheological characterisation of blended cement mixes.

#### **3.2 Materials**

##### ***3.2.1 OPC 43 grade cement clinker***

The OPC 43 grade cement clinker was procured from M/S Ultra Tech Cement Ltd., Dadri. The properties of clinker satisfies the all the requirements as per IS: 16353-2015. It is greyish black in colour. It has diameter between 10-25 mm. The photographic view of clinker is shown in Fig. 3.1



**Fig. 3.1: Photographic view of clinker**

##### ***3.2.2 Lime Sludge***

The lime sludge was procured from Ruchira Industries, Kala Amb, Himachal Pradesh. It is yellowish white in colour. Its main constituent is CaO which comprises of 85.5% of its composition. It has specific gravity of 3.076. About 90% of particles are finer than 68  $\mu\text{m}$ . The

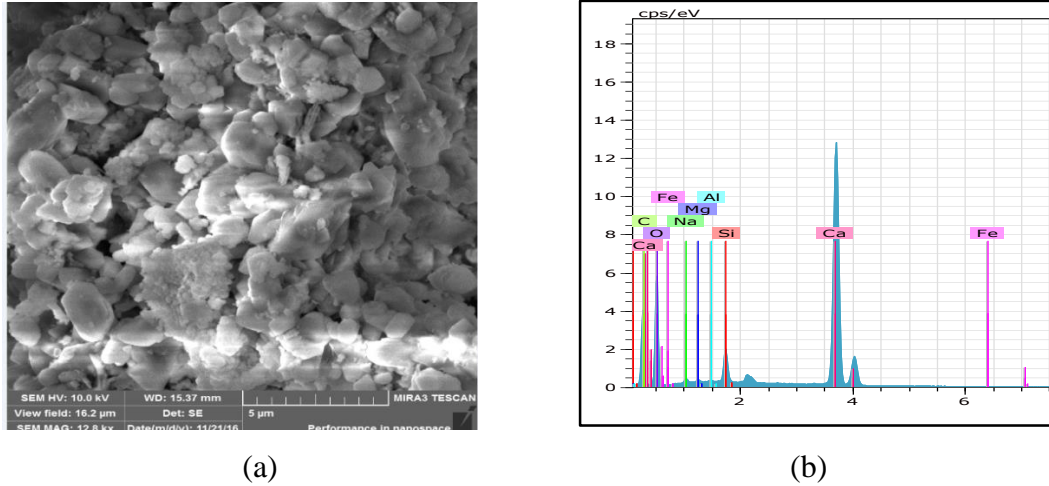
physical and chemical properties of lime sludge are shown in Table 3.1 and Table 3.2 respectively. Fig. 3.2 shows raw lime sludge from paper industry. Table 3.3 shows the particle size distribution of raw lime sludge. Raw lime sludge from paper industry contains 48% water content. Fig. 3.3 (a) shows the elemental analysis of lime sludge which shows presence of calcium and silica element and Fig. 3.3 (b) shows the SEM image of raw lime sludge. The particles are irregular in shape and seem to be non-segregated. Fig. 3.4 shows the XRD of raw lime sludge which shows the presence of calcite in lime sludge.

**Table 3.1: Physical and chemical characteristics of raw lime sludge**

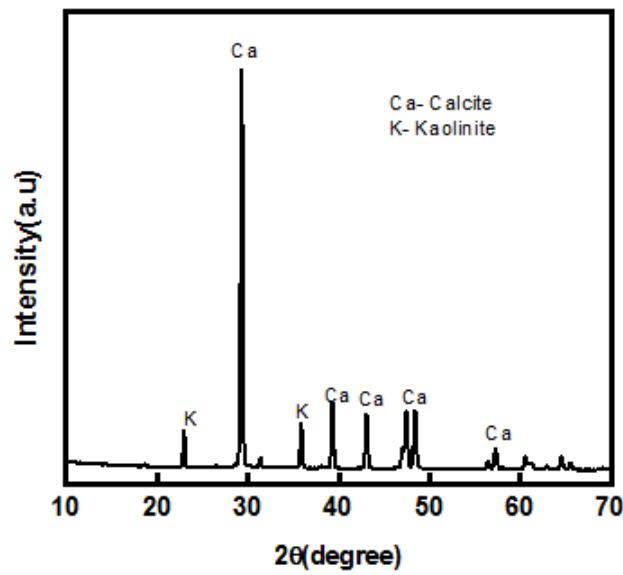
Property	Value
Refractivity	1.65
Colour	Pale white
Specific Gravity	3.076
Water Content	48 %
pH	12.72



**Fig. 3.2: Raw lime sludge from paper industry**

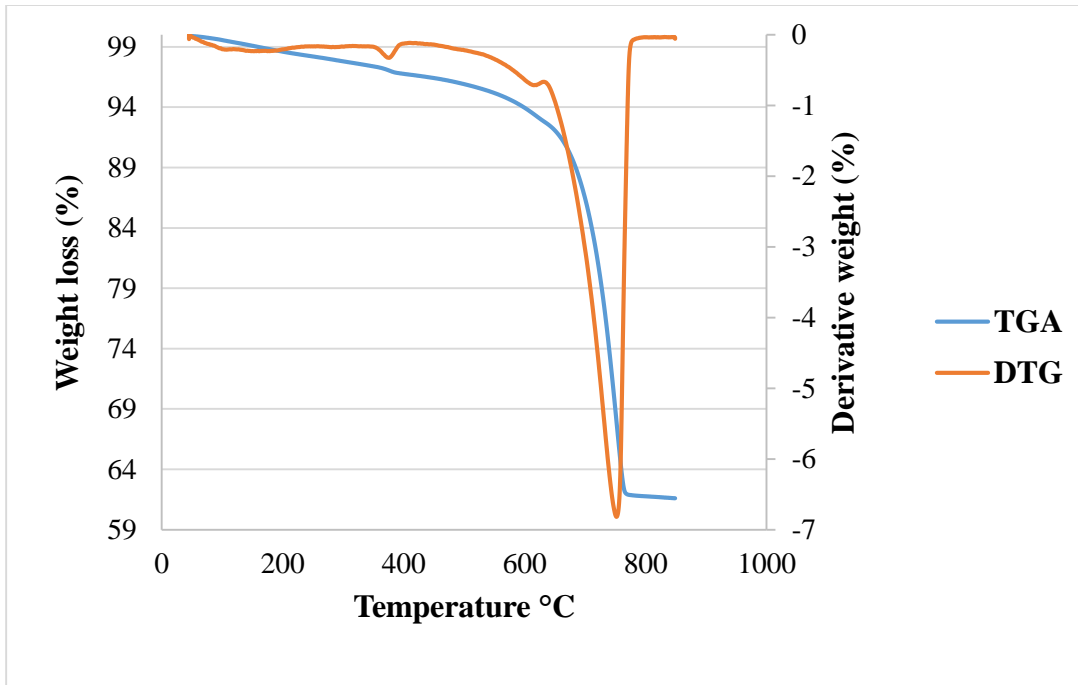


**Fig. 3.3: Characterization of lime sludge (a) SEM image of raw lime sludge (b) EDAX analysis of raw lime sludge showing elements present**



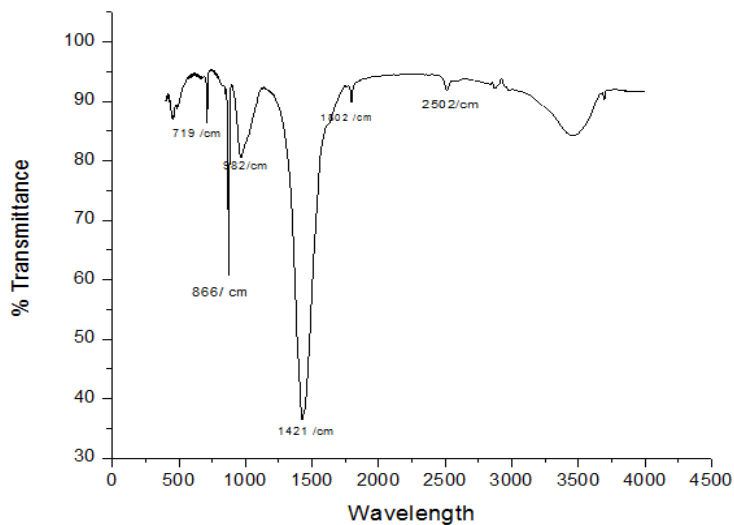
**Fig. 3.4: XRD of raw lime sludge**

Fig. 3.5 shows the TGA/DTG curve of lime sludge. From TGA curve it was observed 37.5% of weight loss due to evaporation of water. At 750°C decomposition of calcium carbonate takes place. This lime is suitable for making binder, it will thermally activate lime sludge. Earlier lime sludge was in hydrated form which was inert and when it will be treated above 750°C, it will become hydraulically reactive.



**Fig. 3.5: TGA/DTG of raw lime sludge**

Fig. 3.6 shows the FTIR spectrum of lime sludge. Peak at 1421 gives the strong peak of carbonates. When it is compared with FTIR of limestone, it was observed that peak of carbonate is more intense in limestone as compared to lime sludge, therefore because of that activation is required.



**Fig. 3.6: FTIR of raw lime sludge**



**Table 3.2: The chemical composition of raw lime sludge, calcined clay, GGBFS and fly ash**

<b>Constituents</b>	<b>Lime sludge (%)</b>	<b>Calcined clay (%)</b>	<b>GGBFS (%)</b>	<b>Fly ash (%)</b>
<b>CaO</b>	85.50	0.5	40.73	1.46
<b>SiO<sub>2</sub></b>	11.13	52	31.9	56.82
<b>Al<sub>2</sub>O<sub>3</sub></b>	0.24	45	16.17	30.28
<b>Fe<sub>2</sub>O<sub>3</sub></b>	0.182	0.5	0.8601	5.431
<b>MgO</b>	1.18	0.3	6.519	0.520
<b>Na<sub>2</sub>O</b>	0.989	0.2	0.202	0.110
<b>MnO</b>	-	0.004	0.304	0.0408
<b>TiO<sub>2</sub></b>	-	0.8	0.899	2.451
<b>K<sub>2</sub>O</b>	0.199	0.1	0.490	1.620
<b>CuO</b>	0.02	-	0.009	0.027
<b>SrO</b>	0.0299	-	0.0556	0.0343
<b>SO<sub>3</sub></b>	0.174	-	1.73	0.158
<b>P<sub>2</sub>O<sub>5</sub></b>	0.306	-	-	0.769

**Table 3.3: The particle size distribution of raw lime sludge, calcined clay and limestone.**

Materials	Particle Size Distribution		
	D10 ( $\mu\text{m}$ )	D50 ( $\mu\text{m}$ )	D90 ( $\mu\text{m}$ )
Lime Sludge	12.201	36.657	68.482
Calcined Clay	0.247	2.074	5.092
Limestone	7.40	35.83	77.20

### 3.2.3 Calcined Clay

The calcined clay was procured from Britex Enterprises, New Delhi. The properties of calcined clay satisfies all the physical and chemical requirements as per Draft IS: CED 2 (7821)- 2013. The colour of calcined clay is white. It has specific gravity of 3.33. Its main constituents are  $\text{SiO}_2$  and  $\text{Al}_2\text{O}_3$  comprising of 95% of its composition. Its loss on ignition is 0.1%. About 90% of particles are finer than 5  $\mu\text{m}$ . The chemical and physical properties of calcined clay are given in Table 3.2 and Table 3.4 respectively. The particle size distribution of calcined clay is shown in Table 3.3.

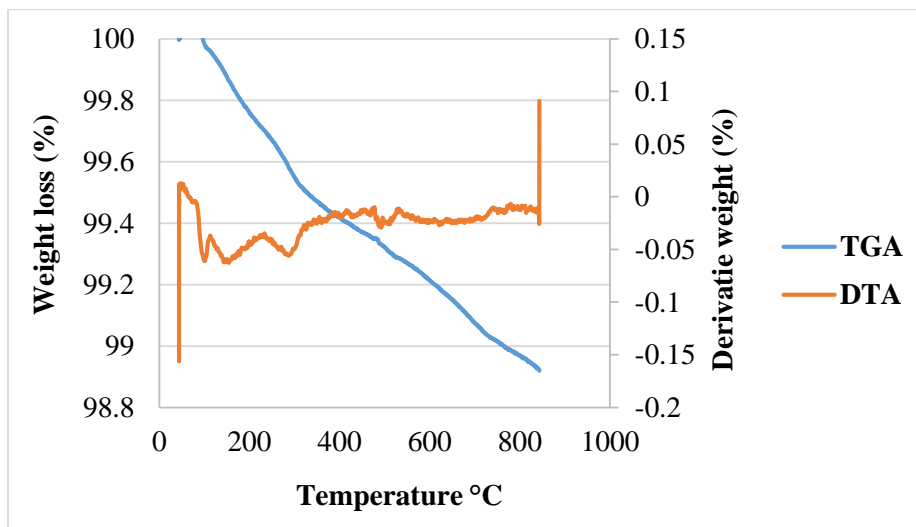


**Fig. 3.7: TGA/DTG curve of calcined clay**

From TGA curve of calcined clay it was observed that weight loss at 900°C is only 1% due to loss of moisture and de-hydroxylation and DTG curve shows several decomposition temperature up to 600°C.

**Table 3.4: Physical characteristics of calcined clay**

Property	Value
Whiteness	$\geq 92$
Refractivity	1.6
Specific Gravity	3.33
Water Content	$\leq 1.0 \%$
pH	6.67

### 3.2.4 Ground granulated blast furnace slag (GGBFS)

The ground granulated blast furnace slag was procured from Vizag Steel Plant,

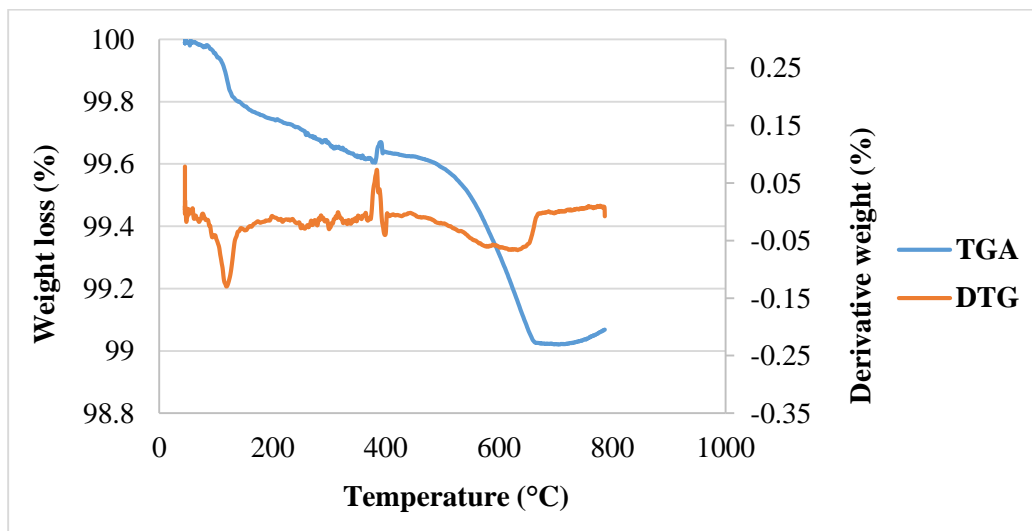


**Fig. 3.8: TGA/DTG curve of GGBFS**

Vishakhapatnam. It is light grey in colour. Its main constituents are  $\text{SiO}_2$  and  $\text{CaO}$ , consisting of 72.63% of its composition. The properties of GGBFS satisfies the requirements as per IS: 12089-1987. The chemical composition of GGBFS is given in Table 3.2. From Fig. 3.8 the TGA curve of calcined clay, it was observed that weight loss at  $787^\circ\text{C}$  is only 0.9% due to loss of moisture and DTG curve shows several decomposition temperature up to  $631^\circ\text{C}$ .

### 3.2.5 Fly Ash

The fly ash was procured from NTPC Dadri. It is grey in colour. Its main constituents are  $\text{SiO}_2$  and  $\text{Al}_2\text{O}_3$ , consisting of 87.1% of its composition. The properties of fly ash satisfies the requirements as per IS: 3812. Table 3.2 gives the chemical composition of fly ash.

### 3.2.6 Limestone

The limestone was procured from Starke & Co. Pvt. Ltd., New Delhi. About 90% of limestone particles are finer than  $77\mu\text{m}$ . The particle size distribution of limestone are shown in Table 3.3. The refractive index of limestone is 1.65. The specific surface area of limestone is  $386.2\text{ m}^2/\text{kg}$ . Fig. 3.9 shows the TGA/DTG analysis of limestone. It was observed that limestone was decomposed at  $800^\circ\text{C}$  with maximum weight loss of 41.1%. Fig. 3.10 shows the FTIR of limestone. When it was compared with FTIR of limestone, it was observed that carbonate peak in limestone is more intense than that of lime sludge, indicating presence of reactive  $\text{CaO}$ .

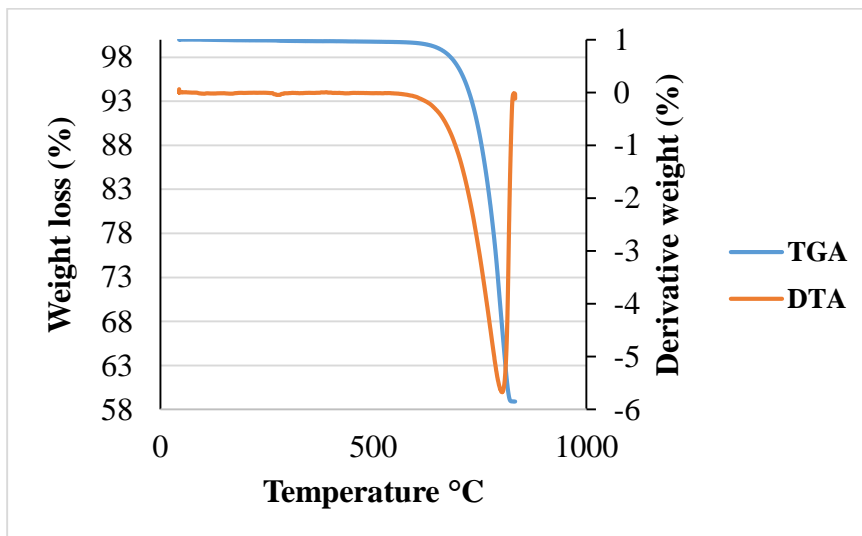


**Fig. 3.9: TGA/DTG curve of limestone**

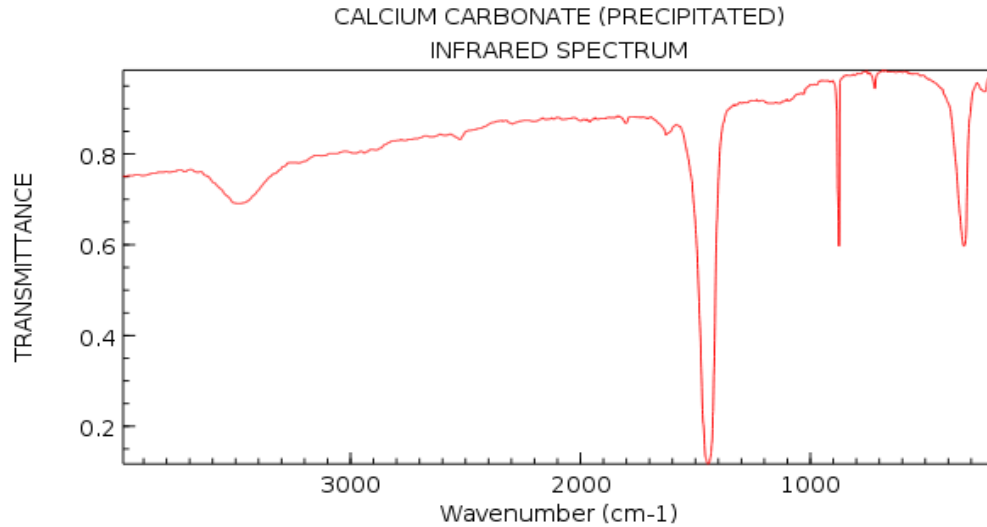


**Fig. 3.10: FTIR spectra of limestone**

### **3.2.7 Gypsum**

The gypsum was procured from Starke & Co. Pvt. Ltd., New Delhi. It is tan in colour. The chemical formula of gypsum is  $\text{CaSO}_4 \cdot 2\text{H}_2\text{O}$ .

## **3.3 Preparation of Materials**

### **3.3.1 Activation of lime Sludge**

The thermo-chemical activation of lime sludge was done to make it reactive. The chemical activation was done by weighing lime sludge in a container, then mixing it with grinded NaOH taken as 5% of weight of the lime sludge. Then, for thermal activation this mix was taken into silicon crucibles and was heated in a furnace at  $850^\circ\text{C}$  for 2 hours.

### **3.3.2 Grinding**

The thermo-chemically activated lime sludge was grinded in a mechanical ball mill of capacity 5 kg with 1:2 ratio of lime sludge and balls respectively for 45 minutes at 60 rpm.

The OPC 43 grade cement clinker was first pulverised 5 times in a pulveriser. This pulverised clinker was then grinded in a ball mill (AIM 441-20) with 1:3 ratio of clinker and balls respectively for 2 hours 50 minutes at 50 rpm.



(a)



(b)



(c)



(d)

**Fig.3.11: Grinding procedure of blended cement (a) Planetary ball mill for grinding (b) Inter-grind mix (c) & (d) Planetary ball mill jars for grinding**

### **3.3.3 Inter-grinding of mixes**

The inter-grinding of mixes for cement paste was done by planetary ball mixer (Retsch PM 400) (Fig. 3.11) with 1:1 ratio of mix and balls respectively for 15 minutes at 150 rpm. For mortar inter-grinding was done by mechanical ball mill of 5 kg capacity with 1:2 ratio of mix and balls respectively for 25 minutes at 60 rpm.

### 3.4 OPTIMIZATION OF MIXES

Firstly mixes as given in Table 3.5 were prepared and their properties such as compressive strength, lime reactivity of pozzolana and pozzolanic reactivity were checked for optimisation of a particular mix for further variation and studies.

**Table 3.5: Blended cement mixes for optimisation**

<b>Mix</b>	<b>Clinker (%)</b>	<b>Activated Lime Sludge (%)</b>	<b>Calcined Clay (%)</b>	<b>GGBFS (%)</b>	<b>Fly Ash (%)</b>	<b>Gypsum (%)</b>
<b>Mix 1</b>	50	15	30	-	-	5
<b>Mix 2</b>	50	15	15	15	-	5
<b>Mix 3</b>	50	15	15	-	15	5
<b>Mix 4</b>	50	-	30	-	-	5
<b>Control</b>	95	-	-	-	-	5

After optimisation, Mix 2 was selected. And content of lime sludge was varied as shown in Table 3.6 and further studies were conducted. Studies were also conducted on blended cements by varying lime sludge and pozzolana content in the optimised proportion (Table 3.7).

### 3.5 TESTING METHODS

#### 3.5.1 Specific Surface Area

Automatic Blaine's apparatus (Fig. 3.12) was used for determination of fineness of raw materials and blended cement mixes. The working principle of this apparatus is drawing a definite quantity of air through a prepared bed of solid containing definite porosity. The number and size of the pores in the prepared bed of definite porosity is a function of the size

of the particles and this determines the rate of air flow. The time elapsed for a given quantity of air to pass through a compacted bed of material determines the fineness of a material.

**Table 3.6: Blended cement mixes for final investigations**

<b>Mix</b>	<b>Clinker (%)</b>	<b>Activated Lime Sludge (%)</b>	<b>Calcined Clay (%)</b>	<b>GGBFS (%)</b>	<b>Gypsum (%)</b>
<b>Control</b>	95	-	-	-	5
<b>Sample 1</b>	50	15	15	15	5
<b>Sample 2</b>	50	20	15	15	5
<b>Sample 3</b>	50	25	15	15	5
<b>Sample 4</b>	50	30	15	15	5

**Table 3.7: Blended cement mixes with variation of lime sludge and pozzolana.**

<b>Mix</b>	<b>Clinker (%)</b>	<b>Activated Lime Sludge (%)</b>	<b>Calcined Clay (%)</b>	<b>GGBFS (%)</b>	<b>Gypsum (%)</b>
<b>Sample 5</b>	50	20	12.5	12.5	5
<b>Sample 6</b>	50	25	10	10	5
<b>Sample 7</b>	50	30	7.5	7.5	5

In an experiment, the perforated disc on the ledge was placed at the bottom of cell and a new filter paper disc was placed over it. About 2.8 g sample was placed in the sample cell. The sample cell was tapped to level the sample. A second new filter paper disc was placed on the



level bed of sample. The plunger was inserted to make contact with the filter paper disc. The plunger was pressed gently but firmly until the lower face of the cap came in contact with the



**Fig. 3.12: The experimental setup of the automatic Blaine's apparatus**

cell. Then slowly the plunger was withdrawn about 5 mm, and it was rotated through 90° and again it was pressed to ensure that the plunger cap is in contact with the cell. Then the plunger was withdrawn slowly and the fineness of the samples was recorded.

### **3.5.2 Particle Size Distribution**

The average particle size of blended cement mix and its particle size distribution were determined by a laser particle size analyser (Horiba LA-950V2). The working principle of analyser is laser diffraction, which relates the intensity and angle of the scattered light with the size of the particles. Light scatters more intensely for a large particle and at smaller angles than that for smaller particles. The measured angle and intensity of light scattered is passed on to algorithm designed to use Mie's scattering theory which transforms scattered light data into particle size information.

In this experiment, about 10 g of blended cement was dispersed in 200 ml of iso-propyl alcohol to form a suspension. This suspension was kept in the sample cell. Then, laser beam was allowed to pass through the sample. Particle size distribution of a blended cement was measured after a sonic vibration of 5 minutes. A plot between cumulative percentage passing and sieve size gives the average particle size.

### 3.5.3 X-Ray Diffractometer

The XRD analysis was performed to study the phase analysis of lime sludge and different blended cement mixes. XRD depends on the constructive interferences of monochromatic X-rays and a crystalline sample. X-rays that are generated by a cathode ray tube are filtered to produce monochromatic radiation, align to concentrate, and directed towards the sample. When there is interaction between incident rays and sample, and Bragg's Law ( $n\lambda=2d\sin\theta$ ) is satisfied then constructive interference is produced. This law relates the wavelength of electromagnetic radiation with the diffraction angle and the lattice spacing in the crystalline sample. Then, these diffracted X-rays are detected, processed and counted. All possible diffraction directions of the lattice can be attained because of random orientation of the powdered material, by scanning the sample through a range of  $2\theta$  angles. Each mineral has a set of unique d-spacing and conversion of the diffraction peaks to d-spacing will allow to identify the mineral. This is achieved by comparing d-spacing with standard reference patterns.

The analysis of phases present in blended mixes are done by Bruker D8 X-ray diffractometers. The sample of fine powder was placed into sample holder or onto the sample surface, make



**Fig. 3.13: The photographic view of X-ray Diffractometer**

upper surface flat and pack it into a sample container and sprinkle it on double sticky tape. And then sample will be analysed for different phases. The photographic view of XRD is as shown in Fig. 3.13.

#### **3.5.4 FE-SEM and EDAX**

The FE-SEM/EDAX analysis was performed to study the microstructure of different blended cement mixes and fractured surfaces of their respective hydrated pastes. The microscope was operating at an accelerating voltage of 20 keV. Due to repeated scattering and absorption within a teardrop-shaped volume, the electrons of the high energy electron beam emitted from electron gun losses its energy. After energy exchange between the electron beam and sample, there was a reflection of high energy electrons by elastic scattering emission of secondary electrons by inelastic scattering and emission of electromagnetic radiation. To collect low energy secondary electrons that are ejected from the K-orbitals is the most common imaging mode. They originate within a few nanometres from the sample due to this low energy. Brightness depends upon the amount of secondary electron reaching detected.

A field emission scanning electron microscope (ULTRA plus, Carl Zeiss, coupled with the Oxford EDX) (Fig. 3.14) was used for studying the interfacial transition zone and the surface morphology of raw materials and blended cement mixes. The samples were mounted on the



**Fig. 3.14: Field emission scanning electron microscope for fractographic examination**

stub of 10 mm diameter and a gold (Au) coating was done over it using sputter coater at a pressure of  $10^{-2}$  mbar. These samples were then placed over a sample holder of the microscope for fractographic examination.

### 3.5.5 *Thermogravimetric Analysis (TGA) and Differential Thermal Gravimetric (DTG)*

A method that measures changes in chemical and physical properties as a function of increasing time or increasing temperature is known as Thermogravimetric analysis (TGA). TGA provides information about the physical phenomena such as absorption of moisture content of materials, vaporization, desorption, sublimation, etc. and chemical process like decomposition, reduction, oxidation etc. TGA measures the amount of weight loss with respect to change in temperature in the presence of atmosphere of nitrogen, vacuum or helium. Differential thermal gravimetric analysis is also thermal analysis which provides data on transformation occurred such as glass transition, crystallization, melting, sublimation etc. (Ramachandran, 1969). The differential temperatures between study material and inert reference material is then plotted against time or temperature that depicts the exothermic or endothermic reaction respectively. TGA/DTG instrument is shown in Fig. 3.15.



**Fig. 3.15: TGA/DTA instrument for determining weight loss of a material**

### 3.5.6 *Fourier Transform Infrared Spectroscopy (FTIR)*

FTIR was performed to obtain an infrared spectrum of absorption or emission of a solid. The FTIR microscope (Perkin Elmer, Spectrum GX) (Fig. 3.16) was used for analysing the bonds present in the molecule. FTIR is based on that most molecules absorb light in the infrared region of the electromagnetic spectrum. The bonds present in the molecule is corresponding to this light absorption. The frequency range are measured by the wave number over the range of  $4000\text{-}600\text{ cm}^{-1}$ . Firstly the background emission spectrum of the IR source is recorded, which is followed by the emission spectrum with the sample in place of the IR source. The sample's absorption spectrum directly depends on the ratio of sample spectrum to the background spectrum. The resultant absorption spectrum obtained from the bond natural vibration frequencies will indicate the presence of various functional groups and chemical bonds present in the sample.

Firstly Potassium Bromide (KBr) pellet was made in hydraulic/pellet press by taking 100mg of finely grinded KBr for background spectrum. Then oven dried and finely grinded sample was taken with KBr in the ratio 3:97 and pellet was formed with 100 mg sample. Then sample pellet was taken in sample carrier and was scanned for spectrum.

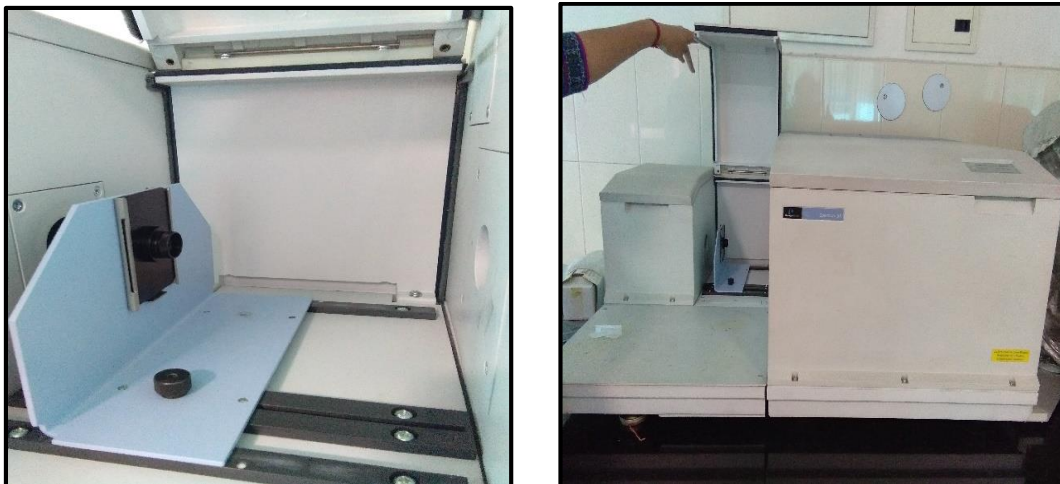


**Fig. 3.16: FTIR instrument for obtaining infrared spectrum of a material**

### 3.5.7 Consistency

Consistency of cement paste and blended cement mixes were determined according to IS 4031 (Part 4) using Vicat's apparatus (Fig. 3.17). The Vicat's plunger of diameter  $10 \pm 0.05$  mm was used to measure the consistency by letting it to penetrate the paste to a point from 5 mm to 7 mm from the bottom of the Vicat's mould. The sample was prepared by mixing a weighted quantity of cement or mixes with distilled or potable water taking into account the gauging time to be between 3 to 5 minutes. The Vicat's mould was completely filled with this paste and the surface was smoothed to make it level with the top surface of the mould. Then, the plunger was gently lowered to touch the surface of the prepared sample in the mould and quickly released, allowing it to sink into the paste.

### 3.5.8 Setting Time

Setting time of blended cement mixes and cement paste was determined according to IS: 4031 (Part 5) using Vicat's apparatus (Fig. 3.18). For measuring the initial and final setting time,



**Fig. 3.17: The Vicat's apparatus for measuring consistency of cement**



**Fig. 3.18: Vicat's apparatus showing setting time of a blended cement**

needle of dia.  $1.13 \pm 0.05$  mm and  $1.13 \pm 0.05$  mm fitted with a brass attachment of  $5 \pm 0.1$  mm were used respectively with the Vicat's apparatus. The sample for setting time was prepared by mixing blended cement mix with 0.85 times the water that was added to give a paste of standard consistency. When the needle fails to penetrate the sample beyond  $5 \pm 0.5$  mm measured from the bottom of the mould, initial setting time is obtained. And final setting of a paste is observed when, upon applying the needle gently to the surface of the block makes an impression while the attachment fails to do so.

### **3.5.9 Flow Table**

For determining water content in lime reactivity mortar cubes flow table was used according to IS: 1727-1967. The water required for  $70 \pm 5$  % flow with 10 drops in 6 sec was taken as water content (Fig. 3.19).

### **3.5.10 Lime Reactivity**

The lime reactivity of pozzolana is determined according to IS: 1727-1967. This test is conducted to check the reactivity of pozzolana with hydrated lime. The materials for standard



**Fig. 3.19: Flow table for mortar flow**

test mortar were taken as lime: pozzolana: standard sand in the proportion 1:2 M:9 by weight, where M is ratio of specific gravity of pozzolana to specific gravity of lime. Where in place of hydrated lime, lime sludge was used. Three different pozzolana were used that are fly ash, GGBFS and calcined clay. And water was taken according to flow table (3.5.10). Fig. 3.20 shows the mortar cubes for lime reactivity.



**Fig. 3.20: Mortar cubes for lime reactivity**



### 3.5.11 Fratini Test

The pozzolanicity of the pozzolana was assessed as per the procedure described in BS EN 196-5. 20 gm of test sample consisting of 80% ordinary Portland cement (43 grade) and 20% pozzolana was mixed with 100 ml of distilled water and was kept in an oven at 40°C in the sealed plastic bottle. Like this 3 test samples of each pozzolana (calcined clay, fly ash and GGBFS) were prepared. After 8 days, Whatman filter paper no. 542 was used for vacuum filter of sample, the filtrate was analysed for hydroxyl ion by a titration dilute hydrochloric acid with methyl orange as an indicator and for calcium oxide, adjusting pH of filtrate to 13, followed by the titration with 0.03 mol/l EDTA solution using a Patton and Readers indicator (Fig. 3.21). The solubility curve of calcium oxide in the solution was plotted as a function of hydroxyl ion concentration to assess pozzolanicity of the pozzolana.



**Fig.3.21: Experimental setup of Fratini test**

### 3.5.12 Isothermal Calorimeter

Isothermal conduction calorimeter (TAM Air, TA instruments) (Fig. 3.22) was used to study the hydration behaviour of blended cement mixes. Calorimeter measures the heat flow when heat is produced in a sample. The sample is placed in an ampoule that is in contact with the heat flow sensor that is also in contact with the heat sink. A temperature gradient across the sensor is developed when heat is produced or consumed by any process, which generates a

voltage which is measured. The voltage is proportional to the heat flow across the sensor and to the rate of process taking place in the sample ampoules. This signal is recorded continuously.

The samples were prepared by thoroughly mixing 4 g of blended cement mix with 10 ml of water at 25°C. The sample was placed into specimen vial and inserted into the calorimeter (Fig. 3.). Sample loading time was 1 min. The thermal power was recorded up to 7 days. The heat flow and rate of hydration of blended mixes were recorded.



**Fig. 3.22: Isothermal calorimeter for hydration kinetics**

### **3.5.13 Specific Gravity**

The specific gravity of blended cement mixes is determined according IS: 4031 (Part 11). The Le-Chatelier's flask is used as an apparatus for determining specific gravity. The sample was prepared by filling kerosene in the flask to a point on the stem between the zero and 1 ml mark. Then the flask was immersed in water bath at  $27 \pm 0.2^\circ\text{C}$  and initial reading was observed. Then, introduce about 64 g of blended cement mix in the flask and stopper was placed over the mouth of the flask. And then at same temperature final reading was taken. The experimental setup of specific gravity is as shown in Fig. 3.23.

### **3.5.14 Soundness**

The soundness of a cement is determined to check any appreciable volume change after it has set. It is determined according to IS: 4031 (Part 3). Le-Chatelier's apparatus conforming to IS: 5514-1969 was used (Fig. 3.24). The sample for soundness was prepared by mixing blended



**Fig. 3.23: The experimental setup of determining specific gravity of blended cement mixes**

cement mix with 0.78 times the water required for standard consistency of the respective mix. The mould was placed on a thin glass plate and edges of mould were kept together while placing sample in the mould, it is then covered with another thin glass plate and weight was putted on it and was immediately submerged in water at a  $27 \pm 2^\circ\text{C}$  and was kept there for 24 hours. The distance separating the indicators was measured and was taken as initial reading. This assembly was again immersed in water at  $100^\circ\text{C}$  for 3 hours. Again, distance between the indicators was measured and it was taken as final reading. Fig. 3 shows the experimental setup of soundness of blended cement mixes.

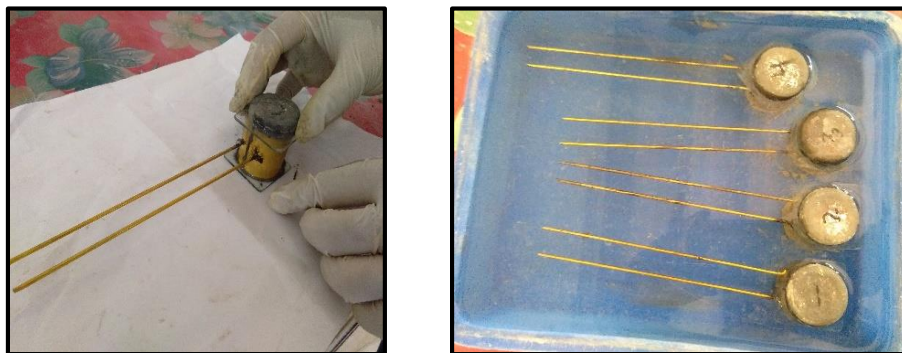


**Fig. 3.24: The experimental setup of soundness of blended cement mixes**

### 3.5.15 pH

The pH of blended cement mixes is determined by using pH meter (Fig. 3.25). pH meter is calibrated before taking reading. A sample was prepared by taking about 10 g of sample in 100 ml of distilled water, and it was stirred and was left for 1 hour. After this reading for each sample will be taken by keeping sample undisturbed for 3 minutes.



**Fig. 3.25: The experimental setup for determining pH of blended mixes**

### 3.5.16 Rheology

The flow behaviour of blended cement mixes were studied by rotational viscometer. It helps in simulating the shear rate closer to reality encountered in the practical handling and placing of fresh concrete. Basic rheological parameters are plastic viscosity and yield stress which may enable to predict flow which would go beyond measurement of useful traditional slump.

Rotational rheometer (Model 3500 Viscometer, Grace Instrument Company) is an automated system which works on the principle of a co-axial cylinder (Fig. 3.26). The rotational velocities it applies is in the range of 0.01-600 rpm, shear stress in the range 0.5-500 Pa and shear rate in the range of 30-500  $s^{-1}$ . Before commencing the test, rheometer was calibrated. The blended mixes with a constant w/c ratio were prepared. The paste was mixed for two to three minutes in the homogenizer. It was then transferred to the sample cup of viscometer and was sheared

in steps from 20 to 300 rpm. The viscosity and yield stress of pastes were noted. And hysteresis loop was generated by shearing from 5 to 50 rpm and from 50 to 5 rpm.



**Fig. 3.26: M3500 viscometer for determining rheology of a blended cement paste**

### ***3.5.17 Compressive Strength***

The compressive strength test of blended cement pastes (25 x 25 x 25 mm) was performed on applied, starting from zero at the rate of 25 kg/cm<sup>2</sup>/min. Three paste were tested to represent the compressive strength of that particular batch.



**Fig. 3.27: Universal testing machine for compressive strength of paste**

The stress-strain curve for each specimen of cement paste was recorded. The compressive strength of sand-cement mortar cubes (70.6 x 70.6 70.6) was performed on 1000 kN capacity (Fig. 3.28). The load was steadily and uniformly applied, starting from zero at a rate of 140 kg/cm<sup>2</sup>/min as per IS: 516-1959.



(a)



(b)



(c)



(d)

**Fig. 3.28: Compressive strength of specimens (a) & (b) Casting of mortar cubes for different blended cements and (c) & (d) mortar testing on compressive testing machine**

# CHAPTER 4

## RESULTS AND DISCUSSION

### 4.1 Characterisation of Cementitious Binders

#### 4.1.1 Lime Reactivity and Pozzolanicity

Lime reactivity of lime sludge pozzolana mix (fly ash, calcined clay and GGBFS) used in making cementitious binders is given in Table 4.1. The slump flow and consistency of mixes were kept 165-175 mm and 31-34% respectively. It was observed that pozzolanic index of all the mixes was in the range of 2.43 to 3.05 MPa which satisfied the requirement of LP 40 grade of IS: 4098-1983. Subsequent experiment was further performed to enhance the pozzolanic index of lime sludge to make it suitable for use in blended cement. To meet the requirement of lime reactivity of 4-4.5 MPa for cement, the lime sludge was thermo-chemically activated. It was found that the pozzolanic activity of mix was lying in the range of 3.61-4.36 MPa. The improvement in the particle size distribution, specific surface area and soluble fraction were responsible for reactive centres of lime absorption. It was observed that GGBFS and calcined clay have better lime reactivity in comparison to fly ash. The reactive silica and alumina present in pozzolana may react with lime to produce major phases such as C-S-H,  $C_2ASH_8$  and  $C_4AH_{13}$  (Shi and Day, 1995). The lime reactivity strength is basically obtained due to calcium silicate hydrate formation.

**Table 4.1: Lime reactivity of pozzolana with lime sludge**

Pozzolana	Slump flow (mm)	Consistency (%)	Lime reactivity	
			Lime sludge (MPa)	Lime sludge + NaOH (MPa)
Fly ash	175	31	2.43	3.61
Calcined clay	170	33	2.89	4.36
GGBFS	165	34	3.05	4.28

Fig. 4.1 shows lime solubility curve of various pozzolana as per EN196-5 between CaO concentration and hydroxyl ion concentration at 40°C. The solubility data of Ca(OH)<sub>2</sub> in the range of 35-90 mmol/l [OH<sup>-</sup>] range can be expressed as in equation (1):

$$\text{Theoretical max. [CaO]} = \frac{350}{[\text{OH}^-]-15} \quad \text{-----(1)}$$

According to standard, the value lying below the line of saturation shows pozzolanic reactivity whereas, the value lying on or above the line of saturation exhibited zero pozzolanic reactivity. It was observed that the mixes prepared with thermo-chemically activated lime sludge showed values below the line of saturation in the curve indicating a removal of calcium ions from the solution attributable to their pozzolanicity. The CaO reduction obtained from the difference between the theoretical and experimental values was 80.07% for calcined clay based binder, 88.85% for GGBFS based binder and 48.23% for flyash based binder (Table 4.2). This may be attributed to the participation of lime sludge in the hydration process. It is concluded that the mix containing GGBFS showed highest pozzolanicity whereas, mix with fly ash showed lowest pozzolanicity.

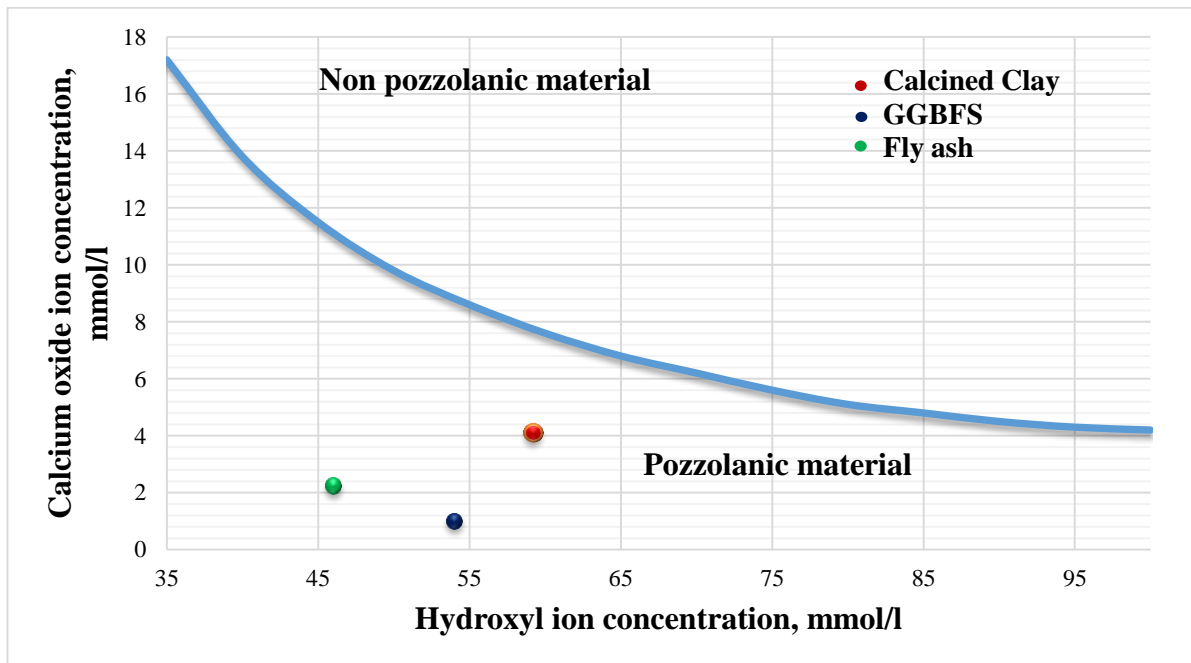


Fig. 4.1: Fratini curve showing pozzolanic reactivity of pozzolana



**Table 4.2: Fratini test results for pozzolanic materials**

<b>Pozzolana</b>	<b>[OH]<sup>-</sup> mmol/l</b>	<b>[CaO] mmol/l</b>	<b>Theoretical max [CaO] mmol/l</b>	<b>CaO reduction %</b>
<b>Calcined Clay</b>	46	2.25	11.29	80.07
<b>GGBFS</b>	54	1.00	8.97	88.85
<b>Fly Ash</b>	59.2	4.10	7.92	48.23

#### ***4.1.2 Blaine Specific Surface Area***

Blaine surface area of various cementitious binders is given in Table 4.3. It was observed that Portland cement had 285.2 m<sup>2</sup>/kg Blaine surface area. Contrary to this, the Blaine surface area of cementitious binders was found in the range of 500-626 m<sup>2</sup>/kg probably due to the fine particles of pozzolana. The higher surface area of the binders would expect to enhance their cementitious properties, consequently the strength of binders. It can also be observed that increasing lime sludge in the slag contain mix resulted in increase of Blaine surface area of the resulting binders probably due to the fineness of lime sludge particles.

#### ***4.1.3 Particle Size Distribution***

Fig. 4.2 shows cumulative particle size distribution of Portland cement and various cementitious binders. It can be seen that Portland cement had particle size range from 5.122 to 262.37 µm. The average particle size (D50) was 41.77 µm. Contrary to this, the cementitious binders exhibited particle size distribution ranging between 0.58 and 300 µm. The average particle size of various mixes ranged from 16.78 to 41.77 µm (Table 4.4). The specific area of cementitious binders (8038.5 – 12171 cm<sup>2</sup>/cm<sup>3</sup>) was also higher than the Portland cement (2298.3 cm<sup>2</sup>/cm<sup>3</sup>). This indicated that cementitious binders had smaller particle size than the Portland cement throughout the distribution range.

Based on the fineness, the mix containing calcined clay and GGBFS was selected because of its similarity with limestone calcined clay cement (LC3). The various percentage of thermo-

chemically activated lime sludge (15 – 30% by weight) was added into the mix. The particle size distribution of these mixes is given in Fig. 4.2 and Table 4.3. It was found that cementitious binder had narrow particle size distribution than the Portland cement showing more uniformity in its particle sizes. The addition of thermo-chemically activated lime sludge into mix resulted in decrease in average particle size (except 25% may be due to some treatment issue). The average particle size of binder was about 20 - 23  $\mu\text{m}$ .

**Table 4.3: Blaine surface area of lime sludge based cementitious binders**

<b>S.No.</b>	<b>Mix</b>	<b>Blaine surface area (<math>\text{m}^2/\text{kg}</math>)</b>
1	Portland cement	285.2
2	Clinker 55%, Pozzolana 25%, Lime Sludge 20%	525
3	Clinker 55%, Pozzolana 20%, Lime Sludge 25%	500.2
4	Clinker 55%, Pozzolana 15%, Lime Sludge 30%	528
5	Clinker 55%, Pozzolana 30%, Lime Sludge 15%	561
5A	Lime Sludge 20%	587
5B	Lime Sludge 25%	602.5
5C	Lime Sludge 30%	626.5

\*Pozzolana: calcined clay and GGBFS in equal ratio

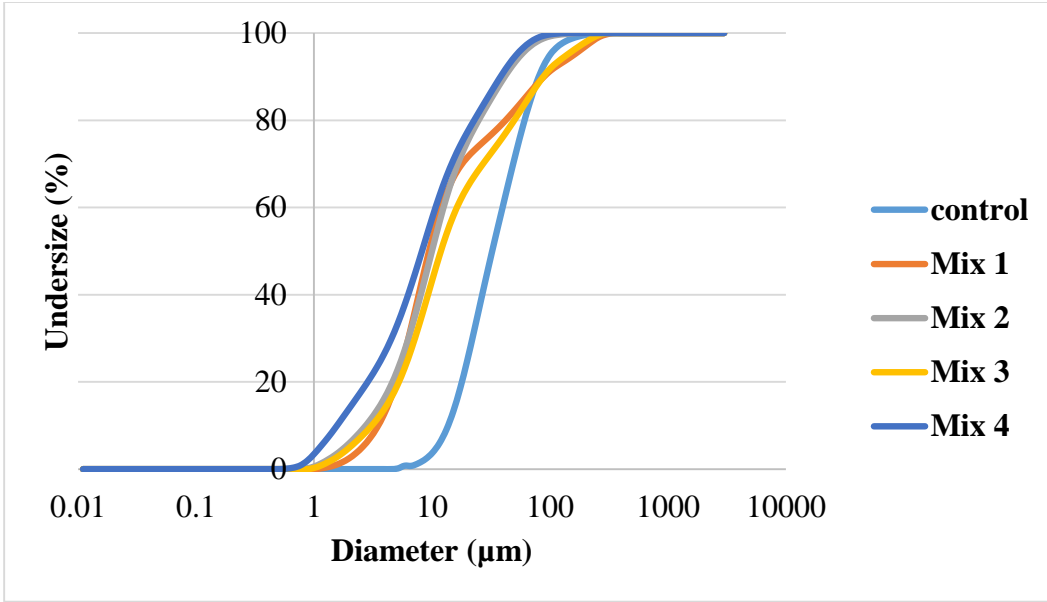


**Fig. 4.2: Particle size distribution curve of Portland cement and various cementitious binders.**

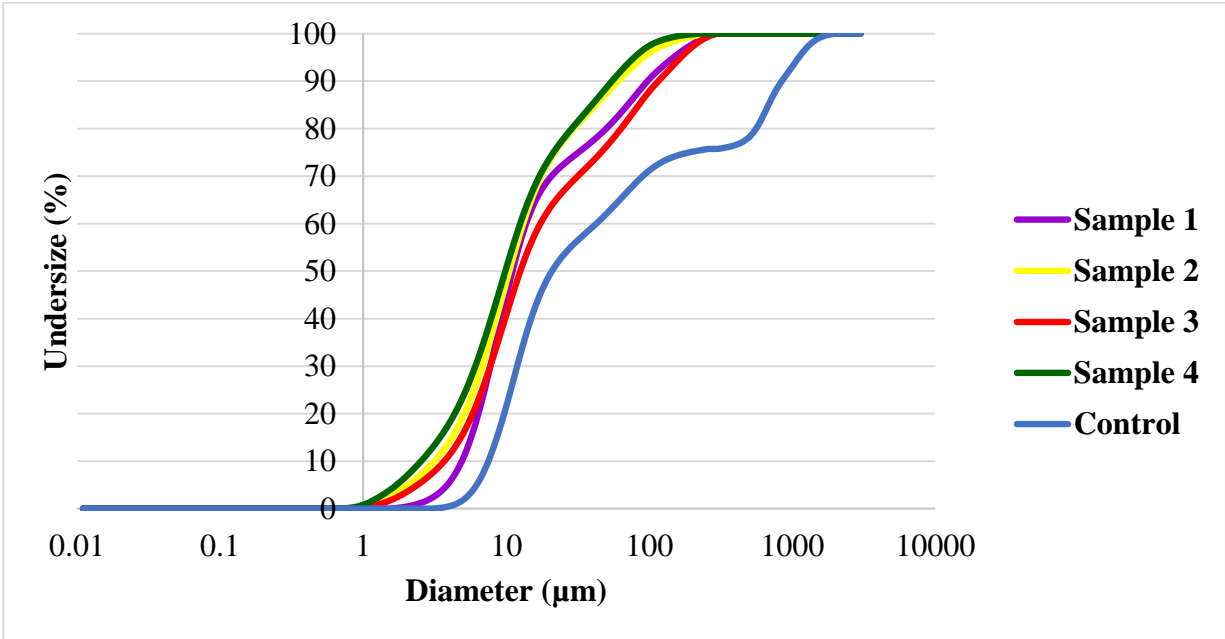


**Fig. 4.3: Particle size distribution curve of cementitious binder (calcined clay and GGBFS) containing different percentage of thermo-chemically activated lime sludge.**

**Table 4.4: Particle size distribution of lime sludge based cementitious binders**

S. No.	Mix	Particle Size Distribution		
		D10 (µm)	D50 (µm)	D90 (µm)
1	Portland cement	13.650	41.770	80.760
2	Clinker 55%, Calcined clay 30%, Lime Sludge 15%	3.490	31.330	89.080
3	Clinker 55%, Calcined clay 30%, Limestone 15%	1.790	16.780	43.730
4	Clinker 55%, Calcined clay 15%, Fly ash 15%, Lime Sludge 15%	3.084	32.280	87.930
5	Clinker 55%, Calcined clay 15%, GGBFS 15%, Lime Sludge 15%	2.740	16.920	41.420
5A	Lime Sludge 15%	4.880	32.870	97.320
5B	Lime Sludge 20%	3.140	22.800	60.720
5C	Lime Sludge 25%	3.680	38.030	115.83
5D	Lime Sludge 30%	2.540	20.280	54.910

#### **4.1.4 X-ray Fluorescence spectroscopy (XRF)**

The oxide composition of Portland cement and cementitious binder as obtained from XRF is given in Table 4.5. When compared with the Portland cement, the CaO content was significantly low while SiO<sub>2</sub> and Al<sub>2</sub>O<sub>3</sub> were on higher side. SiO<sub>2</sub>/Al<sub>2</sub>O<sub>3</sub> and CaO/SiO<sub>2</sub> ratio in the cementitious binder (Mix 2) was 1.59 and 1.75 respectively compared with the 4.64 and 3.26 of Portland cement. This suggested the role of aluminosilicate precursors for strength development in the binder. The alkali content in the binder was higher than the OPC because

of chemical treatment of the lime sludge. However, sulphate content in OPC was higher than the developed binder. MgO content for all the mixes is well below limit (6% by mass) (IS: 269-2013).

**Table 4.5: Chemical composition of lime sludge based cementitious binders with different pozzolana**

Constituents	Mix 1	Mix 2	Mix 3	Mix 4	Control
CaO	38.38	46.79	41.72	37.58	62.91
SiO <sub>2</sub>	30.73	26.77	30.11	31.16	19.32
Al <sub>2</sub> O <sub>3</sub>	23.56	16.85	18.51	24.65	4.165
Fe <sub>2</sub> O <sub>3</sub>	1.991	2.313	2.832	2.041	4.184
Na <sub>2</sub> O	0.979	1.23	1.22	0.364	0.729
MgO	1.378	2.383	1.773	1.326	4.053
K <sub>2</sub> O	0.441	0.525	0.673	0.456	0.8219
SO <sub>3</sub>	1.56	2.074	1.90	1.43	3.013

#### 4.1.5 X-ray Diffraction (XRD)

XRD pattern of Portland cement and cementitious binder with different percentage of thermo-chemically activated lime sludge is shown in Fig. 4.4. When compared with the OPC, the intensity of the peak at 30° 2θ and 31° 2θ (weak peak) associated with belite increased for cementitious binder. This suggest the overlapping of calcite peak (calcined clay) with belite. There was a well-defined alite doublet peak at 33.25° 2θ in the XRD pattern for all the cases. It was observed that the peak intensity of this doublet in OPC was higher than the cementitious binder indicating more alite content in the Portland cement. The peak intensity at 51.7° 2θ corresponding to MgO content decreased in the case of cementitious binder compared to OPC.

A slight humps in the case of cementitious binder around  $30^\circ 2\theta$  was viewed but it is not very distinct due to overlapping of many peaks. This indicates the presence of amorphous phases.

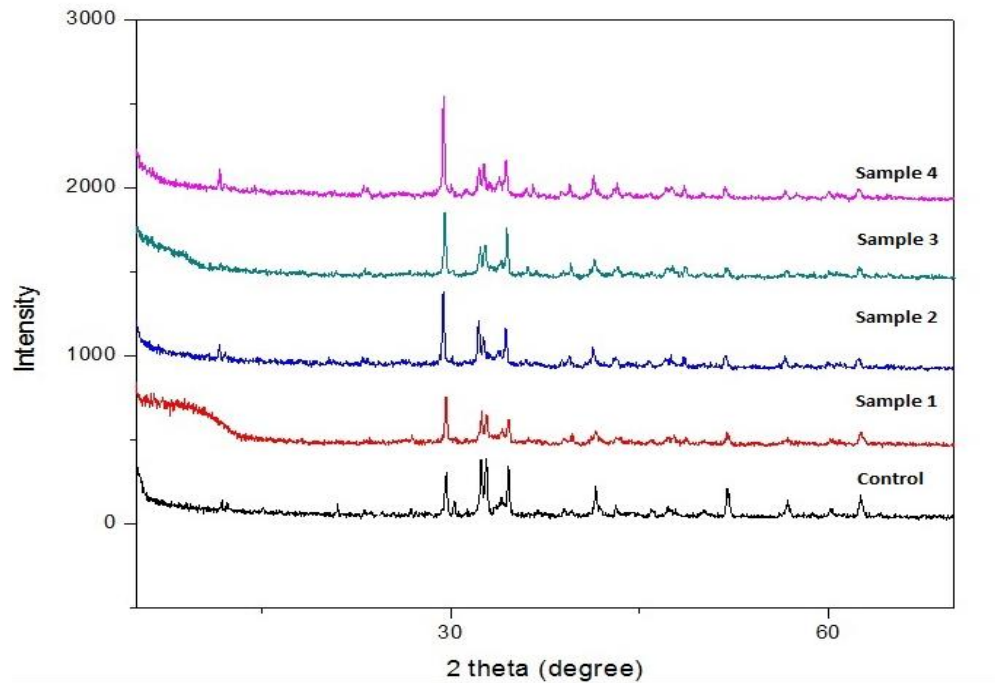


**Fig. 4.4: XRD of lime sludge based cementitious binders**

#### ***4.1.6 Fourier Transform of Infrared Spectroscopy***

FTIR of various cementitious binders was carried out to know their structural functional groups (Fig. 4.5). It was noted that the peak at  $1100\text{ cm}^{-1}$ ,  $900\text{ cm}^{-1}$  and  $550\text{ cm}^{-1}$  were more intense compared to Portland cement. The absorption band at  $1100\text{ cm}^{-1}$  corresponds to Si-O-Si asymmetrical stretching. The intensity and area of this peak varied with respect to composition of mixes. The peak at around  $925\text{ cm}^{-1}$  and  $525\text{ cm}^{-1}$  are associated with aluminosilicate/alite phase. Increasing pozzolana in the mix resulted in increased peak intensity of binder, which suggests more reactive content in it. The intensity of peak at  $1425\text{ cm}^{-1}$  due to carbonate varied with composition of the binders. The weak peaks at  $3450 - 3500\text{ cm}^{-1}$  and  $1650\text{ cm}^{-1}$  were attributed to hydrogen bonded -OH group and water. These bands were absent in the case of Portland cement probably due to anhydrous in nature. It is noted that broad peak at around  $1100\text{ cm}^{-1}$  could be responsible for formation of different phases other than CSH.

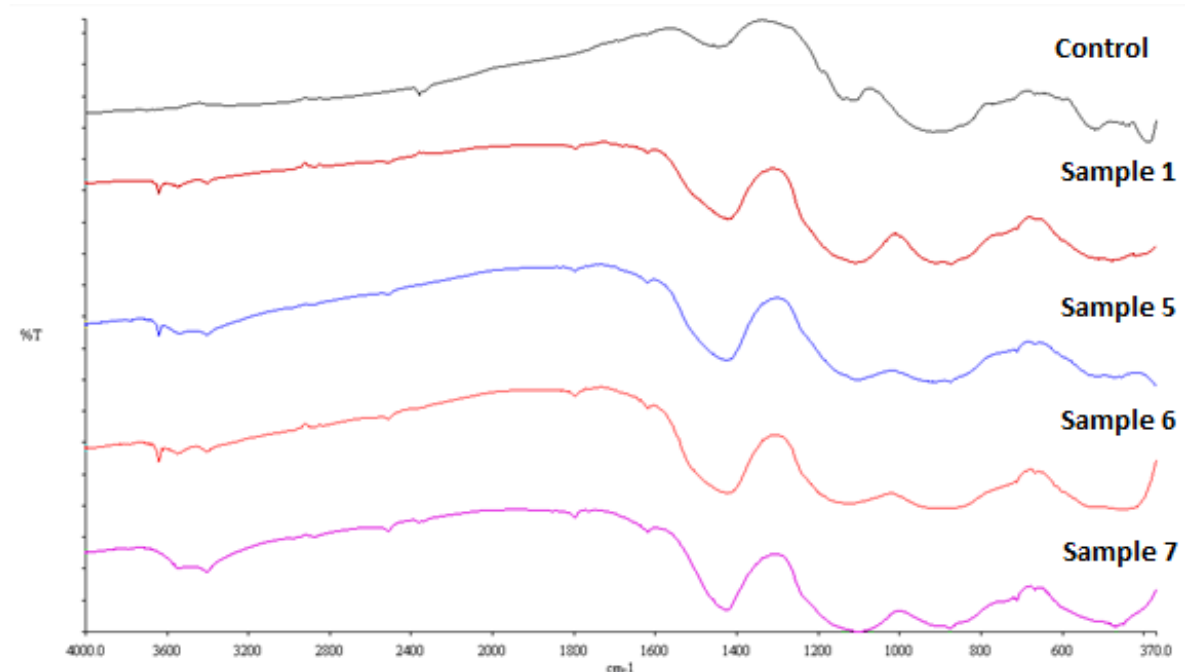
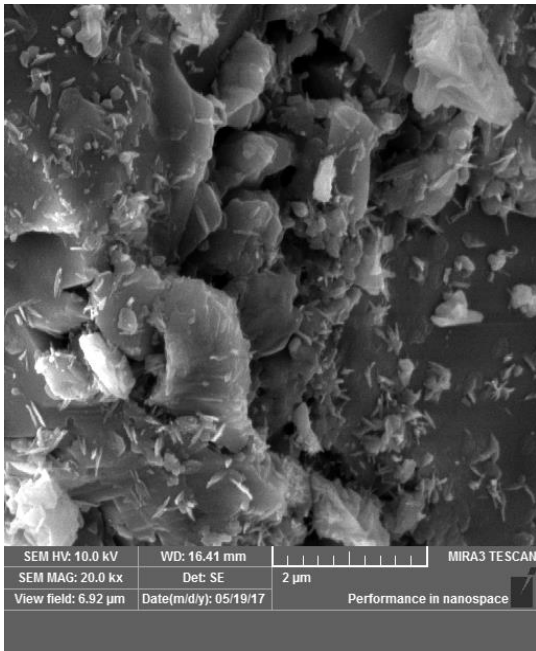


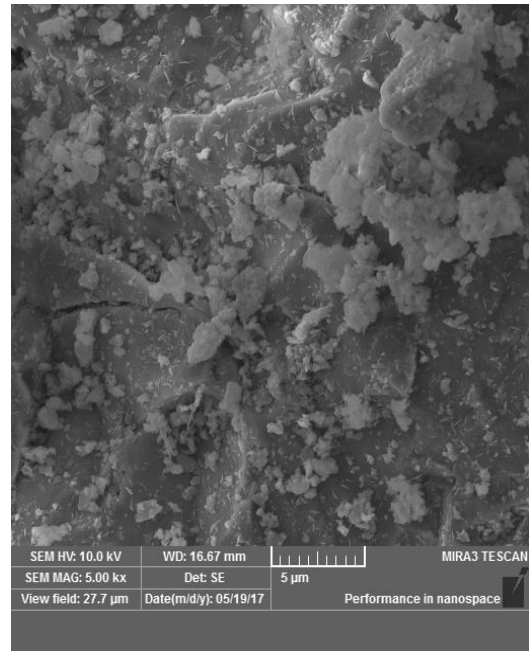
**Fig. 4.5: FTIR of un-hydrated cementitious binder with varying GGBFS, calcined clay and lime sludge.**

#### **4.1.7 FE-SEM - EDAX**

The engineering properties of cement based materials largely depend on their microstructure. Fig. 4.6 shows the SEM images of Portland cement and unhydrated cementitious binders. For Portland cement, crystals were irregular. Morphology seems to be fibrous. Contrary to this, the morphology of cementitious binders based on calcined clay, GGBFS and lime sludge seems to be different because of pozzolana dominancy. Increasing thermo-chemically activated lime sludge in the mix resulted in agglomeration of particles because of its fineness. EDAX of samples was also carried out to know the elemental/oxide composition (Fig. 4.7 & Table 4.6). It was found that CaO content increased and SiO<sub>2</sub> and Al<sub>2</sub>O<sub>3</sub> decreased with increasing thermo-chemically activated lime sludge. CaO/SiO<sub>2</sub> in the mix was in the range of 1.32-5.09. SiO<sub>2</sub>/Al<sub>2</sub>O<sub>3</sub> was in the range of 1.43-3.50 (Table 4.7) which were comparable to composition of aluminosilicate with binder. Na<sub>2</sub>O content in the mix increased with increase in thermo-chemically activated lime sludge. The existence of Na<sub>2</sub>O may be utilised for activation of calcined clay and GGBFS in producing alkali aluminosilicate phase in the binder besides calcium silicate hydrate.



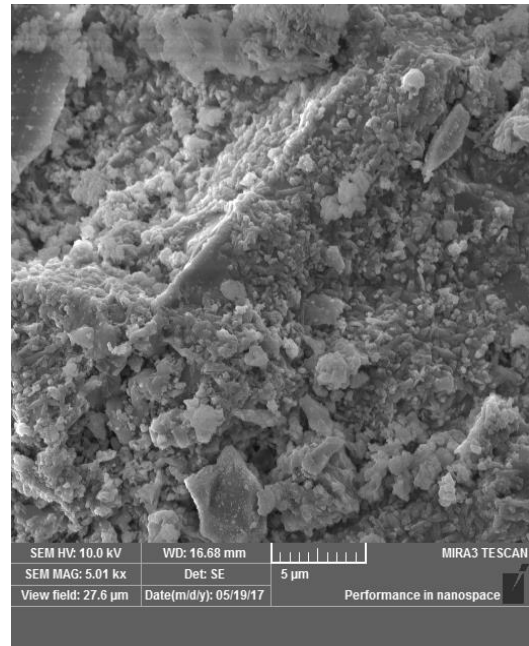
(a)



(b)

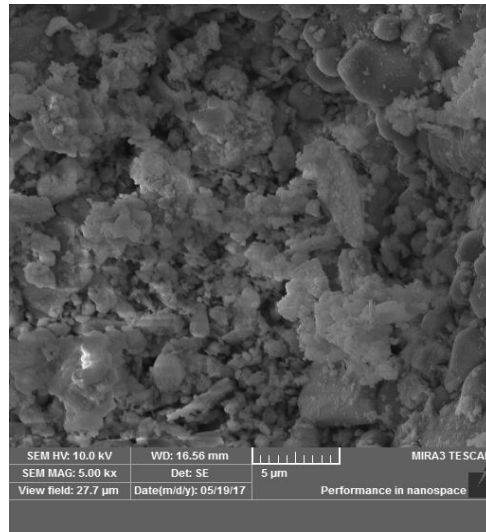


(c)



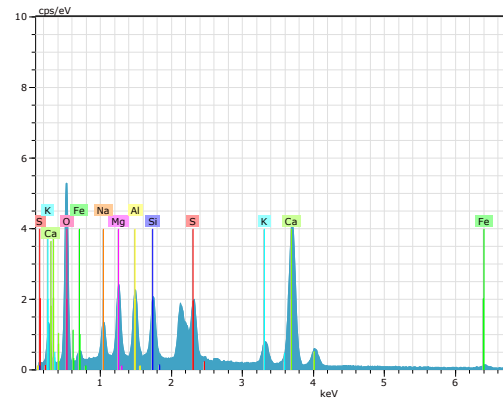
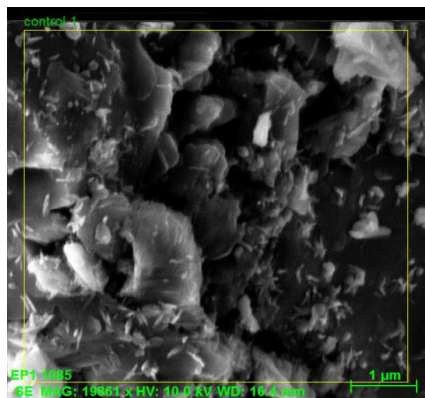
(d)



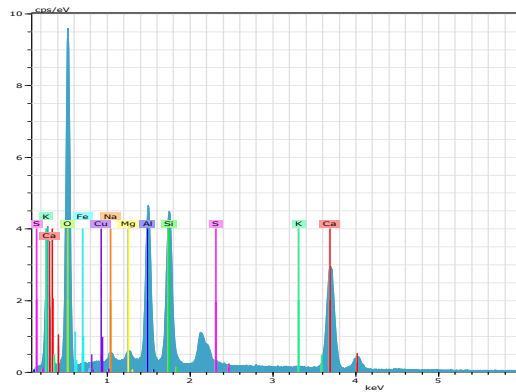
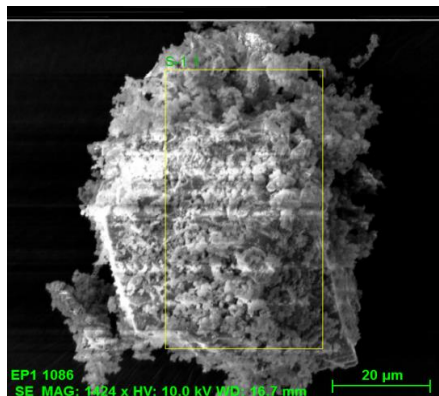


(e)

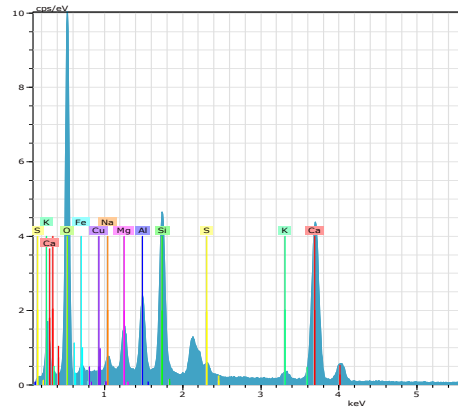
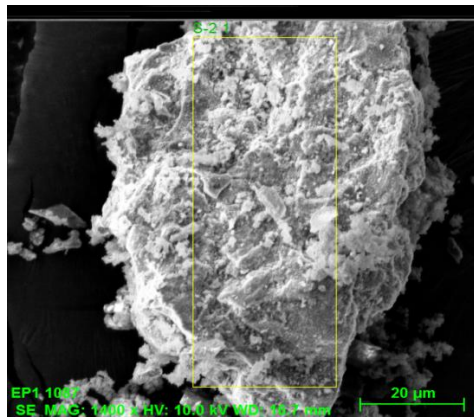
**Fig. 4.6: SEM images of lime sludge based cementitious binder (a) Control (b) sample 1 (c) sample 2 (d) sample 3 (e) sample 4**



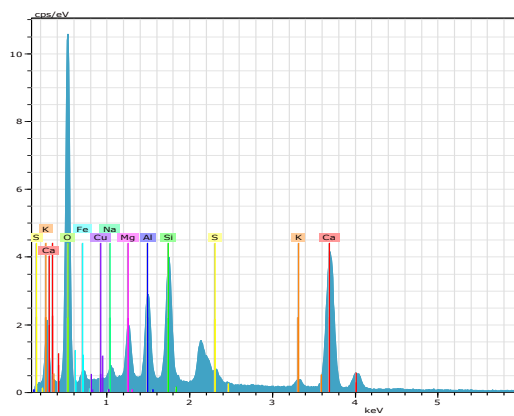
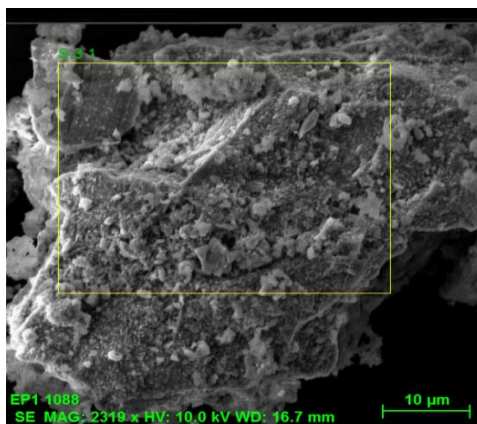
(a)



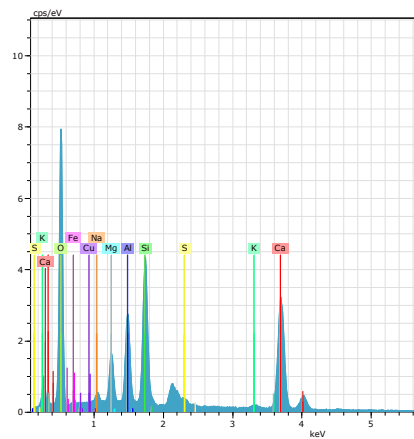
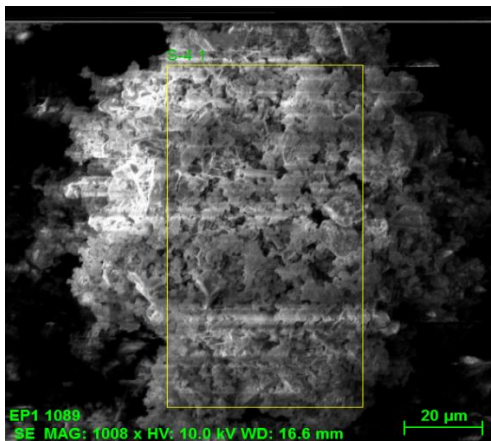
(b)



(c)



(d)



(e)

**Fig. 4.7 EDAX analysis of Portland cement and thermo-chemically activated lime sludge based cementitious binders (a) Control (b) Sample 1 (c) Sample 2 (d) Sample 3 (e) Sample**

**4**

**Table 4.6: EDAX analysis of lime sludge based cementitious binder and Portland cement**

<b>Composition</b>	<b>Sample 1 (%)</b>	<b>Sample 2 (%)</b>	<b>Sample 3 (%)</b>	<b>Sample 4 (%)</b>	<b>Control (%)</b>
CaO	42.79	50.61	50.18	46.67	50.12
SiO <sub>2</sub>	32.45	27.39	22.39	29.70	9.83
Al <sub>2</sub> O <sub>3</sub>	19.66	7.83	10.00	11.39	6.86
Fe <sub>2</sub> O <sub>3</sub>	1.28	3.39	4.43	2.48	6.11
MgO	1.08	4.16	5.32	5.28	6.18
Na <sub>2</sub> O	0.84	1.41	1.48	1.02	2.91
K <sub>2</sub> O	0.19	1.08	1.28	0.68	4.55
SO <sub>3</sub>	1.68	3.54	4.29	2.46	13.44

**Table 4.7: Elemental composition of lime sludge based cementitious binders and Portland cement**

<b>S. NO</b>	<b>Mix</b>	<b>CaO/SiO<sub>2</sub></b>	<b>SiO<sub>2</sub>/Al<sub>2</sub>O<sub>3</sub></b>
1	Portland cement	5.09	1.43
2	Lime sludge based binder 15% Lime sludge	1.32	1.65
3	20% Lime sludge	1.85	3.50
4	25% Lime sludge	2.24	2.24
5	30% Lime sludge	1.57	2.61

#### **4.1.8 Thermal gravimetric analysis (TGA/DTG)**

Thermal gravimetric analysis of Portland cement and cementitious binder containing thermo-chemically activated lime sludge is shown in Fig. 4.8. It can be seen that degradation pattern of Portland cement and lime sludge based cementitious binder were alike. The initial weight loss in the sample was mainly due to moisture loss. The total residue around 800°C was 1.63% in the case of Portland cement, whereas it was 5-9% for lime sludge based cementitious binders. This is attributed to the presence of aluminosilicate based materials (calcined clay/slag). Derivative thermography of lime sludge based cementitious binders showed three decomposition peaks at around 130°C, 400°C and 730°C. The first peak corresponds to dehydration while second small peak was associated with decomposition of amorphous content of slag. Around 800°C, intense peak represents breakdown of skeleton of material. In the case of Portland cement, only two peaks were present, and representing its dehydration and decomposition of alite/belite.

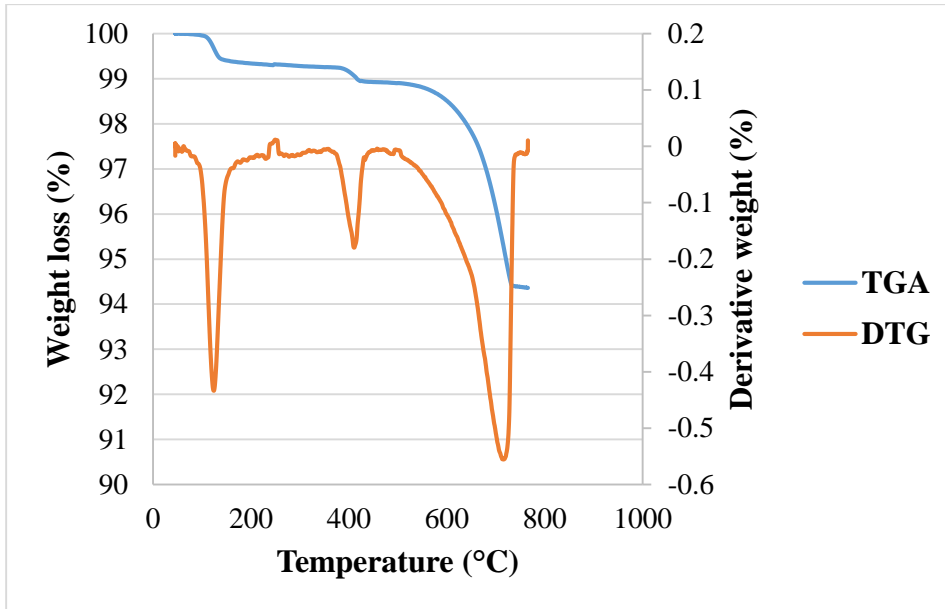
Fig. 4.8 shows the TGA/DTG curve of sample 1 lime sludge based cementitious binders. It was observed that total weight loss up to temperature 770°C is 5.64% due to decomposition of calcium carbonate. And major decomposition peaks were observed at 168°C, 435°C and 800°C.

Fig. 4.9 shows the TGA/DTG curve of Sample 2 lime sludge based cementitious binders. It was observed that total weight loss up to temperature 765°C is 7.17% due to decomposition of calcium carbonate. And major decomposition peaks were observed at 132°C, 408°C and 727°C.

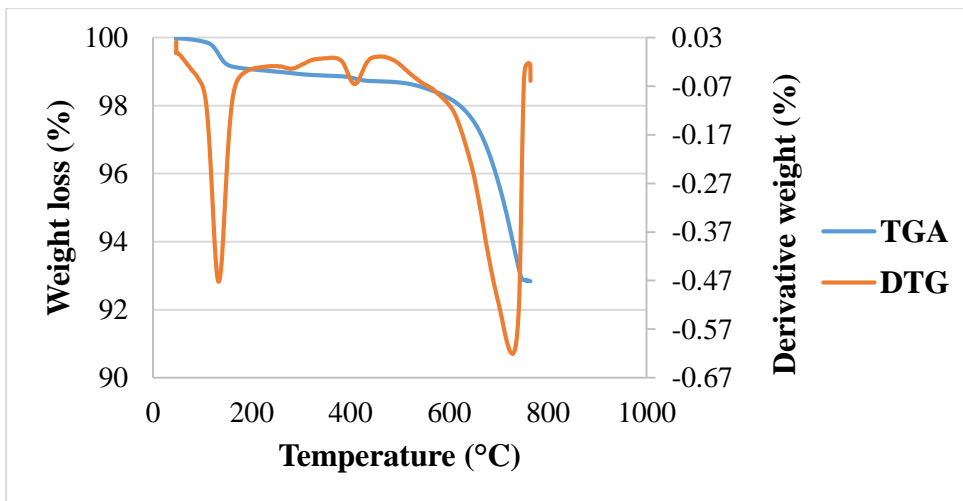
Fig. 4.10 shows the TGA/DTG curve of Sample 3 lime sludge based cementitious binders. It was observed that total weight loss up to temperature 780°C is 7.95% due to decomposition of calcium carbonate. The major decomposition peaks were observed at 129°C, 403°C and 732°C. Also, several decomposition peaks were observed between 129°C and 403°C.

Fig. 4.11 shows the TGA/DTG curve of Sample 4 lime sludge based cementitious binders. It was observed that total weight loss up to temperature 813°C is 8.89% due to decomposition of calcium carbonate. The major decomposition peaks were observed at 124°C, 405°C and 738°C.

Fig. 4.12 shows the TGA/DTG curve of OPC 43 cement sample. It was observed that total weight loss up to temperature 800°C is 1.63% due to decomposition of calcium carbonate. The major decomposition peaks were observed at 126°C and 654°C. Also, several decomposition peaks were observed up to 800°C.



**Fig. 4.8: TGA/DTG curve of Sample 1**



**Fig. 4.9: TGA/DTG curve of Sample 2**

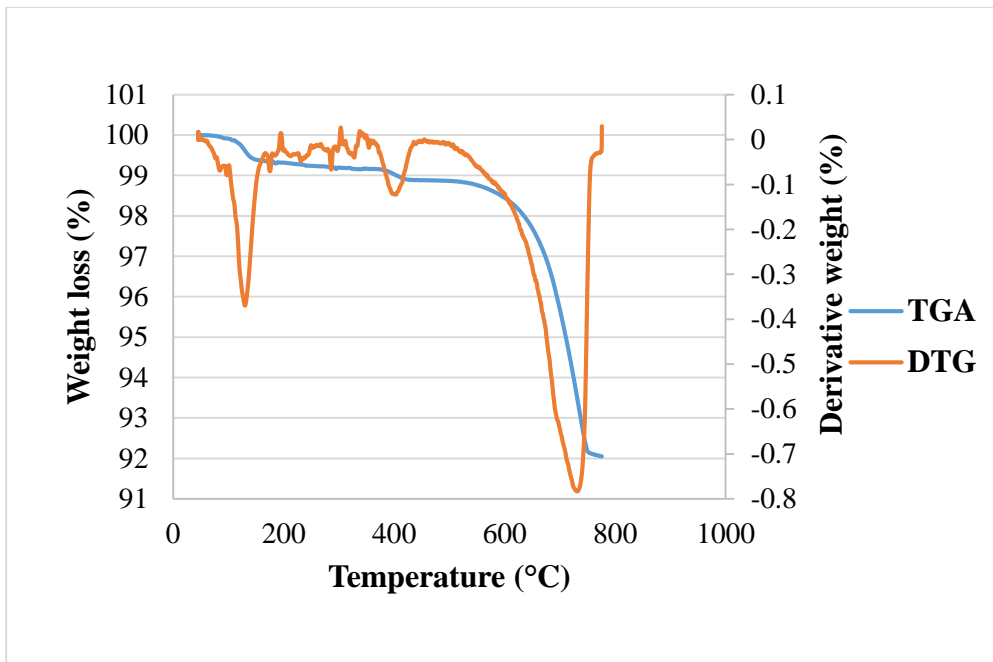


**Fig. 4.10: TGA/DTG curve of Sample 3**

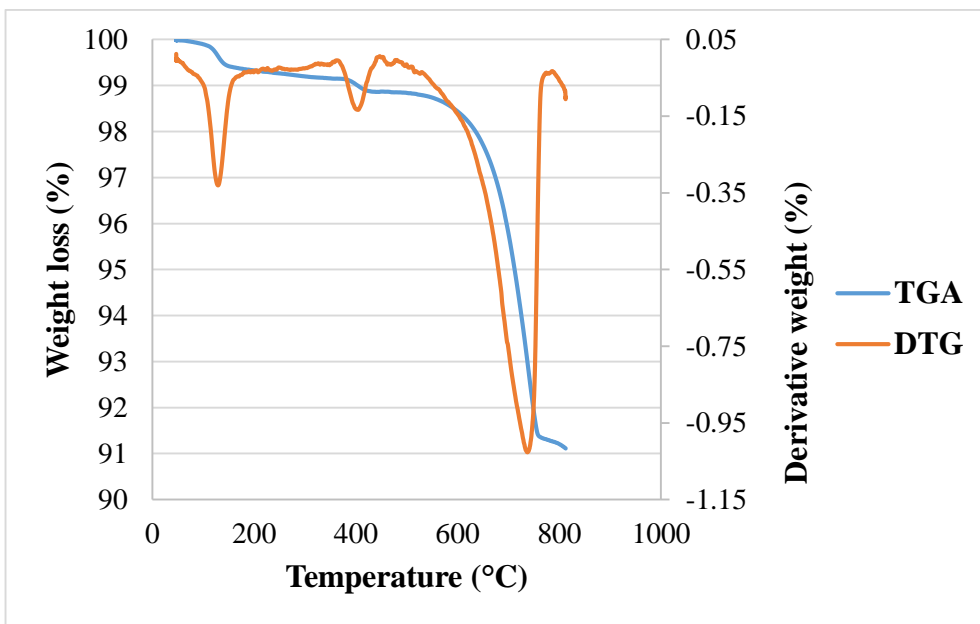


**Fig. 4.11: TGA/DTG curve of Sample 4**

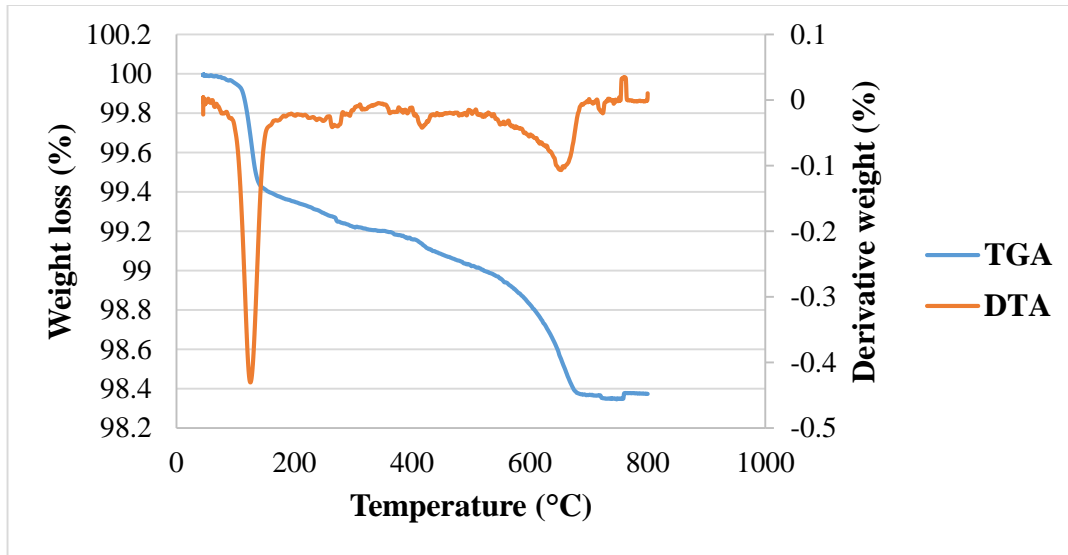


**Fig. 4.12: TGA/DTG curve of OPC 43 cement**

## 4.2 Rheological Studies of binders

Rheological behaviour of thermo-chemically activated lime sludge based cementitious binder was studied with respect to w/c ratio, superplasticizer doses and lime sludge content. It is known that the rheology of cement paste is often categorised by at least two parameters: yield stress and viscosity as defined by Bingham equation (2),

$$\tau = \tau_0 + \mu\gamma \quad \text{----- (2)}$$

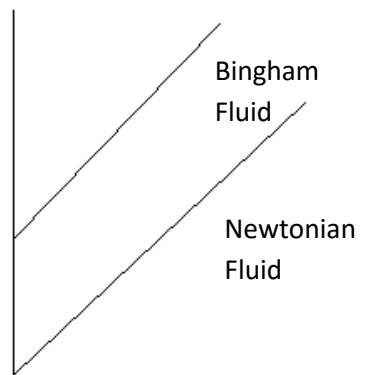


**Fig 4.13: A general flow behaviour of cement paste**

where,  $\tau$  is the shear stress (in Pa),  $\tau_0$  is the yield stress (in Pa),  $\mu$  is the plastic viscosity (in Pa s) and  $\gamma$  is the strain rate (in  $s^{-1}$ ). A general flow behaviour of cement paste can be observed in

Fig. 4.13. Shear stress-shear rate curves of Portland cement and thermo-chemically activated lime sludge based cementitious binder are shown in Fig. 4.14. It was observed that all pastes behaved like Bingham fluid. In each case, a minimum level of yield stress was required to flow. As the lime sludge content was increased, there was no considerable change in the yield stress of the thermo-chemically activated lime sludge based cementitious binder compared to Portland cement except the sample with 25% lime sludge content. The higher value of yield stress indicates its low workability. For all the thermo-chemically activated lime sludge based cementitious binder and Portland cement, the shear stress above 80 Pa was independent of shear rate showing Newtonian plateau.

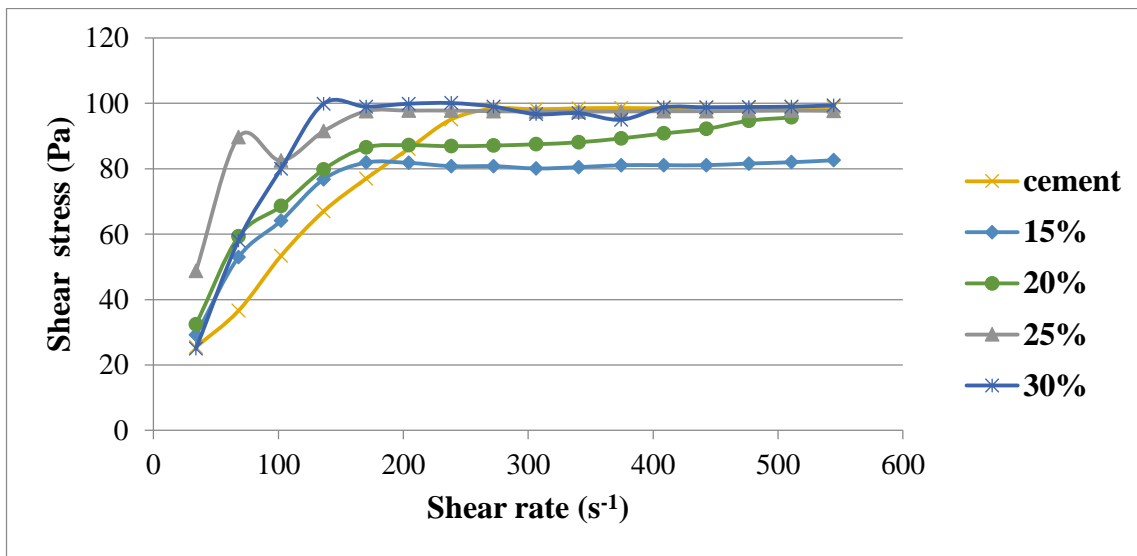
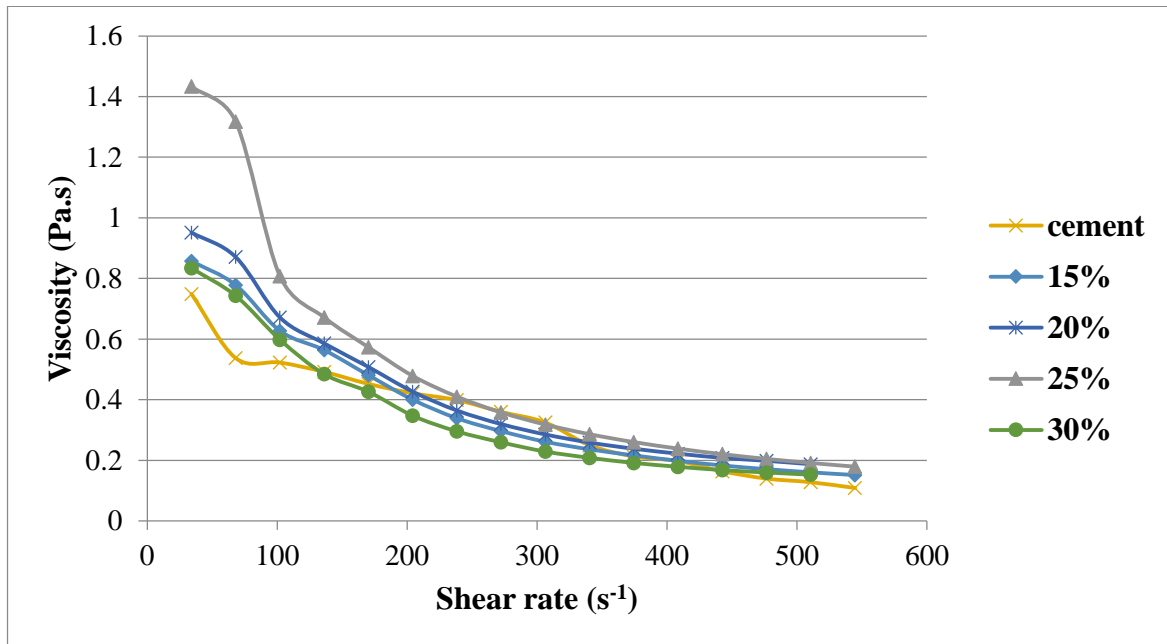


**Fig. 4.14: Shear stress versus shear rate graph of blended cement pastes and OPC 43 cement paste.**

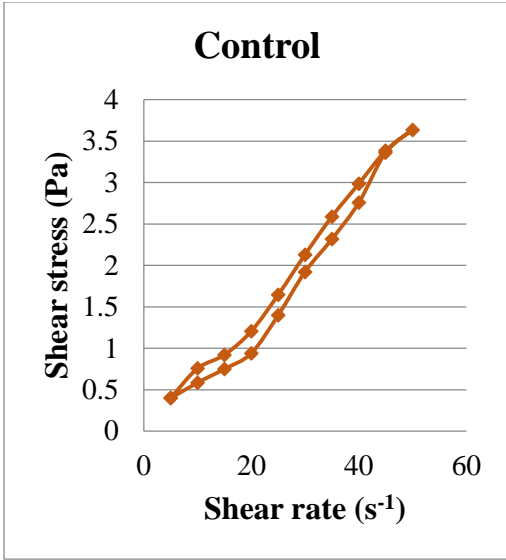
The viscosity of thermo-chemically activated lime sludge based cementitious binder and Portland cement is shown in Fig. 4.15. The pastes exhibited visco-plastic shear thinning behaviour. It was noted that viscosity of pastes decreased with increasing shear rate and then levelled off. The shear rate effect was more pronounced in the case of thermo-chemically activated lime sludge based cementitious binder in comparison to Portland cement. This is because paste tends to make flocs initially and then these flocs are broken down to a large extent as shear rate was increased. A complete dispersion of pastes were observed when a pastes reached minimum viscosity at sufficient pre-shear rate.



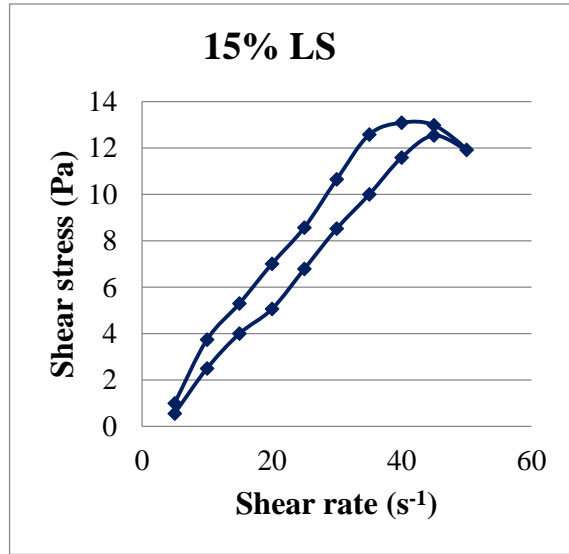
Fig. 4.16 shows hysteresis loop of thermo-chemically activated lime sludge based cementitious binder and Portland cement. In a loop the shear stress of upward curve was higher than the downward curve for all the pastes, supporting partial breaking of bonds in the pastes during shearing. The hysteresis loop area of thermo-chemically activated lime sludge based cementitious binder was higher than the hysteresis loop area of Portland cement. As the lime sludge content was increased in the binder, the area of hysteresis loop also increased. This is attributed to the faster setting of thermo-chemically activated lime sludge based binder. The yield stress of binder increased with the increase of lime sludge probably due to attractive inter-particle forces (flocc. formation) (Fig. 4.17). Experiment was also performed to know the effect of superplasticiser on the rheology of lime sludge based cementitious binder (Fig. 4.18). It was found that at 0.2% of superplasticizer (SP), the paste is not required any force to flow (zero yield stress). Above this level, the superplasticizer is not effective to improve the rheology of lime sludge based cementitious binder probably due to the formation of alkali aluminosilicate phases. The yield stress increased with the increase of SP level.



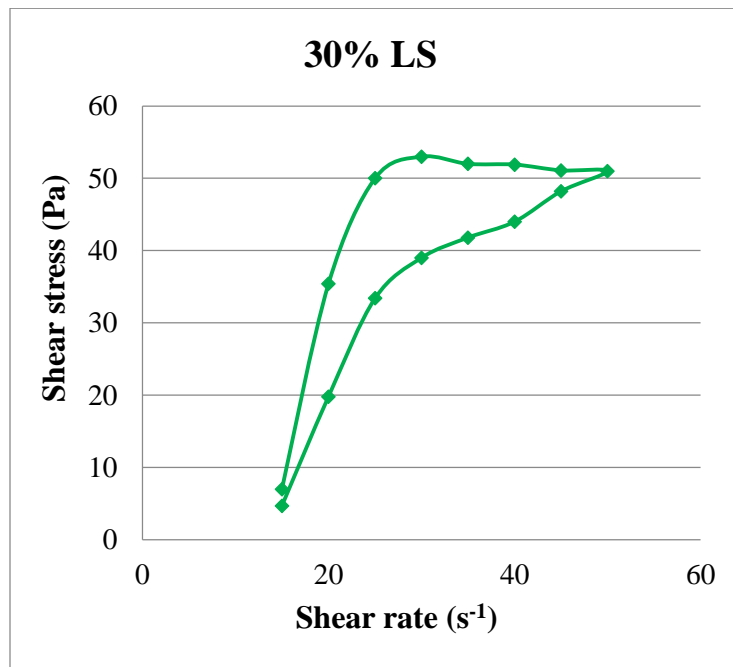
**Fig. 4.15: Viscosity versus shear rate of blended cement pastes and OPC 43 cement paste.**



(a)



(b)



(c)

**Fig. 4.16: Hysteresis loop of shear stress versus shear rate (a) OPC 43 cement paste (b) Blended cement with 15% LS (c) Blended cement with 30% LS**

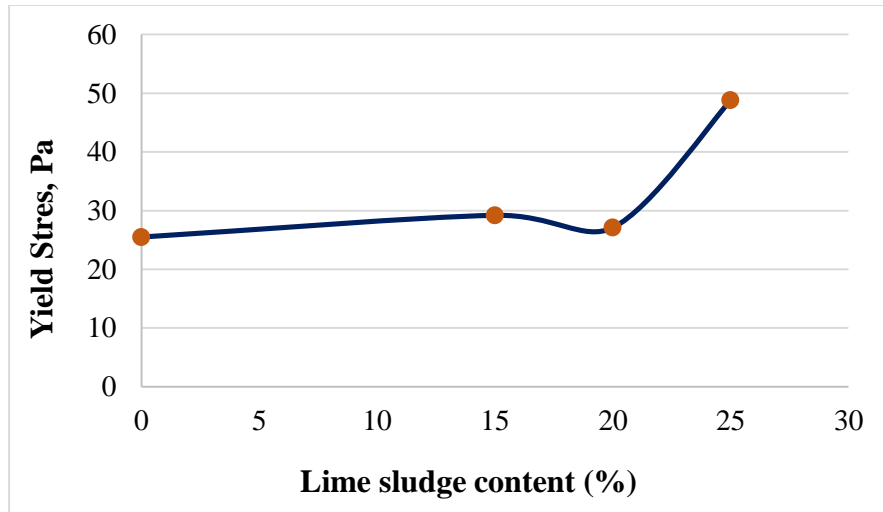


**Fig. 4.17: Yield stress versus lime sludge content**

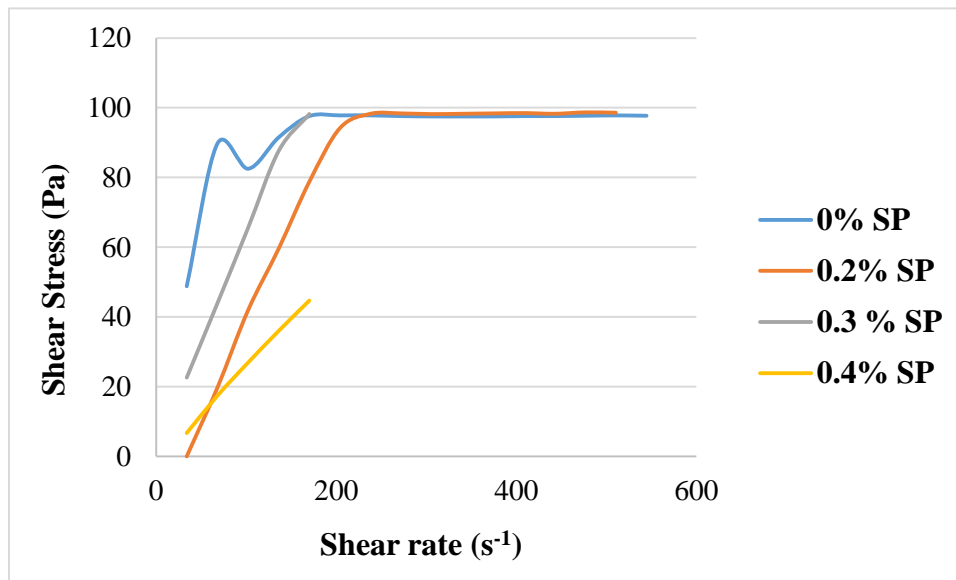


**Fig. 4.18 Shear stress versus shear rate of lime sludge based binder for different superplasticizer doses**

### 4.3 Hydration Studies of binder

Understanding the kinetics of hydration of thermo-chemically activated lime sludge based cementitious binder is crucial in tailoring the materials for desired applications. Depending on the chemistry of the thermo-chemically activated lime sludge based cementitious binder and

grinding process, some acceleration or retardation of the cement hydration might be observed. Longer induction and consolidation time also affects the hydration kinetics of cement paste. The hydration process is divided into four stages as shown in Fig. 4.15, where, rapid initial process is stage 1, the induction period or dormant period is stage 2, acceleration period/setting is stage 3 and retardation period/hardening is stage 4. During the induction period which is within the one hour of adding water, the hydration products formed on the cement grains delay the hydration process to some extent. During this period, cement is workable and this paste is said to be fluid or plastic. The initial setting occurs in the age of 1-3 hours. New hydration products are formed onto the cement grains and hydration products formed in first stage are broken down. Fibrous and strong hydration products are formed. After a while, stiffening of cement paste starts as cement grains become connected. And then stiffness and strength development starts as it approaches hardening process. After some time, reactivity decreases and then finally stops.

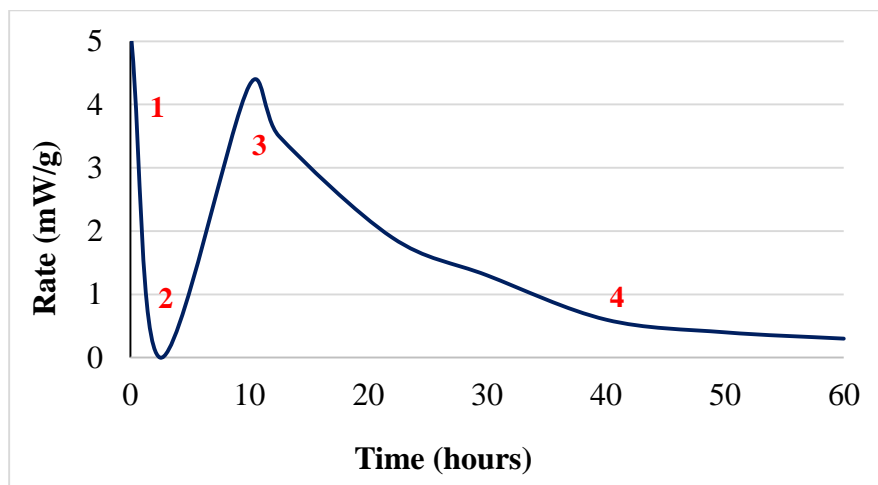


**Fig. 4.19: General representation of hydration of cement paste**

Fig. 4.20 shows the hydration of various cementitious binders. In isothermal calorimetry test, the heat flow rate represents the rate of hydration whereas, cumulative heat evaluation represents the total degree of hydration. The cementitious binders were prepared by cement clinker, GGBFS, calcined clay, fly ash and lime sludge/limestone at 0.4 w/c ratio. The calorimetry response of these pastes observed two peaks, an early dissolution and a later acceleration peak. An early dissolution peak is due to wetting and dissolution of cement

particles. The dormant period after this peak is followed by an acceleration peak which is due to rapid dissolution of alite and the precipitation of calcium silicate hydrate and calcium hydroxide phases. It was observed that dormant period of cement Portland cement was more than the lime sludge based cementitious binder showing its better workability. However, when compared with LC3 (limestone calcined clay cement, Mix 4), the induction period of lime sludge based cementitious binder was more showing it more workable. The setting time calculated from acceleration peak was also more for lime sludge based cementitious binder. The acceleration peak of lime sludge based cementitious binder was splitted compared to Portland cement mainly due to an indicating presence of several strength forming phases. Fig. 4.21 shows total heat released for various cementitious binders. It was found that the reaction product formed in slag based system was more than those of others. The higher the reaction product formation, the higher the strength of the cementitious binder.

Fig. 4.22 shows the normalised heat flow curve of cementitious binders with varying lime sludge and pozzolana content. It was observed that induction period for all the cementitious binders was less than that of portland cement. The acceleration peak was also shifted compared to portland cement. The setting time calculated from acceleration peak was also faster than the portland cement. It is also noted that the height of acceleration peak for lime sludge based binder was more than that of portland cement showing higher reaction product formation for strength development.

Fig. 4.23 shows hydration of cementitious binders with different percentage of thermo-chemically activated lime sludge. It was observed that acceleration peak for lime sludge based binders appeared earlier than the Portland cement showing its faster setting time. The height of acceleration peak was also more than that of Portland cement showing more strength forming phases. Induction period was also reduced as compared to Portland cement. Fig. 4.24 shows cumulative heat released for hydration of cementitious binder as a function of time. It was found that the total heat of Portland cement was more than that of lime sludge based binder after 3 days. It is expected that when the reaction is extended, the reaction product formation in the lime sludge based binder was higher than the Portland cement because of increased acceleration peak height in the heat flow curve. This suggest that the developed binder can be suitably used as an alternative to Portland cement.

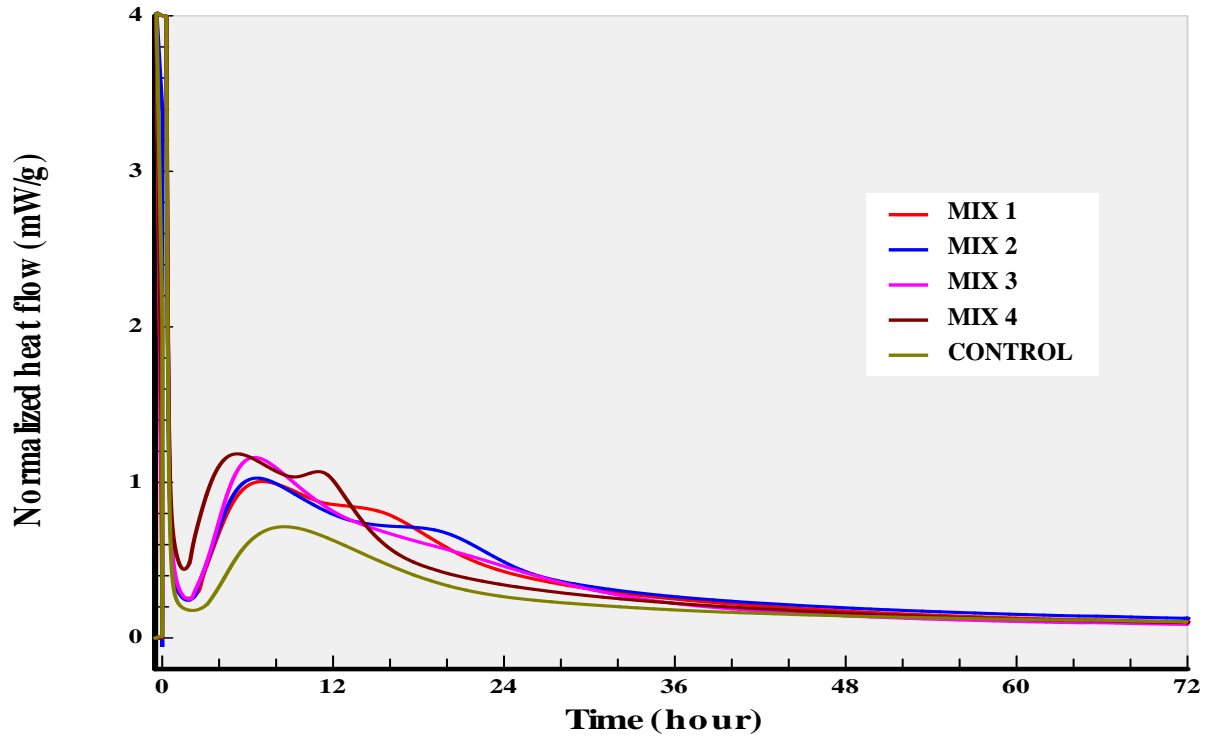


Fig. 4.20: Normalised heat flow versus time curve of blended cements with different pozzolana

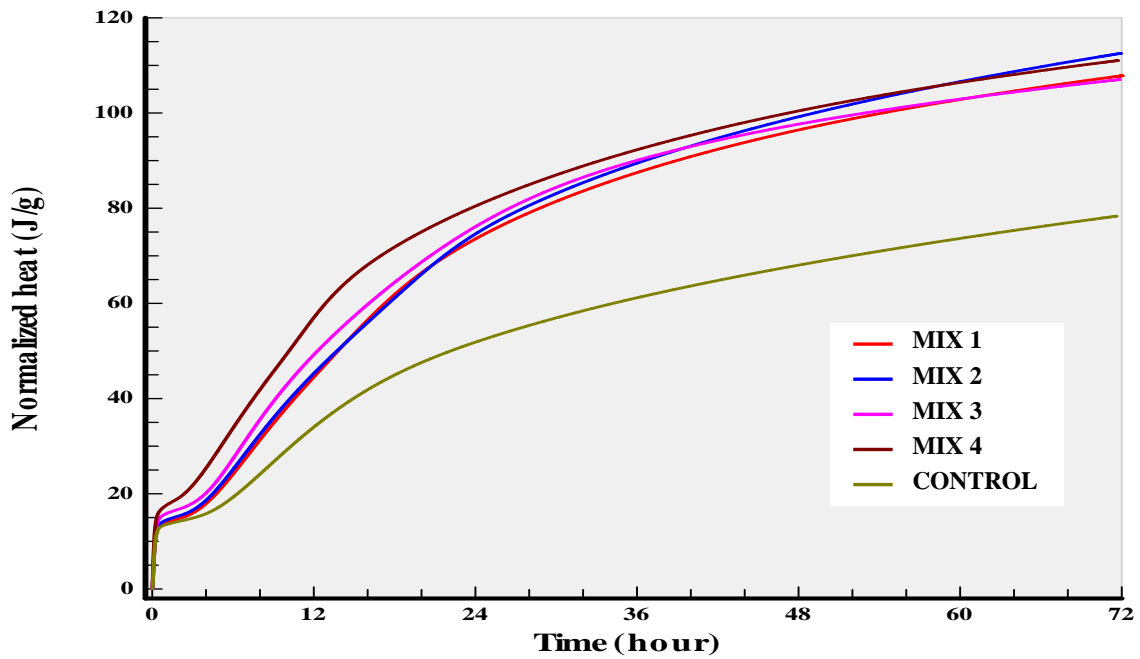


Fig. 4.21: Normalised heat versus time curve of blended cements with different pozzolana

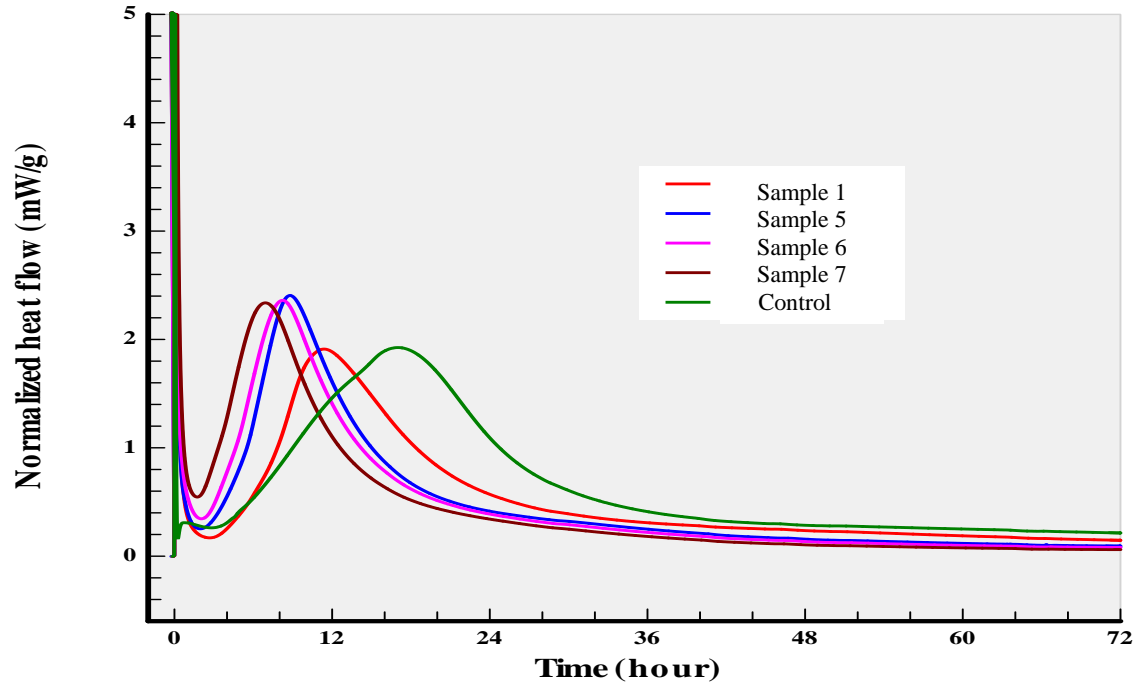


Fig. 4.22: Normalised heat flow versus time curve of blended cements with varying lime sludge and pozzolana content

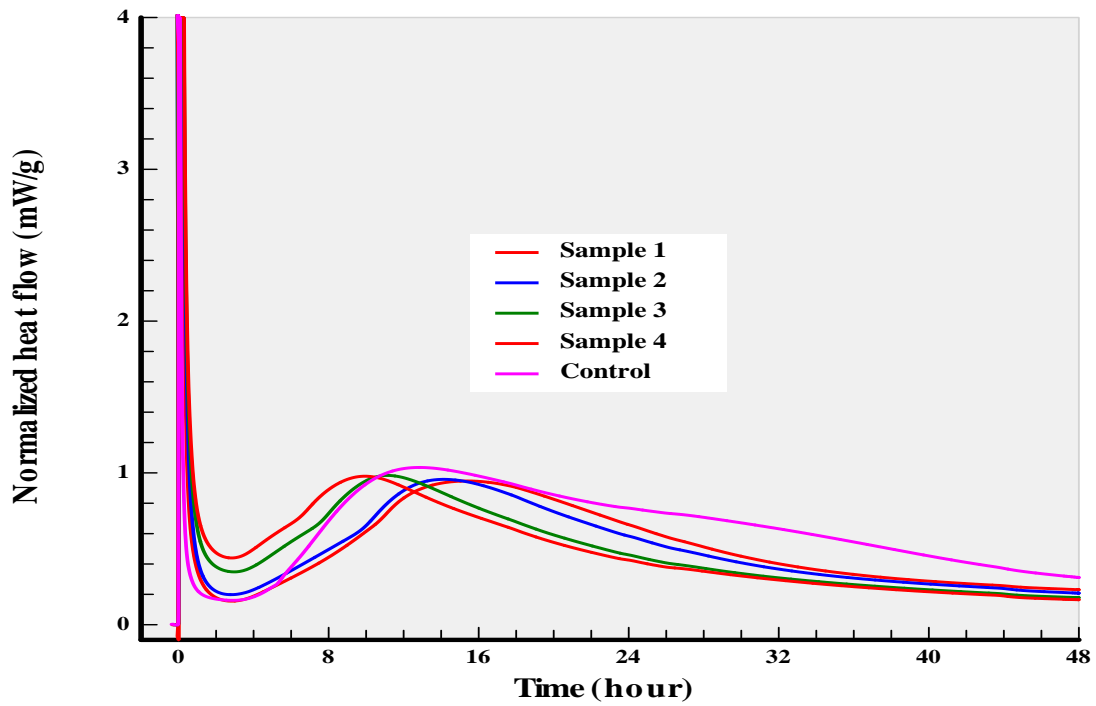
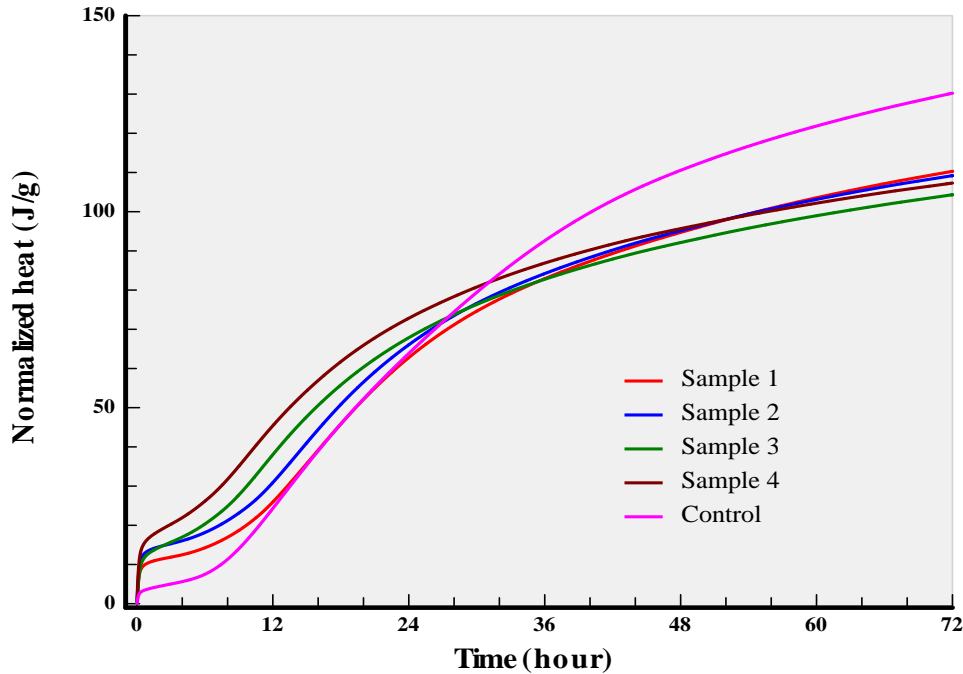


Fig. 4.23: Normalised heat flow versus time for optimised mix with varying lime sludge content



**Fig. 4.24: Normalised heat versus time for optimised mix with varying lime sludge content**

## **4.4 Properties of lime sludge based cementitious binders**

### **4.4.1 Specific Gravity**

The specific gravity of lime sludge based cementitious binders and Portland cement is given in Table 4.8. It was observed that increasing lime sludge in the mix, increased the density of resulting mix. The specific gravity of lime sludge based cementitious binders was comparable to Portland cement.

### **4.4.2 Soundness**

It is reported that the Portland cement after setting should not undergo any appreciable change in volume. Certain cements undergo a large expansion after setting which will cause disruption in set and hardened mass. Due to this expansion, durability of structures is affected. The unsoundness of cement is caused due to presence of excessive lime, or high proportion of magnesium or calcium sulphate content. Other factors responsible for unsoundness of cement are inadequate burning of cement clinker and insufficiency in grinding and inter-grinding



process. For the considerable period of time, unsoundness does not come to the surface therefore accelerated tests are required to detect expansion.

**Table 4.8: Specific gravity of lime sludge based cementitious binders.**

S.NO	Mix	Specific gravity
1	Portland cement	3.08
2	Clinker 55%, Pozzolana 30%, Lime Sludge 15%	3.10
3	Clinker 55%, Pozzolana 30%, Lime Sludge 20%	3.15
4	Clinker 55%, Pozzolana 30%, Lime Sludge 25%	3.20
5	Clinker 55%, Pozzolana 30%, Lime Sludge 30%	3.25

\* Pozzolana: calcined clay and GGBFS in equal ratio

The soundness test of lime sludge based binders was carried out as per IS: 4031 (part 3) using Le-Chatelier method (Table 4.9). It was observed that the values obtained for various mixes were in the range of 0.27-5.45 mm which were under the permissible limit of maximum 10 mm mentioned in the IS: 269-2015. This suggested that all the mixes were sound. Higher values in certain mixes compared to Portland cement may be due to reduction in pozzolana content and increase in lime sludge content, which will leave free available unreacted lime in cement paste.

#### **4.4.3 pH**

The pH of cement plays a critical role in the chemistry of concrete. It should be in the range of 11-13 to maintain alkaline environment in concrete. Table 4.10 shows pH of various lime sludge based cementitious binders. It was found that the values were in the range of 11.8-12.4 which were comparable to the Portland cement (pH 12.03). Under aggressive environment, the sulphate, chloride and acid penetrate through micro-cracks into the concrete and attack its

surrounding materials which will result in lowering of their pH. If pH of cement drops, the passivity of reinforcement is affected. The concrete is also carbonated in case of low pH.

**Table 4.9: Soundness of lime sludge based binder**

S.NO.	Mix	Soundness (mm)
1	Portland cement	0.91
2	Clinker 55%, Pozzolana 25%, Lime Sludge 20%	1.17
3	Clinker 55%, Pozzolana 20%, Lime Sludge 25%	2.62
4	Clinker 55%, Pozzolana 15%, Lime Sludge 30%	5.45
5	Clinker 55%, Pozzolana 30%, Lime Sludge 15%	0.69
5A	Lime Sludge 20%	0.27
5B	Lime Sludge 25%	0.35
5C	Lime Sludge 30%	0.95

\*Pozzolana: calcined clay and GGBFS in equal ratio

**Table 4.10: The pH of lime sludge based cementitious binders.**

S.NO.	Mix	pH
1	Portland cement	12.03
2	Lime sludge based cementitious binder - 15% Lime Sludge -20% Lime Sludge -25% Lime Sludge -30% Lime Sludge	11.79 11.93 12.33 12.38

#### 4.4.4 Consistency and setting time

Consistency of lime sludge based cementitious binder was determined according IS: 4031 (Part 4) using Vicat's apparatus. The results of various mixes are given in Table 4.11. It was found that the consistency lies in the range of 34-36%. On comparing with Portland cement, the consistency of lime sludge based binders was 6-8% higher due to its large surface area. The initial setting time as measured according to IS 4031 (part 5) was found in the range of 35-40 min. It was noted that increasing thermos-chemically treated lime sludge in the mix resulted in increase in setting time probably due to involvement of lime sludge in the hydration process. Contrary to this, the final setting time decreased with the increase of lime sludge in the mix due to involvement of pozzolonic activities. When compared with the Portland cement, lime sludge based binder exhibited lower initial and higher final setting time. The setting time of lime sludge based binders satisfied the requirement of IS: 269-2015 (Initial setting time min. 30 minutes and final setting time max. 600 minutes).

**Table 4.11: The initial and final setting time of lime sludge based blended cements**

<b>Mix</b>	<b>Consistency (%)</b>	<b>Initial setting time (min)</b>	<b>Final setting time (min)</b>
Lime sludge based cementitious			
- Lime Sludge 15%	34.5	35	420
- Lime Sludge 20%	35	35	360
- Lime Sludge 25%	35.5	45	405
- Lime Sludge 30%	36	40	390
Portland cement	28	70	360

#### 4.4.5 Compressive Strength

The compressive strength of thermo-chemically activated lime sludge based binders was determined according to IS 4031 (part 6). The consistency of various mixes was kept at around 34%. Fig. 4.25 shows compressive strength of various mixes. At 7 days, it was found in the range to 29 to 36 MPa whereas at 28 days the values were in the range of 35 to 46 MPa. After comparative evaluation, it was found that the slag containing lime sludge based cementitious binder gave highest compressive strength. On comparing, the value of compressive strength of lime sludge based binder was ~ 12% lower than the Portland cement. In the optimised mix, the thermo-chemically activated lime sludge was added up to a level of 30% into the mix. It was found that increasing lime sludge into the mix resulted in decrease of compressive strength. At higher addition level, lime sludge act as a filler in the system playing negative role in the strength development of the binders.

In another attempt, the lime sludge based binders were formulated by varying pozzolana and lime sludge content for optimisation of mix (Fig. 4.26). The compressive strength of these binders was tested at the age of 7, 14 and 28 days. At 7 days, the value of compressive strength was lying in the range of 21 to 36 MPa. At 14 days, these values were increased ranging between 26 to 45 MPa. At 28 days, the compressive strength of lime sludge based cementitious binder were comparable to Portland cement. Because of this, Sample 1 was identified as optimised mix for lime sludge based cementitious binder.

The strength development in the lime sludge based binder is explained with the help of FTIR, TGA and FE-SEM. FTIR spectra showed the absorption band at  $990\text{ cm}^{-1}$  (Si-O),  $1120\text{ cm}^{-1}$  (Si-O-Si),  $1450\text{ cm}^{-1}$  (O-C-O),  $1650\text{ cm}^{-1}$  ( $\text{H}_2\text{O}$ ) and  $3450\text{ cm}^{-1}$  (-OH) (Fig. 4.28). In Portland cement, the small peak at  $990\text{ cm}^{-1}$  due to CSH phase was obscured from other peaks (ettringite), while in lime sludge based binders, the peak was broaden and intense. The splitting of this peak clearly indicated the existence of mixed phases of CSH and (Ca Na) ASH (formed due to geo-polymerization of calcined clay/slag). The higher intensity of this peak resulted in formation of increased reaction products compared to Portland cement. Because of this, the binder gained adequate strength. In addition to this, an intense peak at  $1450\text{ cm}^{-1}$  related to carbonate occurred due to reaction between the alkali and atmospheric air. The lime sludge based binder also exhibited intense hydroxyl peak at  $3450\text{ cm}^{-1}$  compared with Portland cement

probably due to entrapped water in the cavities formed as a result of geo-polymerization reaction.

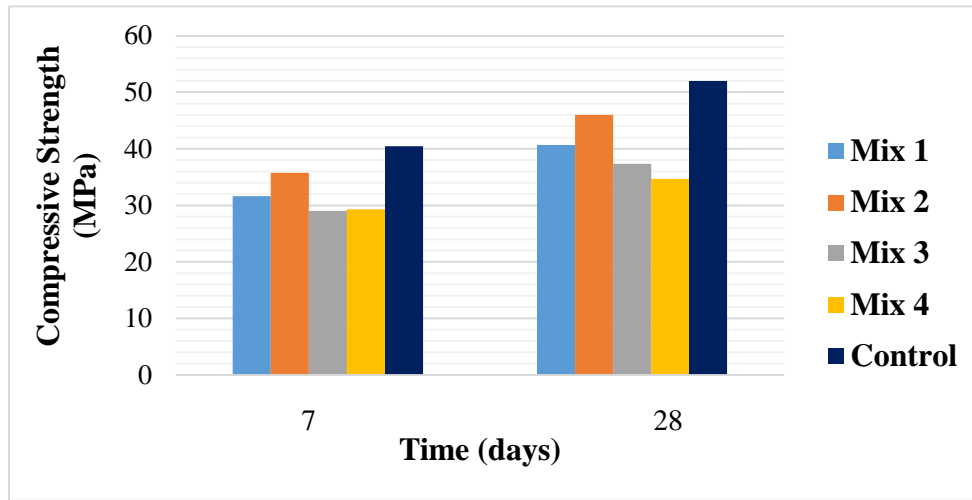


**Fig. 4.25: Compressive strength versus time graph for blended cements with different pozzolana**

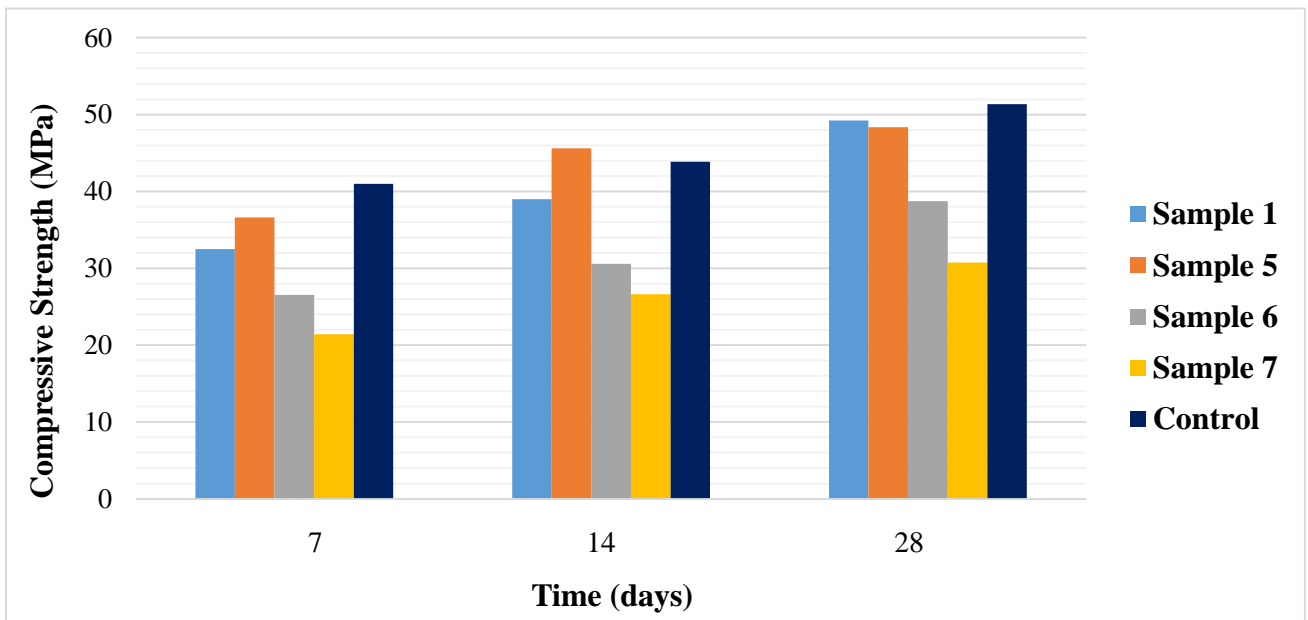


**Fig. 4.26: Compressive strength versus time graph for blended cement with varying lime sludge and pozzolana content**

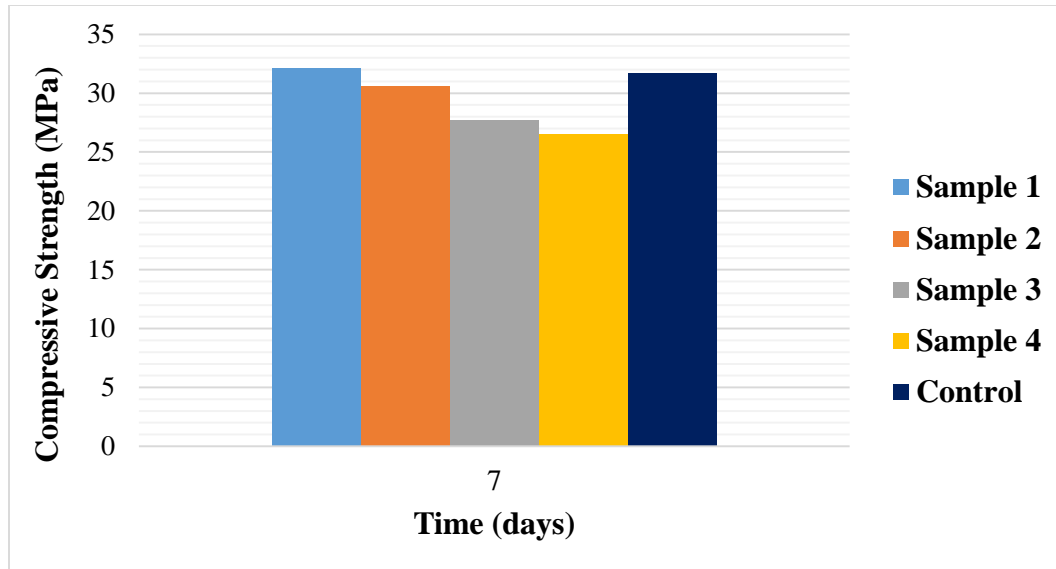


**Fig. 4.27: Compressive strength versus time graph for blended cement with varying lime sludge content**

TGA also supported phase development in the binders (Fig. 4.29 & Fig. 4.30). DTG peak at 461°C showed a peak corresponding to calcium hydroxide decomposition which is smaller in the case of lime sludge binder than Portland cement. This suggested that CSH phase formed in lime sludge based binder was smaller than the Portland cement. Lime sludge based binder showed a plateau between 250 – 700 °C indicating that the reaction products formed as a result of hydration/geopolymerization were thermally stable. No degradation occurred in this temperature range. Contrary to this, Portland cement exhibited a continuous weight loss in the samples probably due to the decomposition of CSH as well as hydrated aluminate phases besides CO<sub>2</sub> emission. (Fig. 4.29 shows the TGA/DTG curve of hydrated cement paste. It was observed that at about 115°C, all the physically bounded water gets evaporated. At about 461°C, decomposition of calcium hydroxide takes place. About 19.2% weight loss was observed up to 750°C. Fig. 4.30 shows the TGA/DTG curve of hydrated blended cement paste of Sample 1. It was observed that at about 112°C, all the physically bounded water gets evaporated. At about 449°C, decomposition of calcium hydroxide takes place. About 23.95% weight loss was observed up to 740°C. Another decomposition peak was observed at 709°C). As also evidenced in FE-SEM (Fig. 4.31), Portland cement showed fibrous and prismatic type features in the microstructure showing presence of CSH, ettringite and another phases. Voids

were also seen in the microstructure. Contrary to this, lime sludge based binder showed needle and plate type of crystals along with some agglomeration of particles. These features can be useful in correlation with strength development in both the binders.

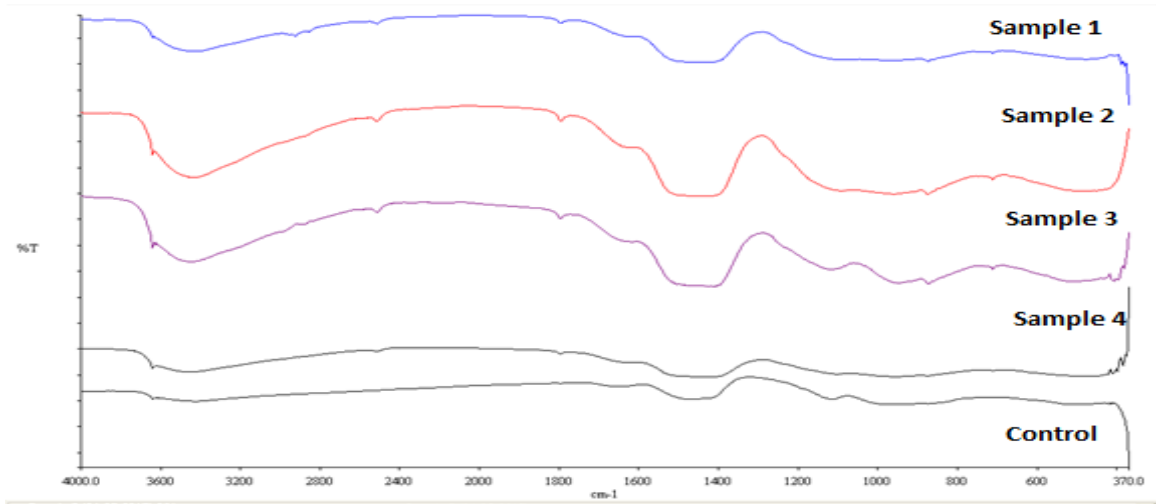


**Fig. 4.28: FTIR spectra of hydrated cementitious binders.**

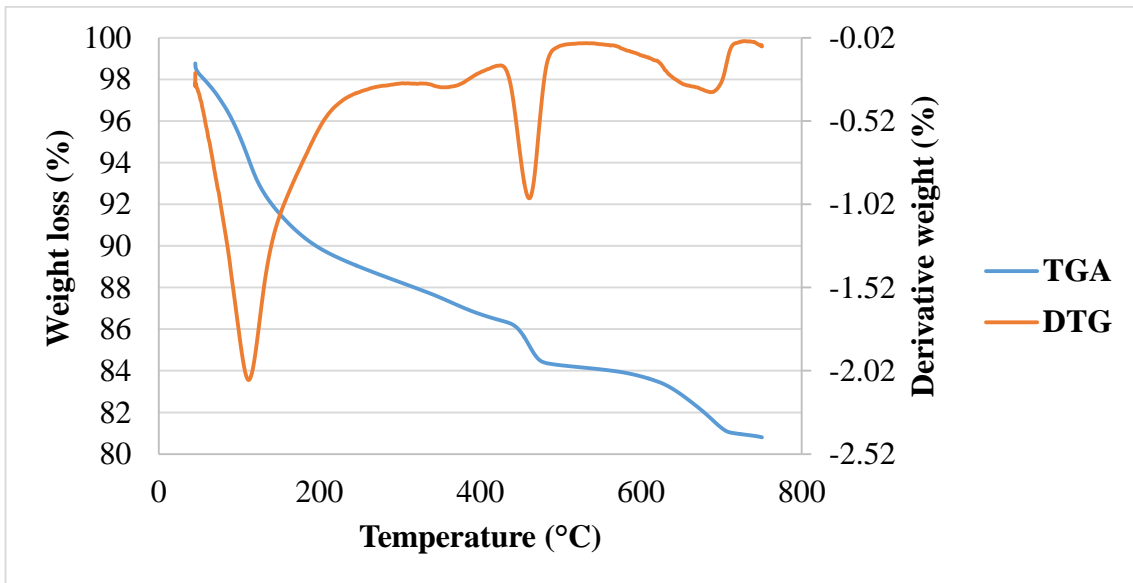


**Fig. 4.29: TGA curve of hydrated cement paste**

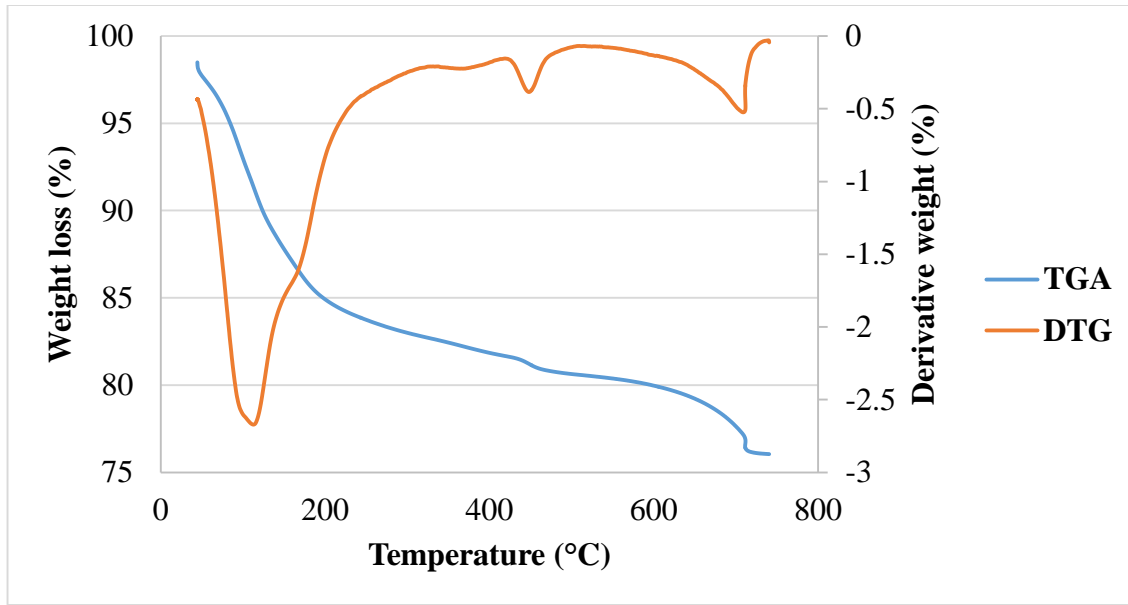
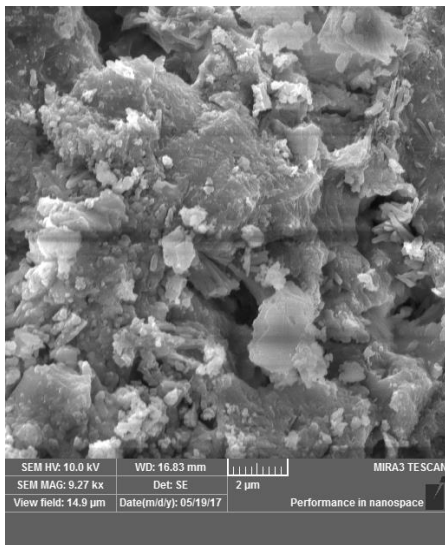
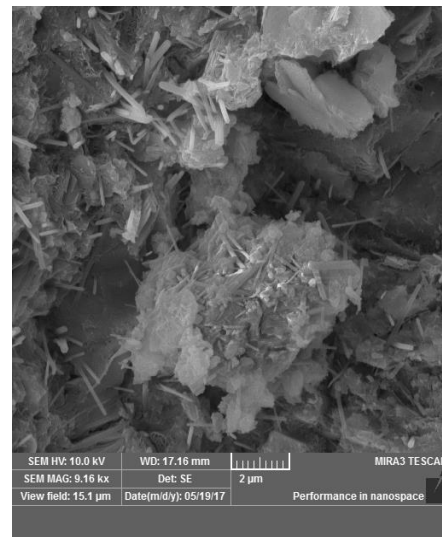


**Fig. 4.30: TGA curve of hydrated lime sludge based binder.**



(a)



(b)

**Fig. 4.31: FE-SEM images of hydrated cementitious binder (a) Portland cement (b) lime sludge based binder**



Suitability of developed binder was assessed with the requirements of IS: 269-2015 of Portland cement. It was found that physical properties of lime based binder satisfied the requirement of IS: 269-2015 of OPC 43 grade. It can be concluded that lime sludge based binder can be suitably used as an alternative to Portland cement for manufacturing of mortar/concrete (Table 4.12).

**Table: 4.12 Comparative properties of lime sludge based binder and ordinary Portland cement**

<b>Property</b>	<b>Ordinary Portland cement (IS: 269-2015) Required value</b>	<b>Lime sludge based cementitious binder</b>
<b>Setting time</b> <b>-Initial (min.)</b> <b>-Final (max.)</b>	30 600	35 420
<b>Fineness (min.) (m<sup>2</sup>/kg)</b>	225	561
<b>Soundness (max.) (mm)</b>	10 (max.)	0.69
<b>Compressive Strength (MPa)</b> <b>7 days</b> <b>28 days (min)</b> <b>(max)</b>	33 43 58	32.51 49.23

## 4.5 Life cycle assessment

The most common approach to assessing potential environmental impact is the method of life cycle assessment (LCA). LCA is the cross-media approach and allows for a more holistic investigation of product and services. LCA examines the product from extraction of raw materials to its production and use of the product, to its final disposal. The product life cycle is shown in Fig. 4.32.

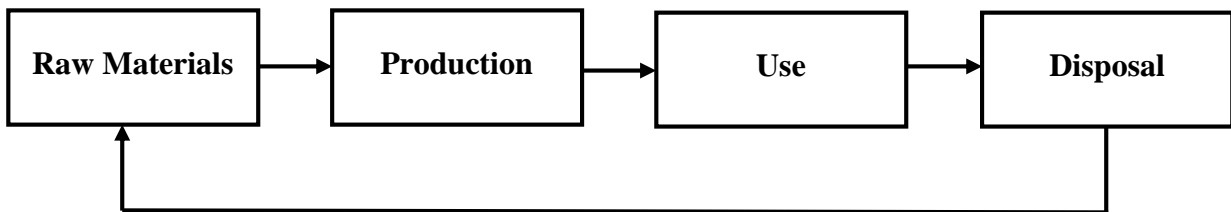


**Fig. 4.32 Product Life Cycle**

A LCA comprises of four major steps:

- a) **Goal and scope:** This step defines the objective and intended application of the investigation (Provis and Deventer, 2009)
- b) **Inventory analysis (LCI):** This step indicates all the inputs and outputs of a product or service system. All raw material consumption and energy are considered on the input side whereas all products and emission into air, water and soil are considered on output side.
- c) **Impact assessment (LCIA):** This step evaluates the potential environmental impacts associated with inputs and outputs determined by the LCI. Some of the impact categories are given below:
  - Depletion of resources (abiotic depletion potential)
  - Acidification (acidification potential)
  - Climate change (global warming potential)
  - Ozone depletion (ozone depletion potential)
  - Human toxicity (human toxicity potential)

*d) Interpretation:* This step identifies significant environmental impacts (e.g., ozone layer depletion, energy use, greenhouse gases) as well as significant unit processes in the system.

In this work, SimaPro 7.0 software was used for LCA. It is a qualified tool which provides you to focus, analyse and monitor the sustainability performance of products and their services. By using SimaPro, one can measure the environmental impact of any product across its life cycle. Table 4.13 shows the weight per m<sup>3</sup> of raw materials taken for lime based cementitious binder. Fig. 4.33 shows the input parameters of lime based cementitious binder in the SimaPro 7.0 software for LCA.

OPC 43 Cement paste production: For processing in the software, the desire information for OPC 43 cement are given in Table 4.14 and Fig. 4.34. The values obtained from different inventories are given in Table 4.15

**Table 4.13: Composition of lime sludge based cementitious binder in LCA**

<b>Material</b>	<b>Quantity (kg/m<sup>3</sup>)</b>
Cement	215.11
Lime Sludge	58.67
GGBFS	58.67
Calcined clay	58.67
Water	116.36

**Table 4.14: Composition of OPC 43 cement paste**

Material	Quantity (kg/m <sup>3</sup> )
Cement	449.27
Water	102

The screenshot displays the SimaPro 7.0 interface with the 'Products' section active. The 'Blended cement' product is selected, showing a quantity of 1 m3. The 'Inputs' section lists the following materials and their quantities:

Name	Amount	Unit	Distribution	SD^2 or 2*SDMin	Max	Comment
Portland cement, strength class Z 42.5, at plant/CH U	215.11	kg	Undefined			
slag	58.64	kg	Undefined			
Water, decarbonised, at plant/RER U	116.36	kg	Undefined			
Clay, at mine/CH S	58.67	kg	Undefined			
Lime, from carbonation, at regional storehouse/CH S	58.67	kg	Undefined			

**Fig. 4.33 Lime sludge based binder production in SimaPro 7.0**

Fig. 4.35 shows LCA of lime sludge based cementitious binder and corresponding Portland cement. It was observed that by using lime sludge based binder instead of conventional OPC 43 grade cement, global warming caused by carbon dioxide emission was decreasing by 51% and ozone layer depletion which was due to emission of chlorofluorocarbon (CFC) was decreased by 48.88%. Abiotic depletion decreased to a level of 50.115%. Acidification which was generally due to sulphur dioxide (SO<sub>2</sub>) emission was reduced by 50.56

**Table 4.15: Utilised inventories with data source in SimaPro 7.0**

Process	Data Source
Portland cement	Ecoinvent
Lime sludge	Ecoinvent
GGBFS	Literature
Calcined clay	Ecoinvent
Water	Ecoinvent

Products							
Known outputs to technosphere. Products and co-products							
Name	Amount	Unit	Quantity	Allocation %	Waste type	Category	
control	1	m3	Volume	100 %		Construction	
(Insert line here)							
Known outputs to technosphere. Avoided products							
Name	Amount	Unit	Distribution	SD^2 or 2*SD Min	Max	Comment	
(Insert line here)							
Inputs							
Known inputs from nature (resources)							
Name	Sub-compartment	Amount	Unit	Distribution	SD^2 or 2*SD Min	Max	Comment
(Insert line here)							
Known inputs from technosphere (materials/fuels)							
Name	Amount	Unit	Distribution	SD^2 or 2*SD Min	Max	Comment	
Portland cement, strength class Z 42.5, at plant/CH U	449.27	kg	Undefined				
Water, decarbonised, at plant/RER U	102	kg	Undefined				
(Insert line here)							
Known inputs from technosphere (electricity/heat)							
Name	Amount	Unit	Distribution	SD^2 or 2*SD Min	Max	Comment	
(Insert line here)							
Outputs							

**Fig.4.34 OPC 43 cement paste production in SimaPro 7.0**

Terrestrial ecotoxicity refers to impact of products and services on the land due to disposal, it was reduced by 51.62%. Photochemical oxidation refers to reaction of chemical change in a substance which leads to loosing its electrons, it is associated with light (UV rays). It was

reduced by 50.61% in lime sludge based binder as compared to same quantity of OPC 43 cement.

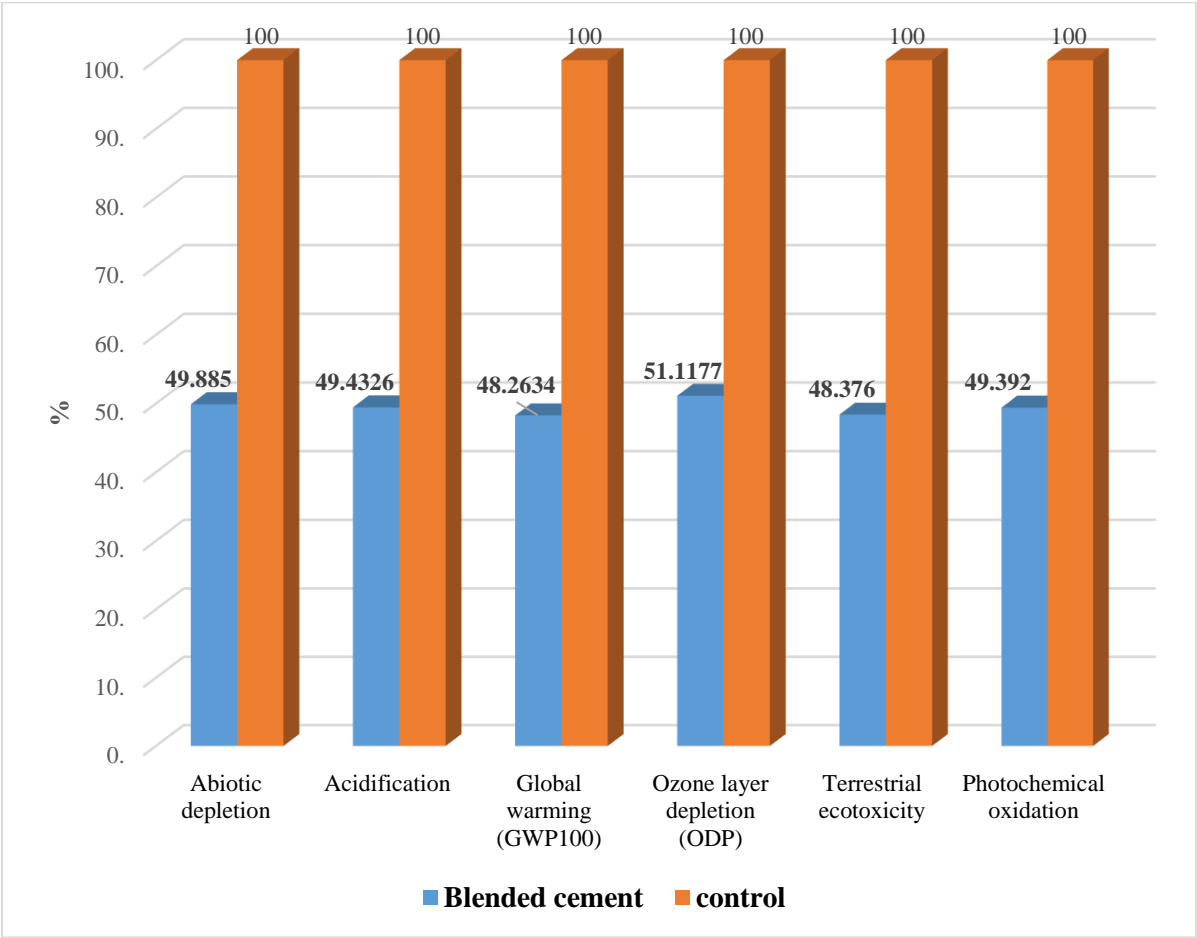


Fig. 4.35: LCA of blended cement and OPC 43 cement

# CHAPTER 5

## CONCLUSIONS

The major conclusions that can be drawn from the results/present work are as listed below

1. Lime sludge obtained from paper industry was thermo-chemically activated to enhance its hydraulic reactivity as well as activating efficiency of pozzolana to be used in binder. The lime reactivity of processed lime sludge satisfied the requirement for use in making cementitious binder. The enhanced reactivity of lime sludge up to a level of 50% is attributed to its conversion from crystalline state to non-crystalline state.
2. Cementitious binder has been developed using cement clinker, pozzolana (calcined clay and GGBFS) and thermo-chemically activated lime sludge. Efficiency of various pozzolan such as fly ash, calcined clay and GGBFS was assessed in terms of its pozzolanicity (Fratini test- lime absorption) prior to use in the mix. It was found that the mix containing GGBFS/calcined clay gave best results. The advantage of this mix is attributed to the formation of CSH as well as (CaNa)ASH phases.
3. Rheological studies indicated that the paste behaved like a Bingham fluid. Shear thickening behavior was noticed in the downward curve of hysteresis loop. Adding superplasticizer up to a level of 0.2% resulted in zero yield stress. The reduction in particle aggregation in the pastes is attributed to the dominance of hydrodynamic forces over the attractive inter-particle forces.
4. Hydration studies of the developed cementitious binders clearly indicated that the total heat (reaction product) released during calorimetric response was comparable with calorimetric response of Portland cement. Induction period was lower than the Portland cement. The reactivities of pozzolana and thermo-chemically activated lime sludge could be considered responsible for such behavior.
5. Comparative assessment of developed binder based on thermo-chemically activated lime sludge was made as per the requirement of IS: 8112 (Specification for 43 grade ordinary Portland cement). Results were comparable.
6. Life cycle impact assessment of developed binder based on thermo-chemically activated lime sludge was made using SimaPro 7.0 software. The developed binder has advantages in terms of climate change (global warming potential), depletion of resources (abiotic depletion potential) and terrestrial toxicity.

7. Based on these results, the developed binder can be suitably used as an alternative to Portland cement in making mortar and concrete for several applications.

### **Scope of future work**

1. Optimisation of parameters for thermo-chemical activation of lime sludge will be carried out at pilot plant scale to develop confidence during implementation in the industry.
2. Potential of developed binder in the production of concrete will be assessed. Durability studies will also be proposed under accelerated conditions.
3. Manufacturing of cementitious binder based on thermally activated lime sludge will be carried out at commercial scale.



## REFERENCES

- Banfill, P. and Frias, M. (2007) 'Rheology and conduction calorimetry of cement modified with calcined paper sludge', *Cement and Concrete Research*, 37, pp.184–190.
- Barnett *et al.* (2005), 'Strength development of mortars containing ground granulated blast-furnace slag: Effect of curing temperature and determination of apparent activation energies', *Cement and Concrete Research*, 36, pp.434 – 440.
- Barrett *et al.* (2014), 'Early-Age Shrinkage Behavior of Portland Limestone Cement', *Cement & Concrete Composites*, pp.1-14.
- Beuntner, N. and Thienel, K. C. (2015), 'Properties of calcined lias delta clay-technological effects, physical characteristics and reactivity in cement', *Calcined Clay for Sustainable Concrete*, pp.43-50.
- Bhanumathidas *et al.* (2004), 'Dual role of gypsum: Set retarder and strength accelerator', *The Indian Concrete Journal*, pp.1-4.
- Bijen, J. (1996), 'Blast Furnace Slag Cement for Durable Marine Structures', *Stichting BetonPrisma, Netherlands*.
- Bishnoi *et al.* (2014) 'Pilot Scale Manufacture of limestone calcined clay cement: The Indian experience', *Indian Concrete Journal*, 88(6), pp.22-28.
- Emmanuel *et al.* (2015) 'The Role of Calcined Clay Cement vis a vis Construction Practices in India and their Effects on Sustainability', *Calcined Clays for Sustainable Concrete*, 10, pp.411-417.
- Escalante *et al.* (2001), 'Reactivity of blast-furnace slag in portland cement blends hydrated under different conditions', *Cement and Concrete Research*, 31, pp.1403 – 1409.
- Diab *et al.* (2016), 'Long term study of mechanical properties, durability and environmental impact of limestone cement concrete', *Alexandria Engineering Journal*, 55, pp-1465–1482.

Falchi *et al.* (2015), 'The influence of water-repellent admixtures on the behavior and the effectiveness of Portland limestone cement mortars', *Cement & Concrete Composites*, 59, pp.107–118.

Falla *et al.* (2015) 'The influence of metakaolin on limestone reactivity in cementitious materials', *Calcined Clay for Sustainable Concrete*, pp.11-19.

Fava, G., Ruello, M. L. and Corinaldesi V. (2011) 'Paper Mill Sludge Ash as Supplementary Cementitious Material', *Journal of Materials in Civil Engineering*, 23(6), pp.772-776.

Garcia *et al.* (2001), 'The microstructure and mechanical properties of blended cements hydrated at various temperatures', *Cement and Concrete Research*, 31, pp.695 – 702.

Garg, M. and Singh, M. (2006) 'Strength and durability of cementitious binder produced from fly ash-lime sludge-Portland cement', *Indian Journal of Engineering & Materials Sciences*, 13, pp.75-79.

Global Overview of Construction Technology Trends: Energy Efficiency in Construction (HABITAT, 1995)

Hassan *et al.* (2015), 'Early carbonation curing of concrete masonry units with Portland limestone cement', *Cement & Concrete Composites*, 62, pp.168–177.

Holmes, S. (2002) 'An introduction of Building limes', *Lime Research Conference*.

Ishida *et al.* (2009), 'Application of blended cement in shotcrete to reduce the environmental burden', *Engineering Conferences International*, pp.1-9.

Jain *et al.* (1993) 'An innovative single-tier lime hydrator', *Research and Industry*, 38, pp. 230-233.

Li, G. (2004), 'Properties of high-volume fly ash concrete incorporating nano-SiO<sub>2</sub>', *Cement and Concrete Research*, 34, pp.1043 – 1049.

Luo *et al.* (2003), 'Study of chloride binding and diffusion in GGBS concrete', *Cement and Concrete Research*, 33, pp.1 – 7.

Maheswaran *et al.* (2011) ‘Studies on lime sludge for partial replacement of cement’ *Applied Mechanics and Materials*, 71-78, pp.1015-1019.

Morsy, M. S. (2005), ‘Effect of temperature on hydration kinetics and stability of hydration phases of metakaolin–lime sludge–silica fume system’, *Building Research Center*, pp.237-241.

Naik, T. K., Friberg, T. S. and Chun Y. M. (2004) ‘Use of pulp and paper mill residual solids in production of cellucrete’, *Cement and Concrete research*, 34, pp.1229-1234.

Okeyinka, O. M., Oloke, D. A. and Khatib, J. M. (2015) ‘A Review on Recycled Use of Solid Wastes in Building Materials’, *International Scholarly and Scientific Research & Innovation*, 9(12), pp.1533-1542.

Oner *et al.* (2007), ‘An experimental study on optimum usage of GGBS for the compressive strength of concrete’, *Cement & Concrete Composites*, 29, pp.505–514.

Pandey, S. P. and Sharma, R. L. (2000), ‘The influence of mineral additives on the strength and porosity of OPC mortar’, *Cement and Concrete Research*, 30, pp.19–23.

Pane, I. and Hansen, W. (2005), ‘Investigation of blended cement hydration by isothermal calorimetry and thermal analysis’, *Cement and Concrete Research*, 35, pp.1155-1164.

Parashar *et al.* (2015) ‘Testing of suitability of supplementary materials mixed in ternary cements’, *Calcined Clay for Sustainable Concrete*, pp.419-426.

Pavia *et al.* (2008), ‘A study of the durability of OPC vs. GGBS concrete on exposure to silage effluent’, *Journal of Materials in Civil Engineering*, 20(4), pp.313-320.

Pera, J. and Amrouz, A. (1998) ‘Development of Highly Reactive Metakaolin from Paper Sludge’, *Advanced Cement Based Materials*, 53(7), pp.49–56.

Percherdchoo, A. (2015), ‘Service life and environmental impact due to repairs by metakaolin concrete after chloride attack’, *Calcined Clay for Sustainable Concrete*, pp.35-41.

Ranachandran, V.S. (1969) ‘Application of differential thermal analysis in cement chemistry’, *Chemical Publicating Co. Inc., Chapter V*. pp-92.

Report of ACI Committee 233, Slag Cement in Concrete and Mortar, ACI 233R-03, American Concrete Institute, Farmington Hills, Mich, 2003.

Report of National Council for cement and building materials, CRI-ENG-SP-965, Utilization of lime sludge for value added products and productivity enhancement of lime kilns

Roy *et al.* (1982), 'Hydration, structure and properties of blast furnace slag cements, mortars and concrete', *ACI Journal*, 79 (6), pp.444 – 457.

Sahu, V. And Gayathri, V. (2014) 'The Use of Fly Ash and Lime Sludge as Partial Replacement of Cement in Mortar', *International Journal of Engineering and Technology Innovation*, 4(1), pp.30-37.

Saxena *et al.* (2005), 'Solid wastes generation in India and their recycling potential in building materials', pp.2311-2321.

Schneider *et al.* (2011), 'Sustainable cement production—present and future', *Cement and Concrete Research*, 41, pp.642–650.

Singh M. and Garg M. (2007), 'Durability of cementing binders based on fly ash and other wastes', *Construction and Building Materials*, 21, pp.2012–2016.

Singh M. and Garg M. (2008), 'Utilisation of waste lime sludge as building materials', *Journal of Scientific and Industrial Research*, 61, pp.161-166.

Thomas (1992), 'Carbonation of fly ash concrete', *Magazine of Concrete Research*, 44, pp.217-228.

Thongsanitgarn *et al.* (2011), 'Effect of Limestone Powders on Compressive Strength and Setting Time of Portland-Limestone Cement Pastes', *TICChE International Conference*, pp-1-4.

Trumer, A. and Ludwig, H. M. (2015), 'Sulphate and ASR resistance of concrete made with calcined clay blended cements. *Calcined Clay for Sustainable Concrete*, pp.3-9.

Vicat (1837) 'Mortars and Cements', *English Language Edition*.

Villa *et al.* (2007) 'Mineralogical and morphological changes of calcined paper sludge at different temperatures and retention in furnace', *Applied Clay Science*, 36, pp.279–286.

Weerdt *et al.* (2011), 'Hydration mechanisms of ternary Portland cements containing limestone powder and fly ash', *Cement and Concrete Research*, 41, pp.279–291.

Xu *et al.* (2014) 'The utilization of lime-dried sludge as resource for producing cement', *Journal of Cleaner Production*, pp.1-8.

Yousuf, Adil, B. A. and Rafique, A. (2014) 'Sustainable use of paper wastes (hypo sludge) in Concrete mix design', *First International Conference on Emerging Trends in Engineering, Management and Sciences*, pp.1-10.